Introduction to X-ray Emission spectroscopy
(XES, RXES, RIXS, IXS)

Pieter Glatzel

ESRF | The European Synchrotron

Some acronyms for photon spectroscopy used in literature

XAS – x-ray absorption spectroscopy
XAFS – x-ray absorption fine structure
XANES – x-ray absorption near edge structure
NEXAFS – near edge x-ray absorption fine structure
EXAFS – extended x-ray absorption fine structure
AXAFS – atomic x-ray absorption fine structure
SEXAFS – surface extended x-ray absorption fine structure
DEXAFS – dispersive extended x-ray absorption fine structure

XES – x-ray emission spectroscopy
RXES – resonant x-ray emission spectroscopy
IXS – inelastic x-ray scattering
RIXS – resonant inelastic x-ray scattering
NRIXS or NIXS – non-resonant inelastic x-ray scattering
NIXS - nuclear inelastic scattering
XRS – x-ray Raman scattering
(N,R)XRS – (non-)resonant x-ray Raman scattering

Not all acronyms actually distinguish different processes…

X-ray core level configurations and transitions

Absorption

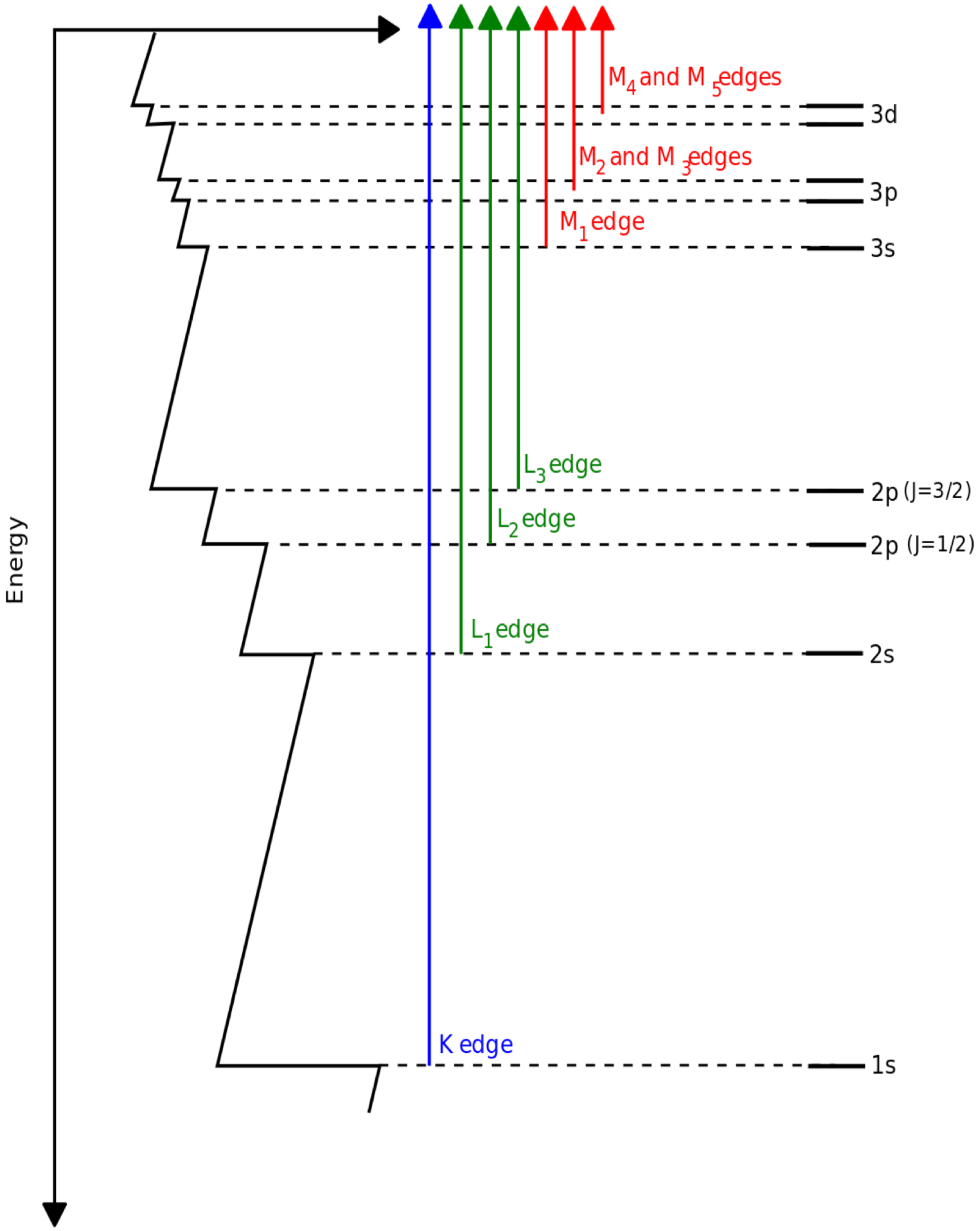

Level	Configuration	Level	Configuration	Level	Configuration
K	$1s^{-1}$	N_1	$4s^{-1}$	O_1	$5s^{-1}$
L_1	$2s^{-1}$	N_2	$4p_{1/2}^{-1}$	O_2	$5p_{1/2}^{-1}$
L_2	$2p_{1/2}^{-1}$	N_3	$4p_{3/2}^{-1}$	O_3	$5p_{3/2}^{-1}$
L_3	$2p_{3/2}^{-1}$	N_4	$4d_{3/2}^{-1}$	O_4	$5d_{3/2}^{-1}$
M_1	$3s^{-1}$	N_5	$4d_{5/2}^{-1}$	$O5$	$5d_{5/2}^{-1}$
M_2	$3p_{1/2}^{-1}$	N_6	$4f_{5/2}^{-1}$	O_6	$5f_{5/2}^{-1}$
M_3	$3p_{3/2}^{-1}$	N_7	$4f_{7/2}^{-1}$	O_7	$5f_{7/2}^{-1}$
				M_4	$3d_{3/2}^{-1}$
				M_5	$3d_{5/2}^{-1}$

Emission

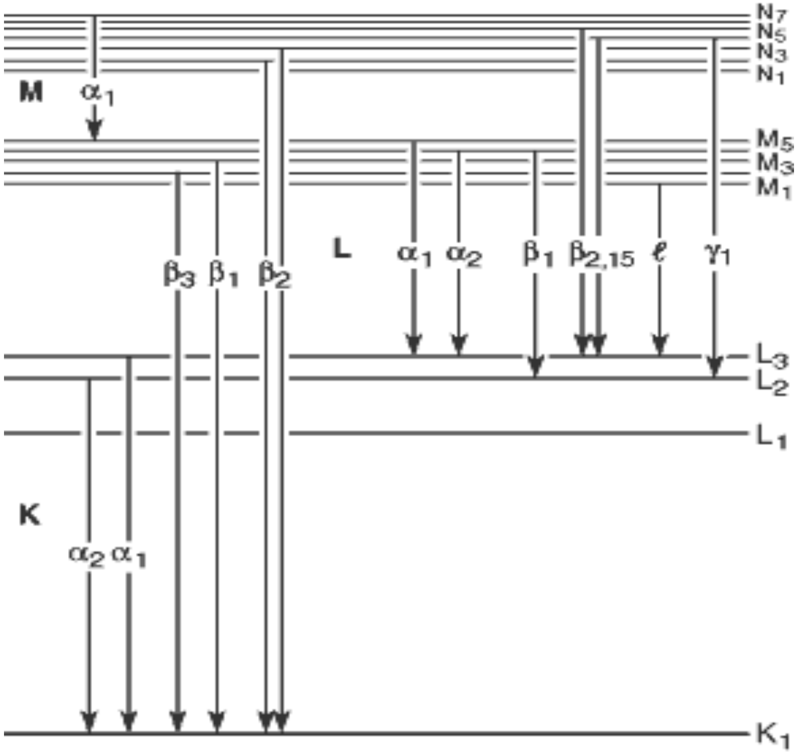

Why x-ray spectroscopy?

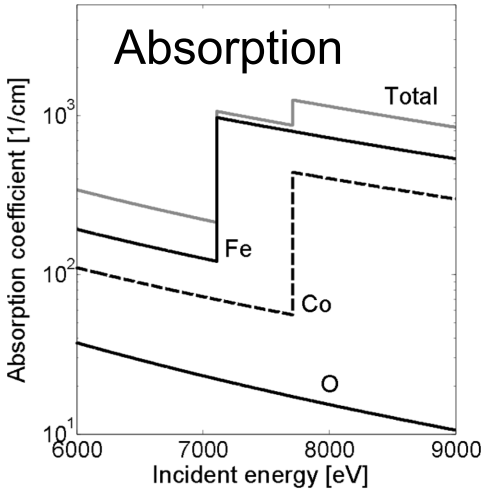

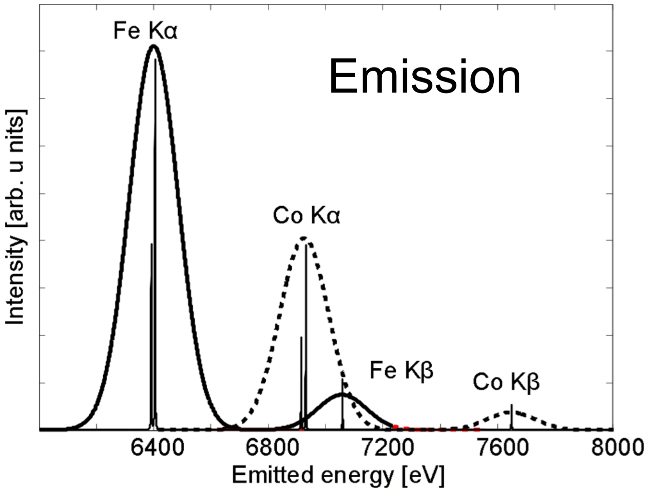

Element specific.

Electronic and atomic structural information on samples with or without long-range order.

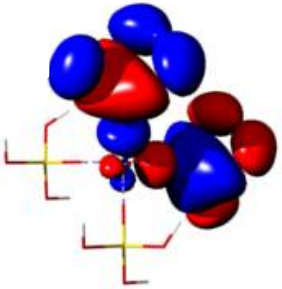

Can be bulk sensitive and compatible with *in-situ* and extreme conditions.

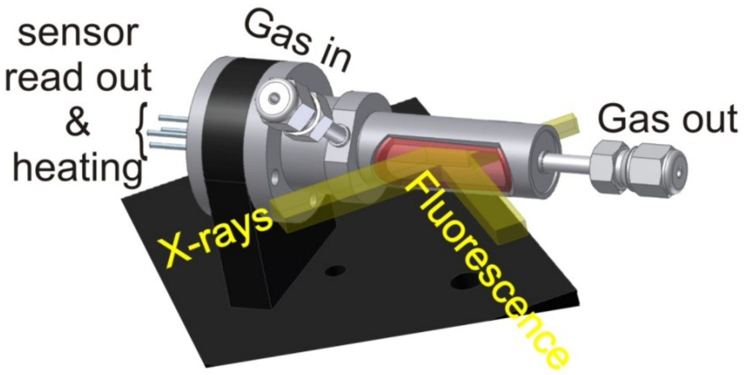

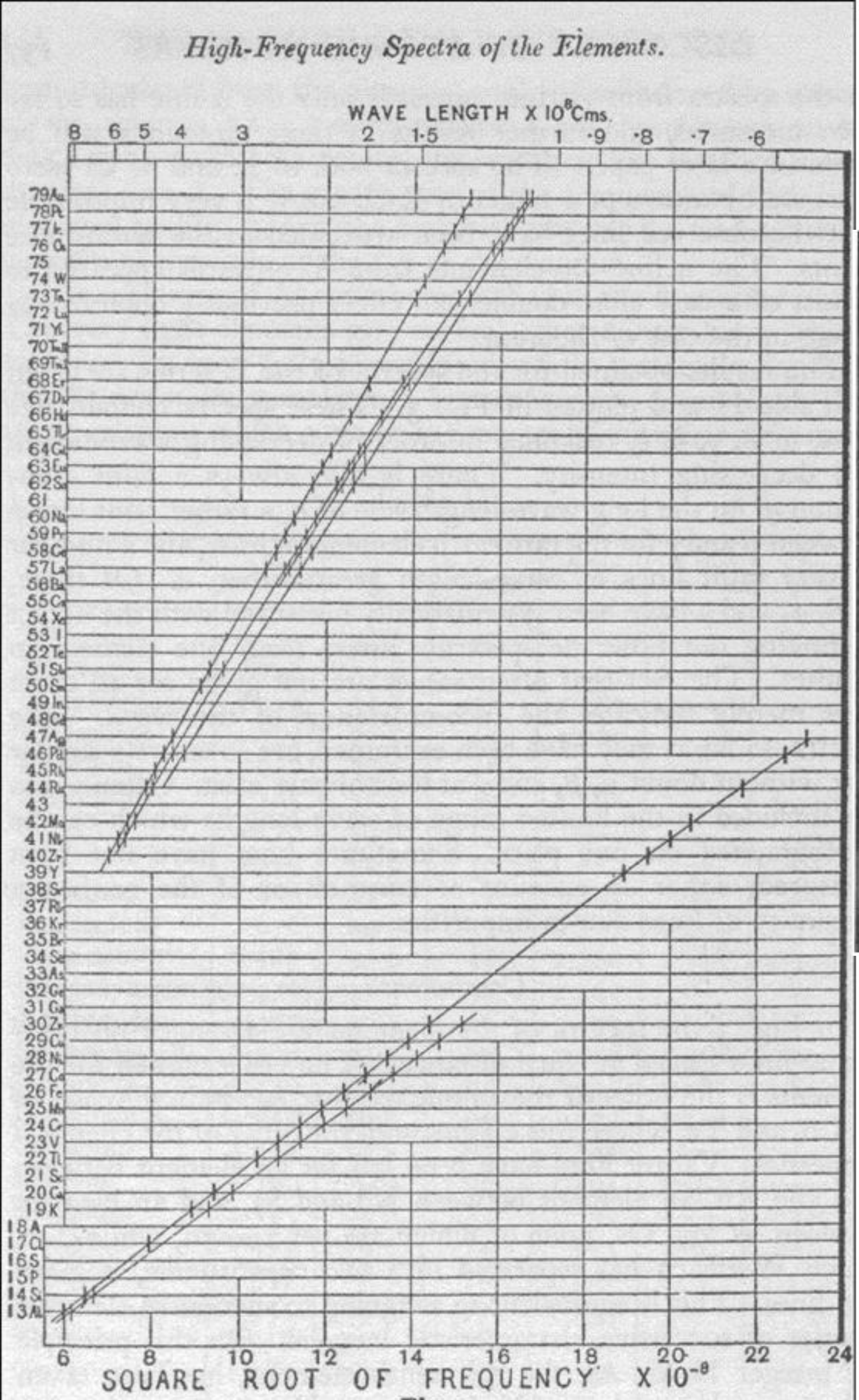

Fig. 3.

Moseley's law

$$\sqrt{\frac{1}{\lambda}} = k_1''(Z - k_2'')$$

Kα and Kβ lines

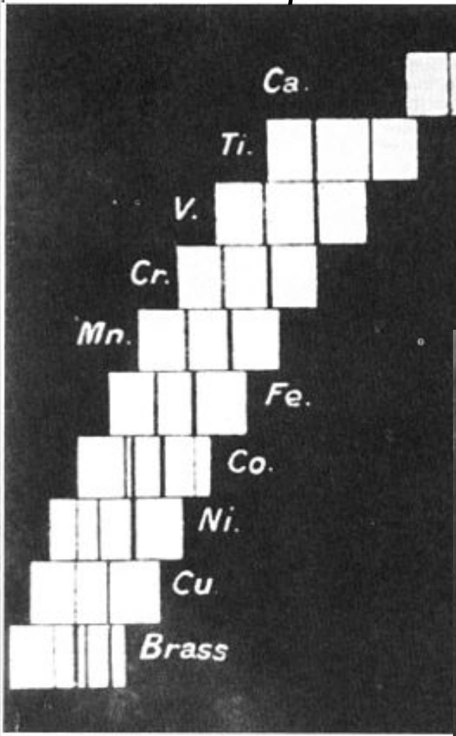

X-ray lines depend on atomic charge Z and not atomic mass A!

Henry Moseley

1887 – 1915

X-ray spectroscopy on Mars

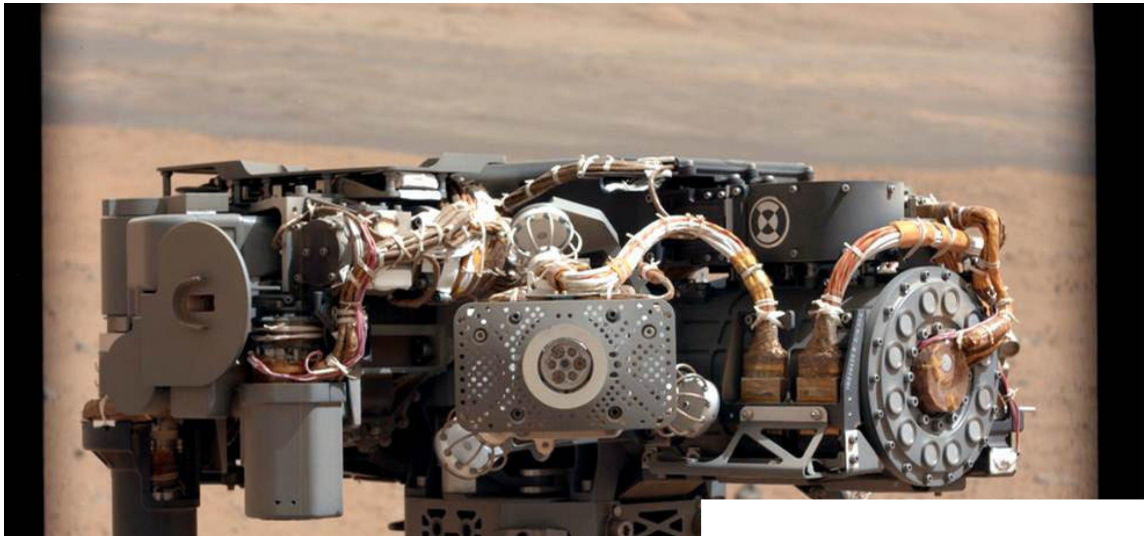

Curium (Cm) decays radioactively emitting α particles and γ-rays. They excite the atoms in the rocks on Mars and the resulting fluorescence spectrum is recorded.

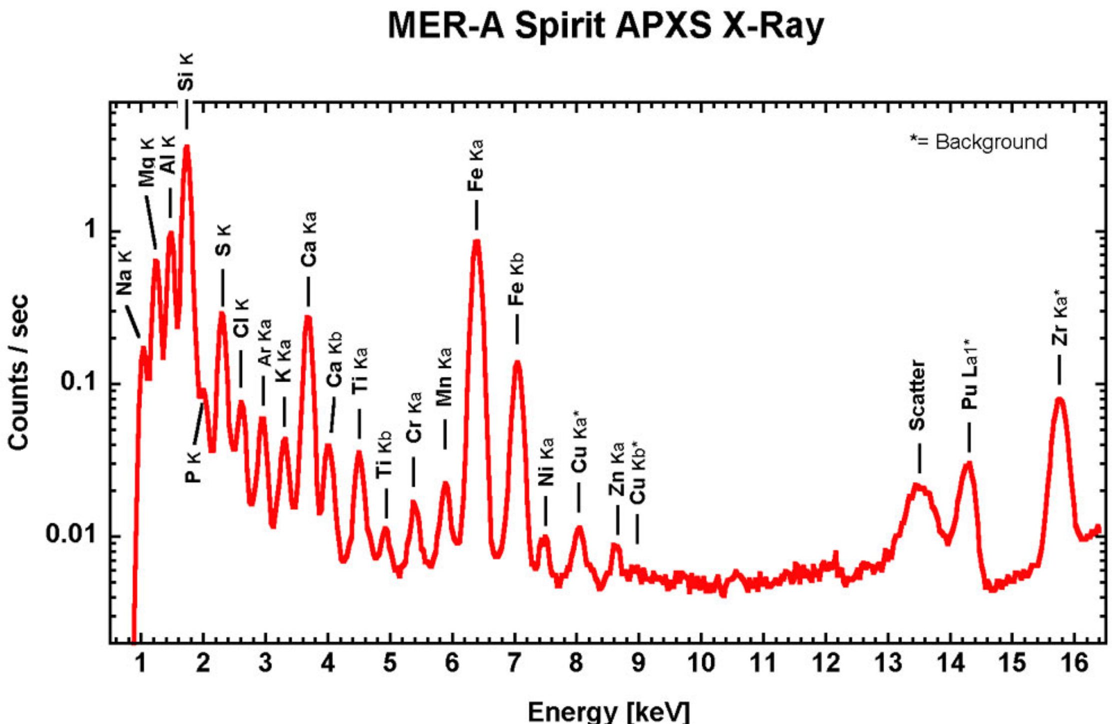

The fluorescence spectrum gives information about elemental composition. For a hydrogen-like atom Z with screening s:

$$\Delta E = 13.6(Z - s)^2\left(\frac{1}{n_i^2} - \frac{1}{n_f^2}\right)$$

XAS-XES

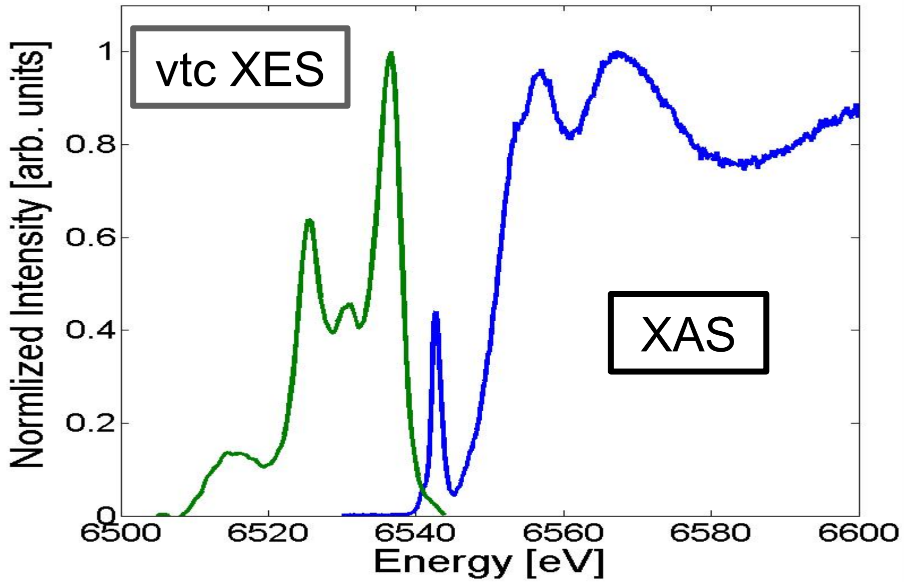

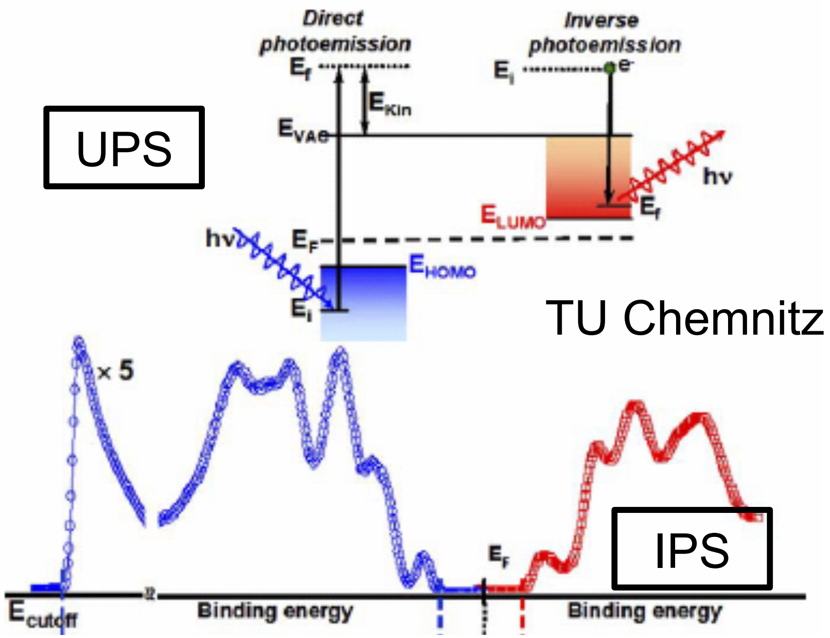

TU Chemnitz

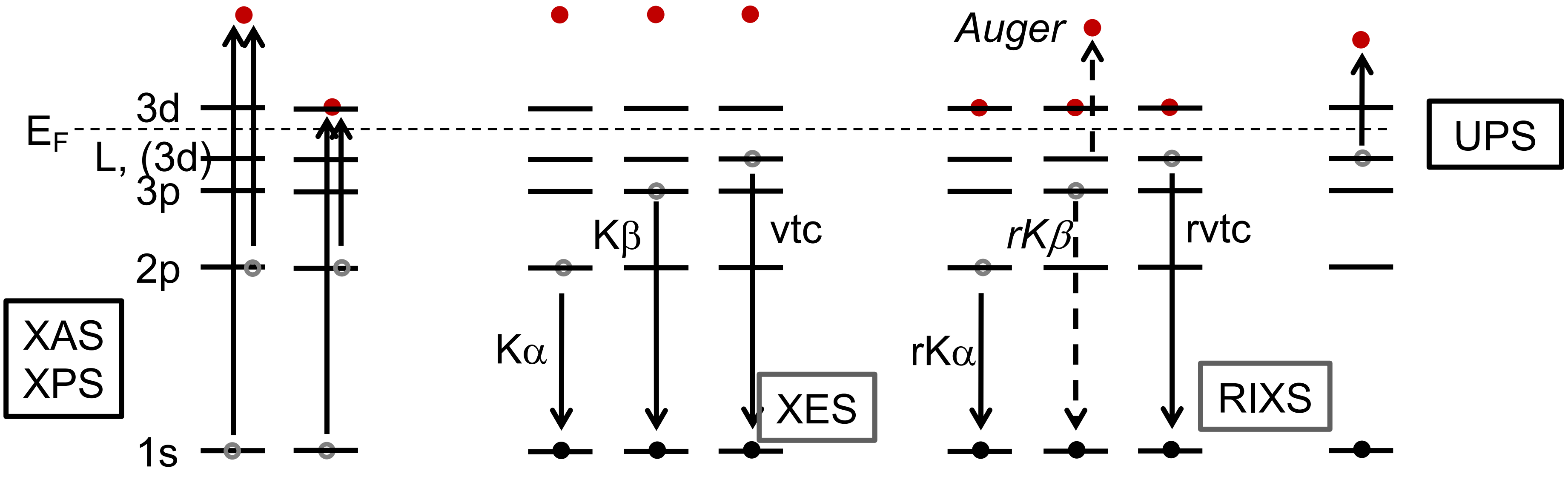

One-electron diagrams for X-ray absorption and (photo)emission.

Transition schemes

Two ways of describing the same process.

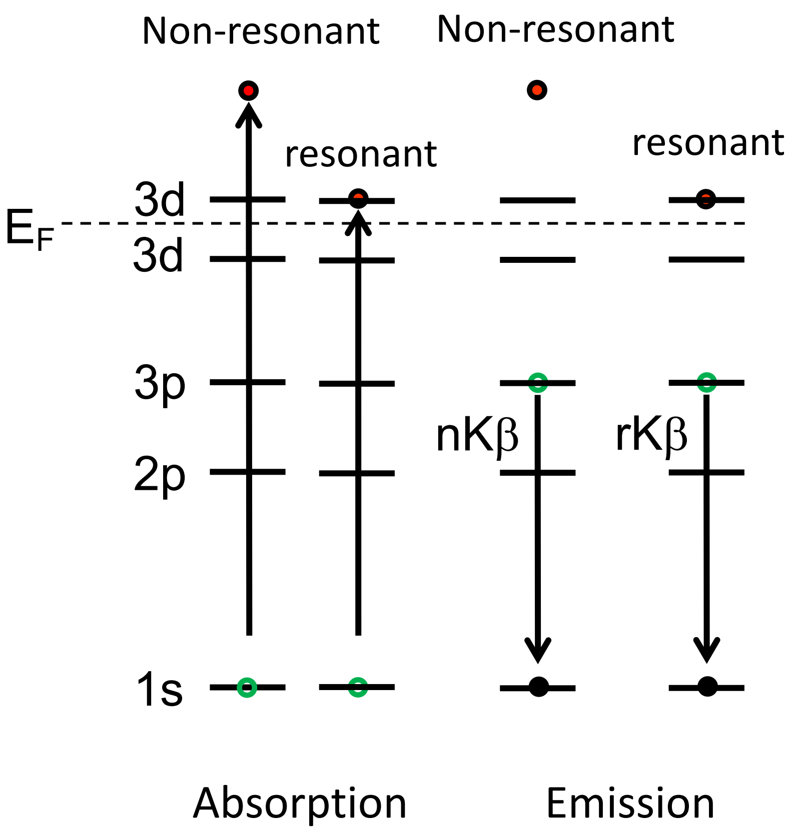

Non-resonant

Non-resonant

resonant

resonant

3d

E_F

3d

3p

2p

1s

nKβ

rKβ

Absorption

Emission

One-electron diagram

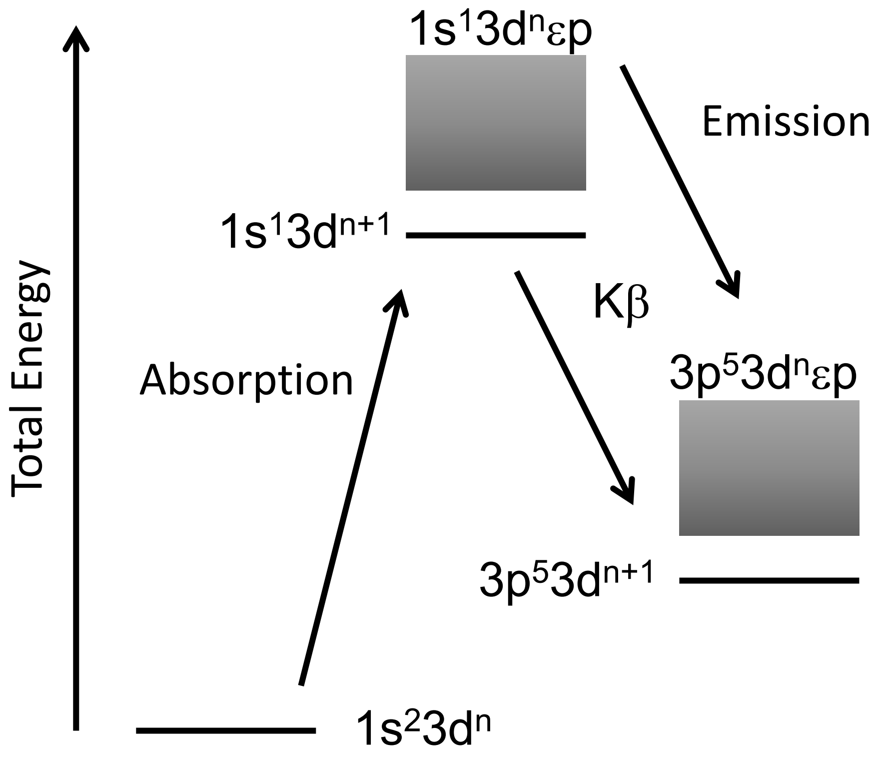

$1s^1 3d^n \varepsilon p$

Emission

$1s^1 3d^{n+1}$

Kβ

Total Energy

Absorption

$3p^5 3d^n \varepsilon p$

$3p^5 3d^{n+1}$

$1s^2 3d^n$

Many body diagram: Observes energy conservation

Some examples for core-to-core (c2c, ctc) X-ray emission lines

Study the oxidation states in Sulfur

XANES

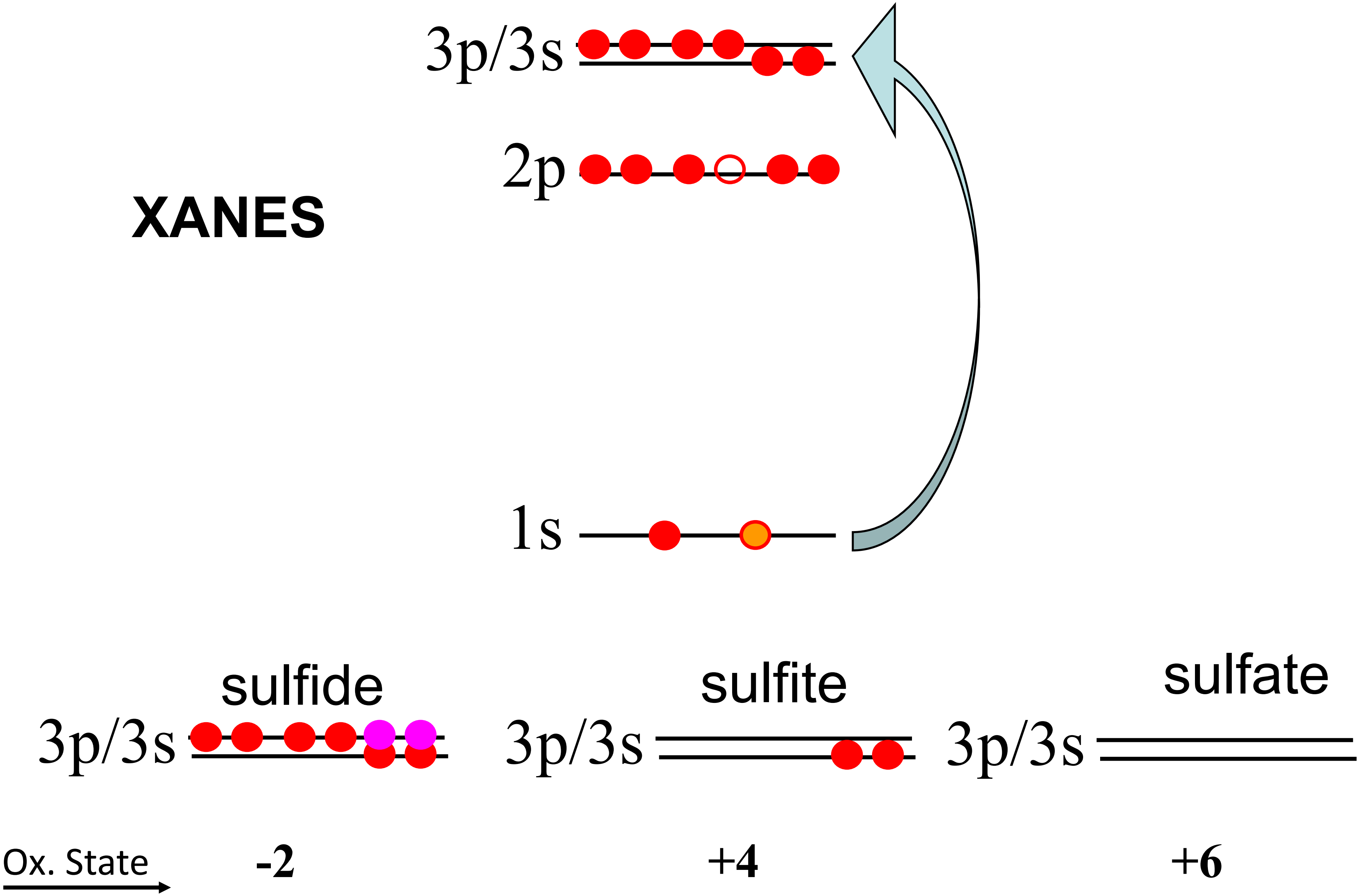

The Sulfur K-edge in Minerals

XANES

Oxidation state derived from edge position
→ rich XANES structure that is difficult to understand

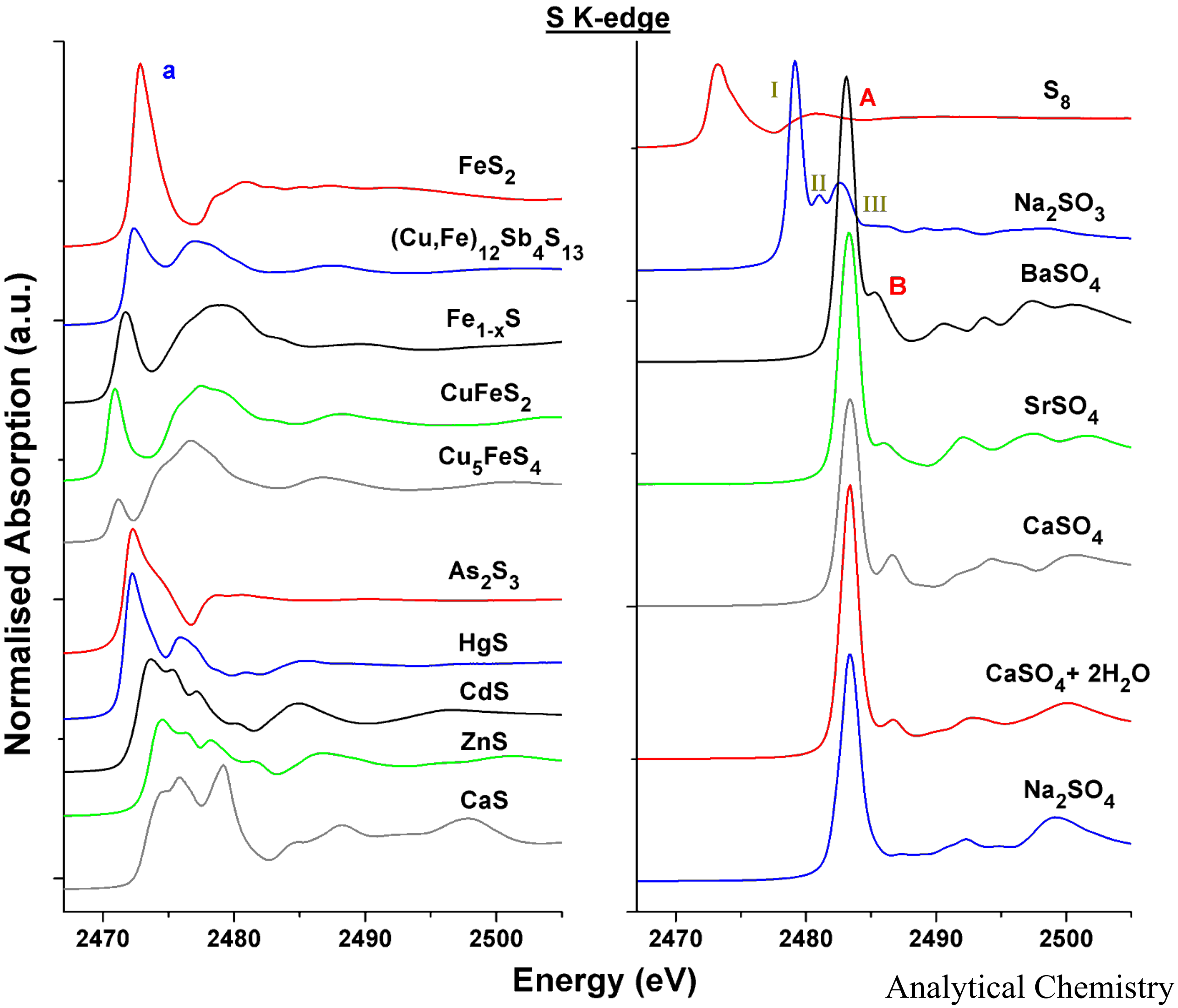

Sulfides

Sulfite

Sulfates

Analytical Chemistry (2009) **81** 6516

Study the oxidation states in Sulfur

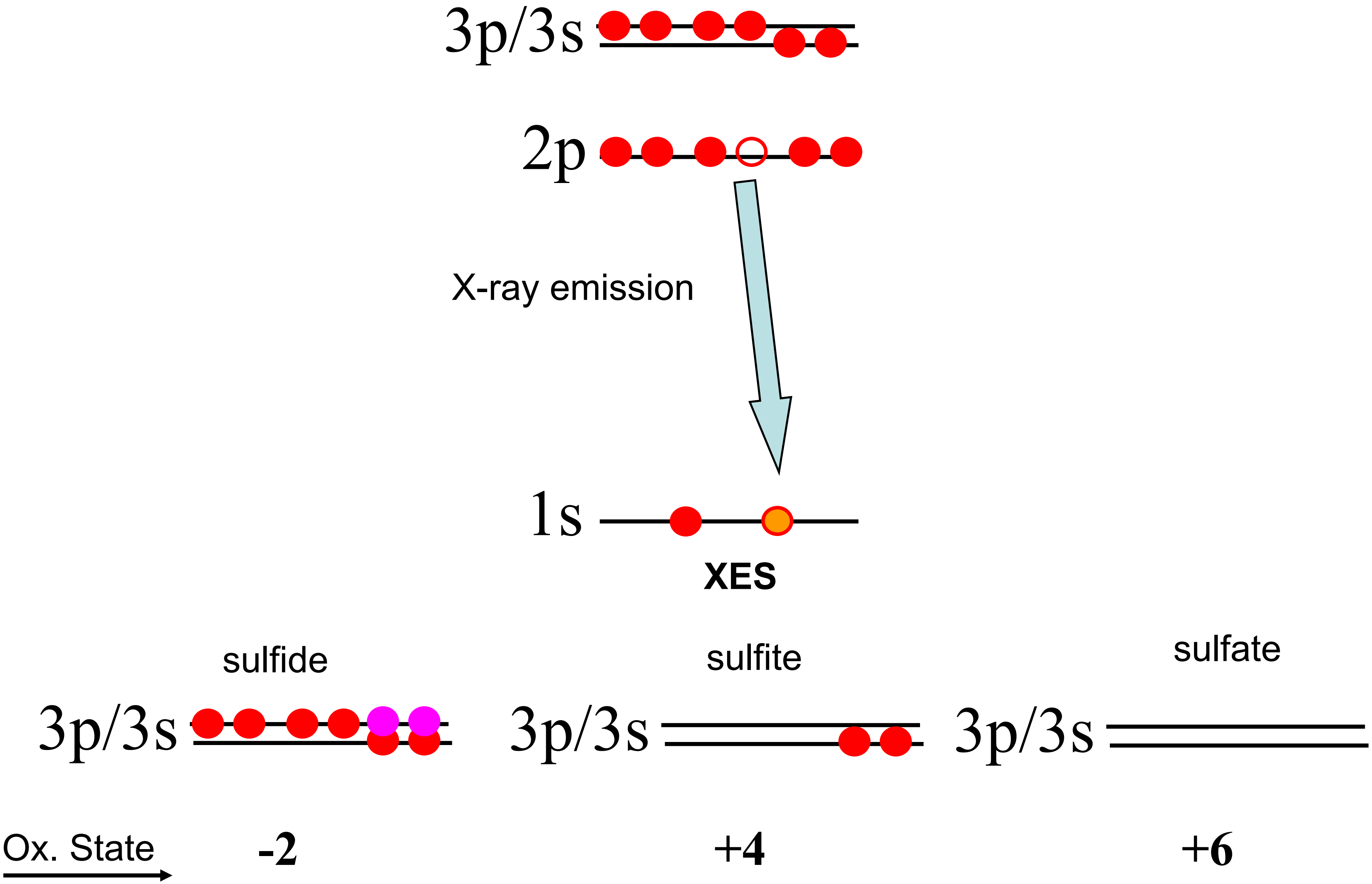

3p/3s

2p

X-ray emission

1s

XES

sulfide

sulfite

sulfate

3p/3s

3p/3s

3p/3s

Ox. State

-2

+4

+6

The Kα fluorescence lines

XES

Oxidation state derived from $K\alpha_1$ position
→ simple structure

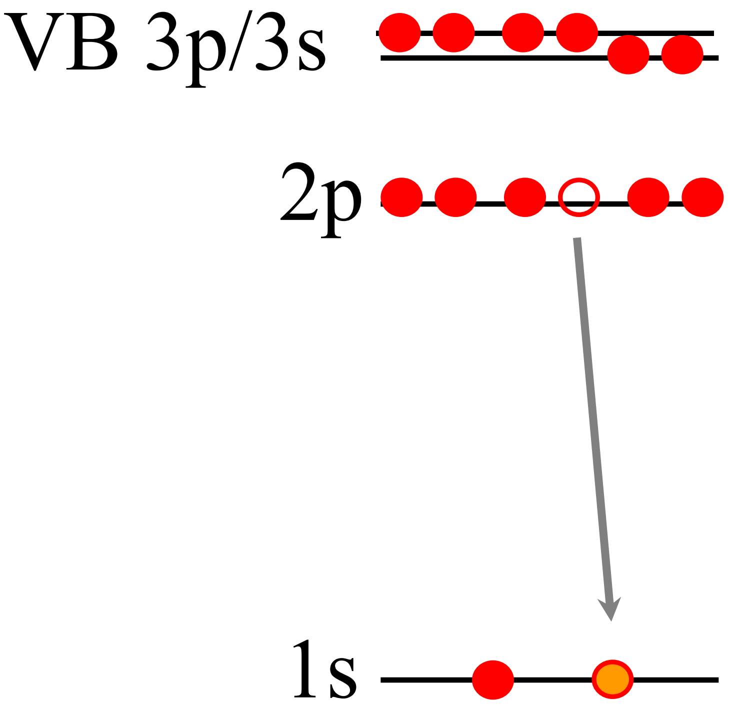

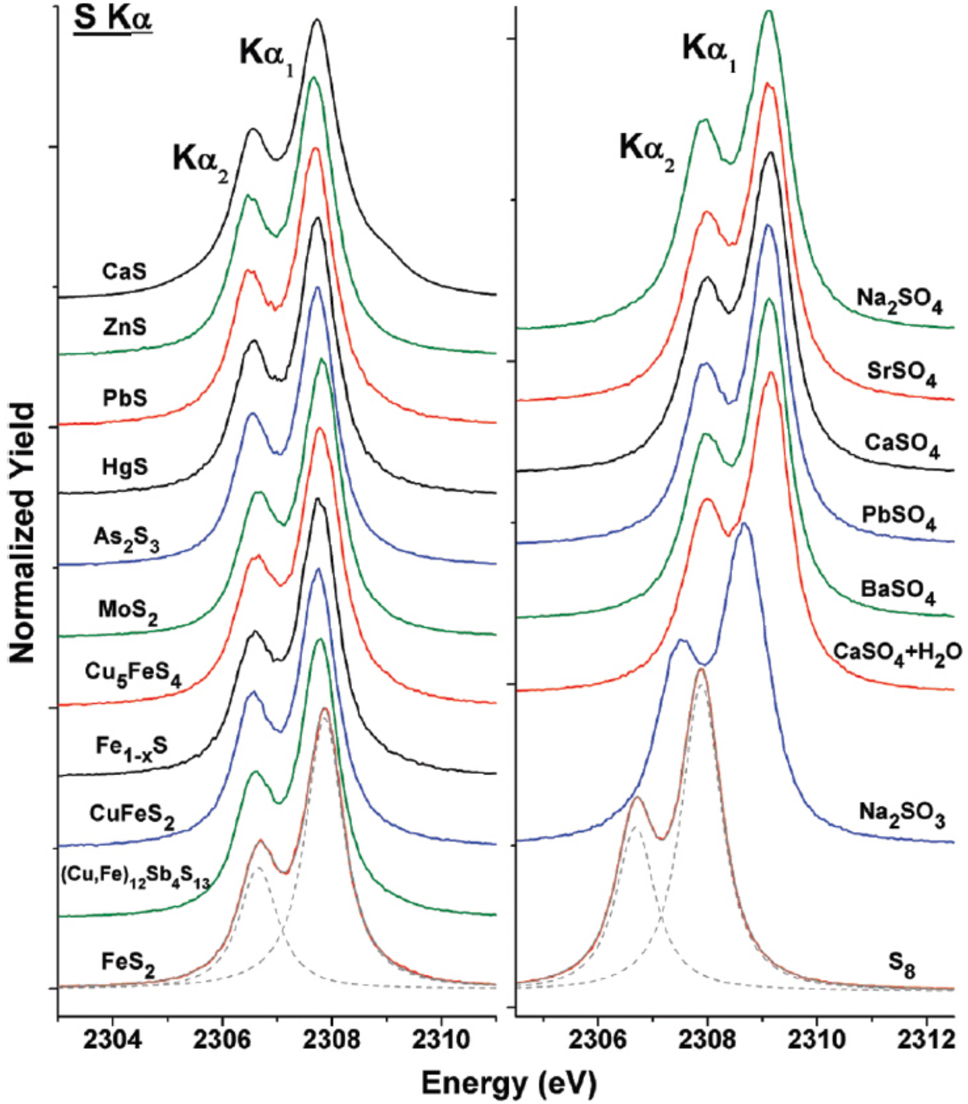

Shifts smaller by an order of magnitude as compared to XANES.

Why is Kα emission chemically sensitive?

Radial wavefunction

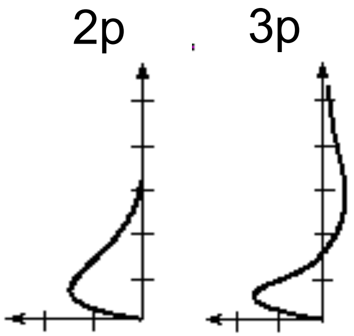

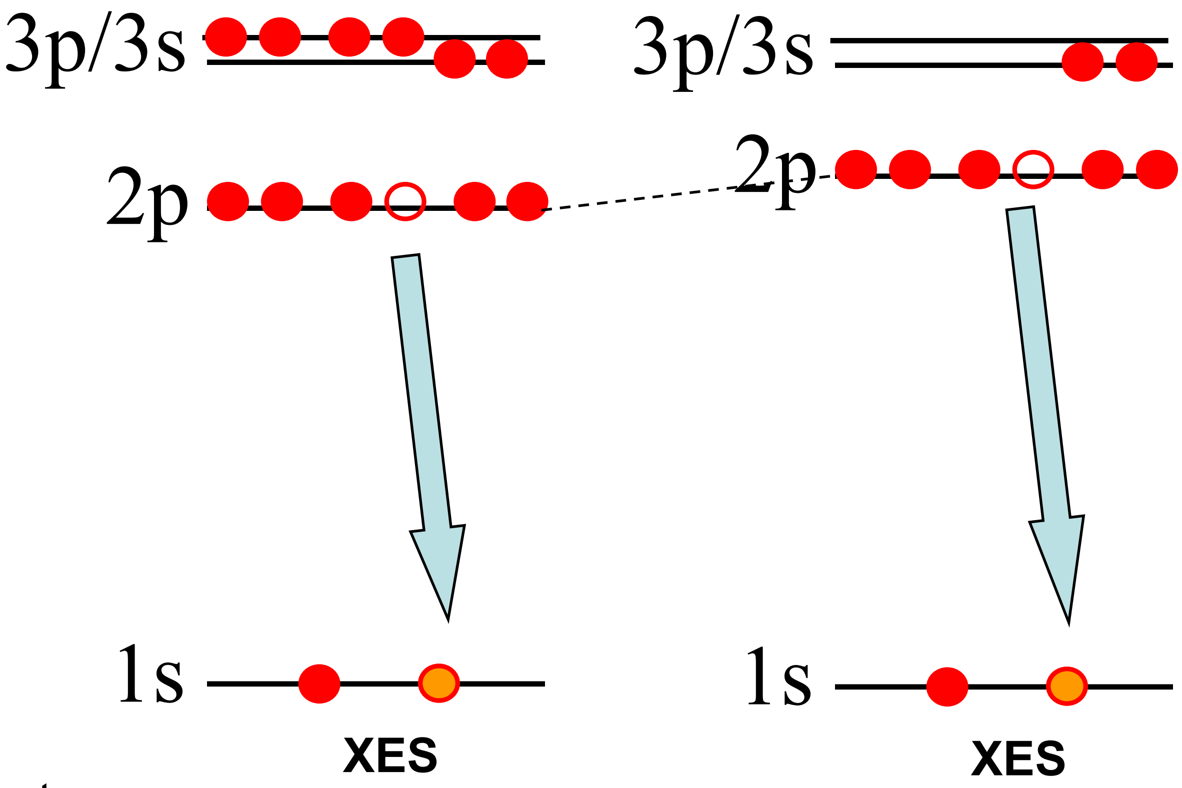

The 3p electrons contribute to the effective nuclear charge experienced by the 2p electrons.

Screening gives rise to chemical sensitivity.

J. C. Slater. *Phys. Rev.*, 36:57 – 64, (1930)

Many body diagram to explain energy shift

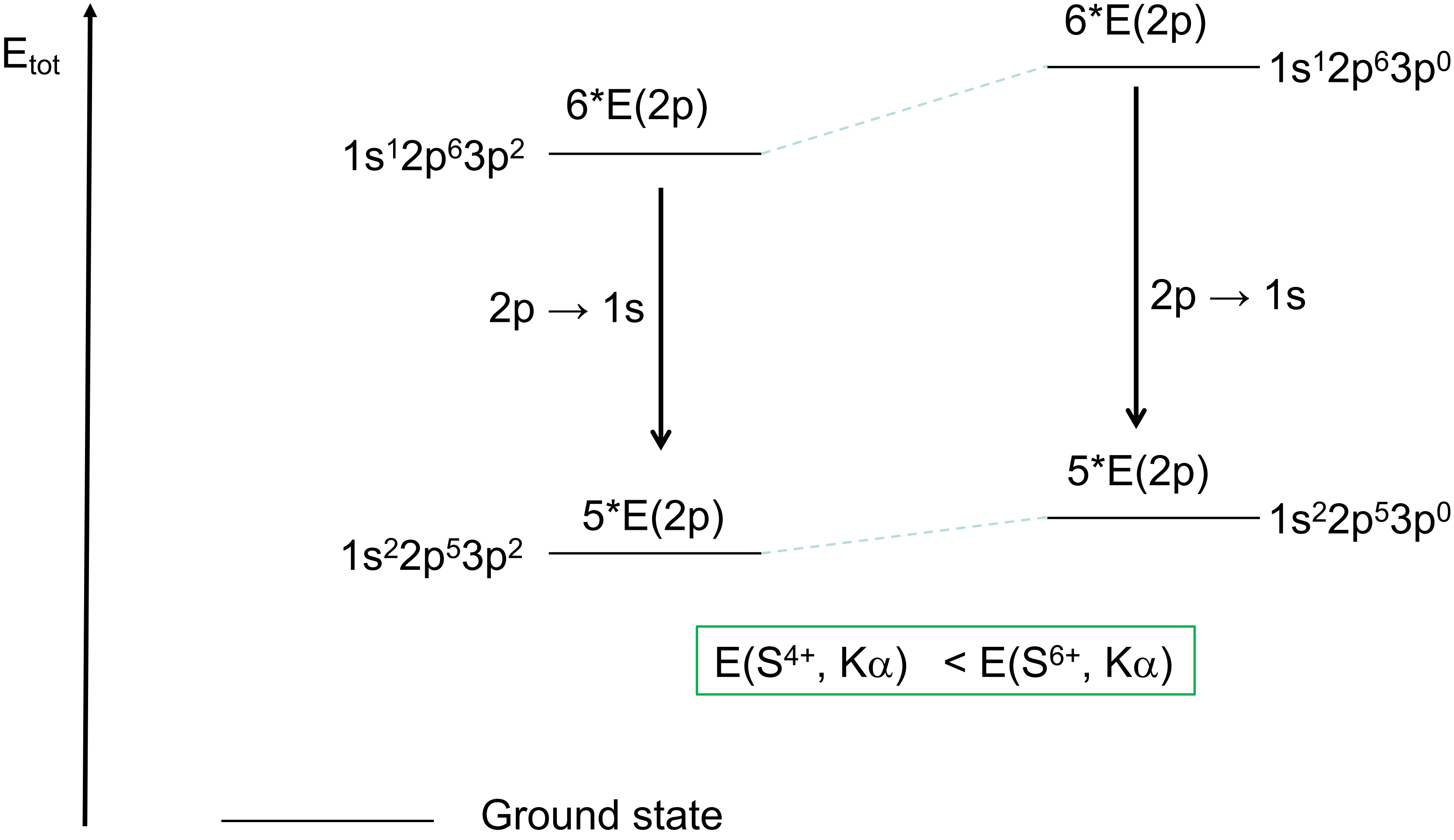

E_{tot}

6*E(2p)

$1s^1 2p^6 3p^0$

6*E(2p)

$1s^1 2p^6 3p^2$

2p → 1s

2p → 1s

5*E(2p)

$1s^2 2p^5 3p^0$

5*E(2p)

$1s^2 2p^5 3p^2$

$E(S^{4+}, K\alpha) < E(S^{6+}, K\alpha)$

Ground state

Total energy diagram assuming that the 1s shell is not affected by the screening by the valence electrons. The binding energy of a 2p electron increases when removing valence electrons

Calculate S Kα shift due to screening

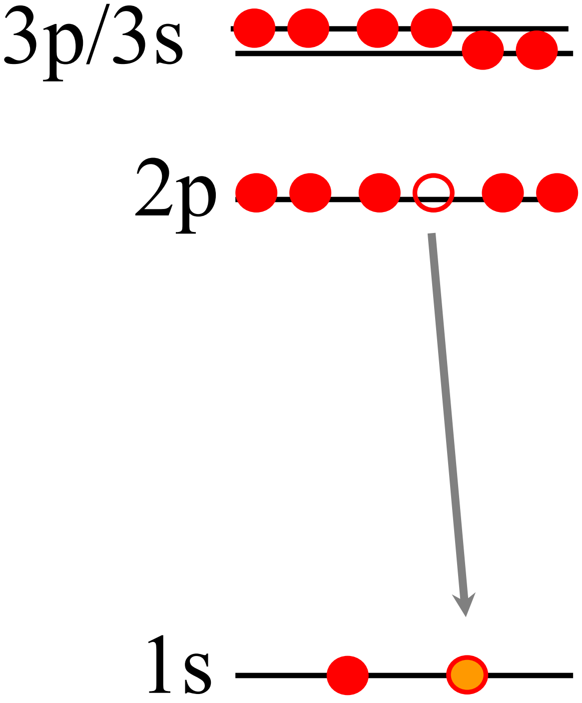

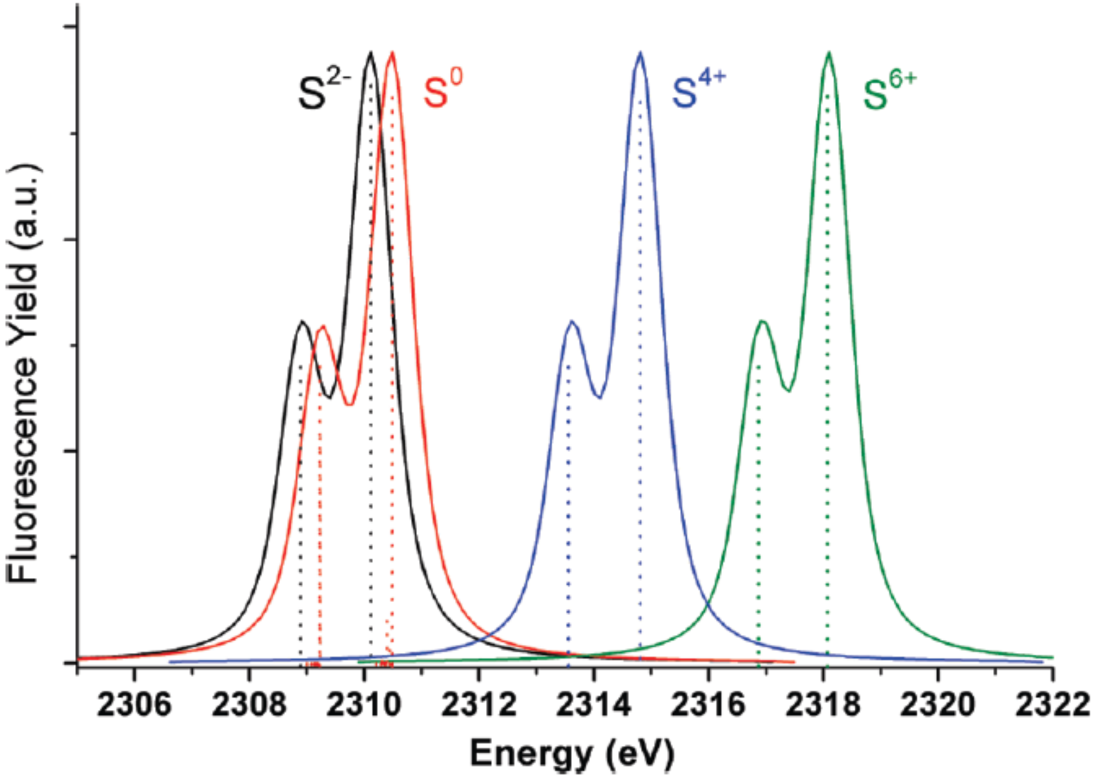

Cowan’s code (atomic)

Atomic orbitals → Shift exaggerated

S 2p XPS and Kα XES

2p XPS

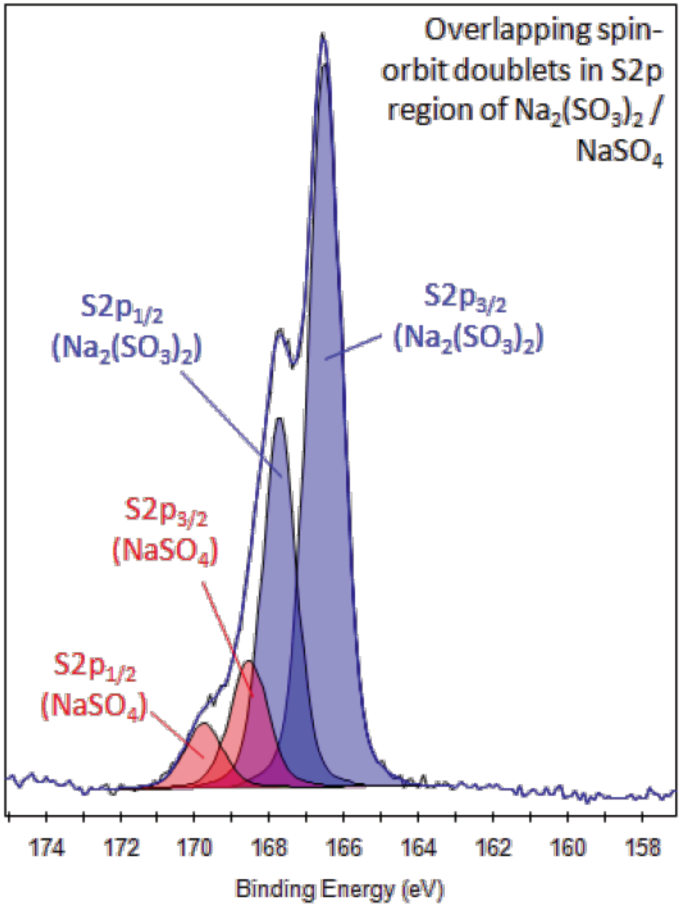

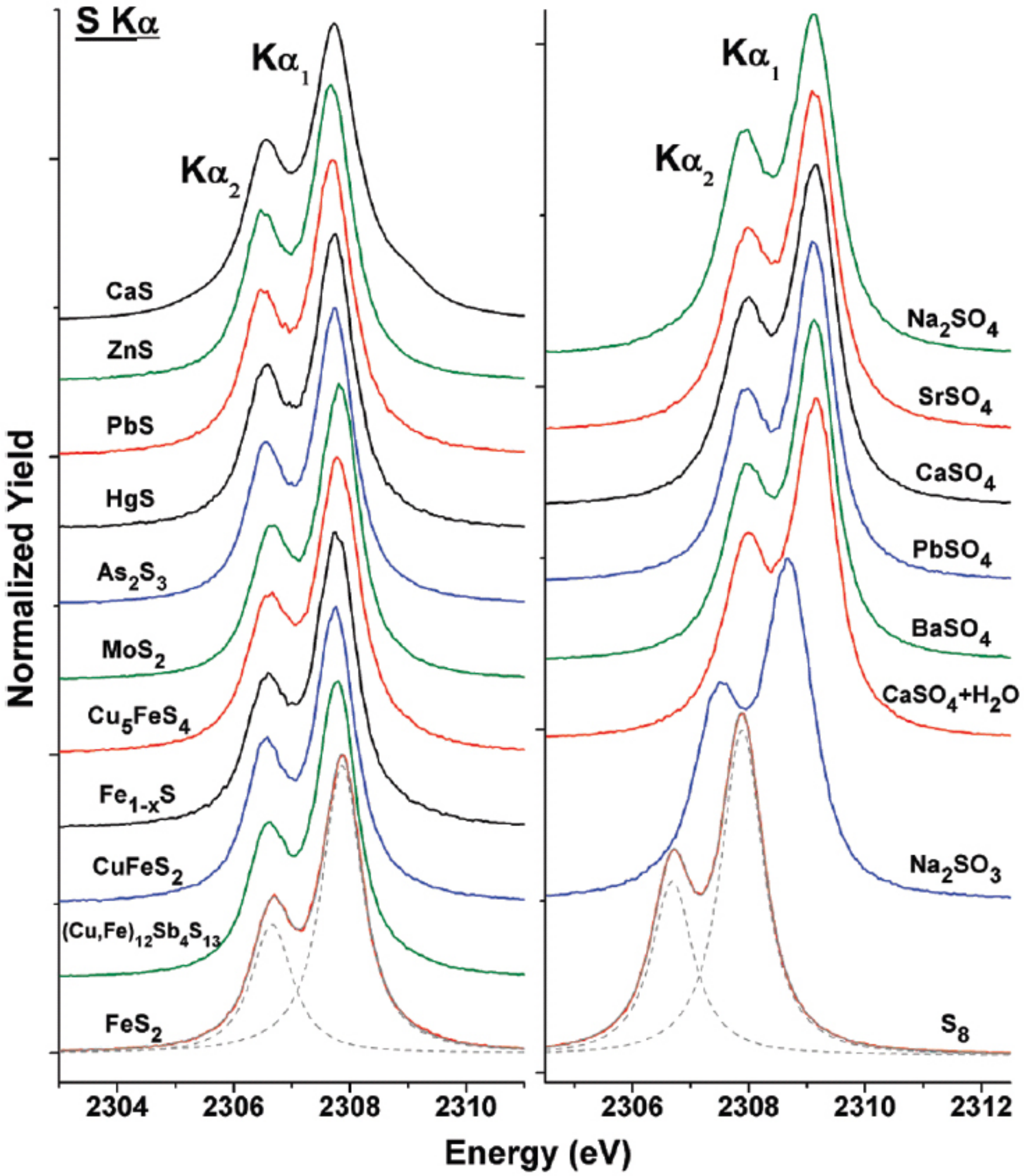

In both cases, the chemical shift arises from changes of nuclear screening.

Summary S XAS-XES

XES is less sensitive to atomic structural changes than XANES

XES can be used to study electronic structure.

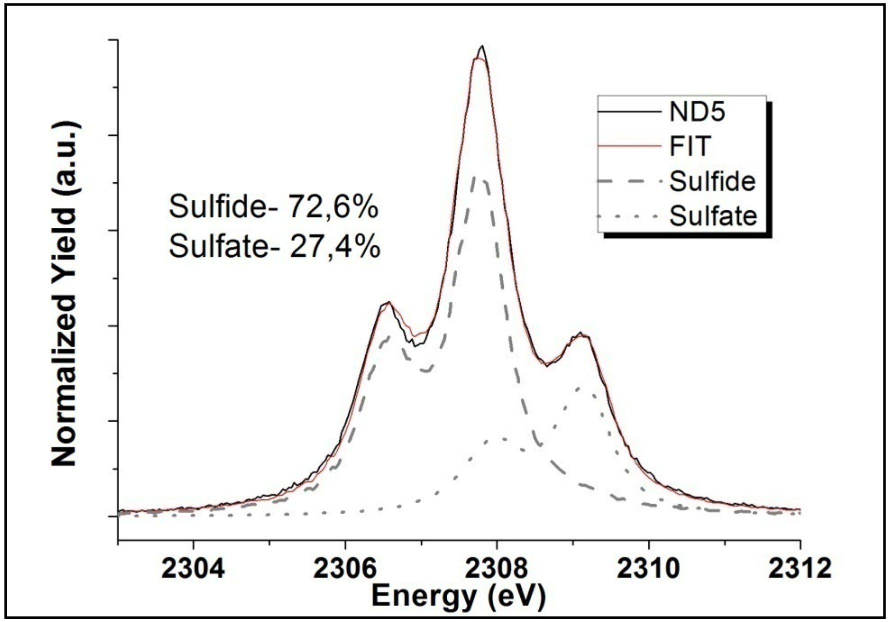

Quantitative analysis in heterogeneous compounds possible.

Analytical Chemistry (2009) **81** 6516

The Kβ lines in 3d transition metals

The K fluorescence lines in 3d transition metals

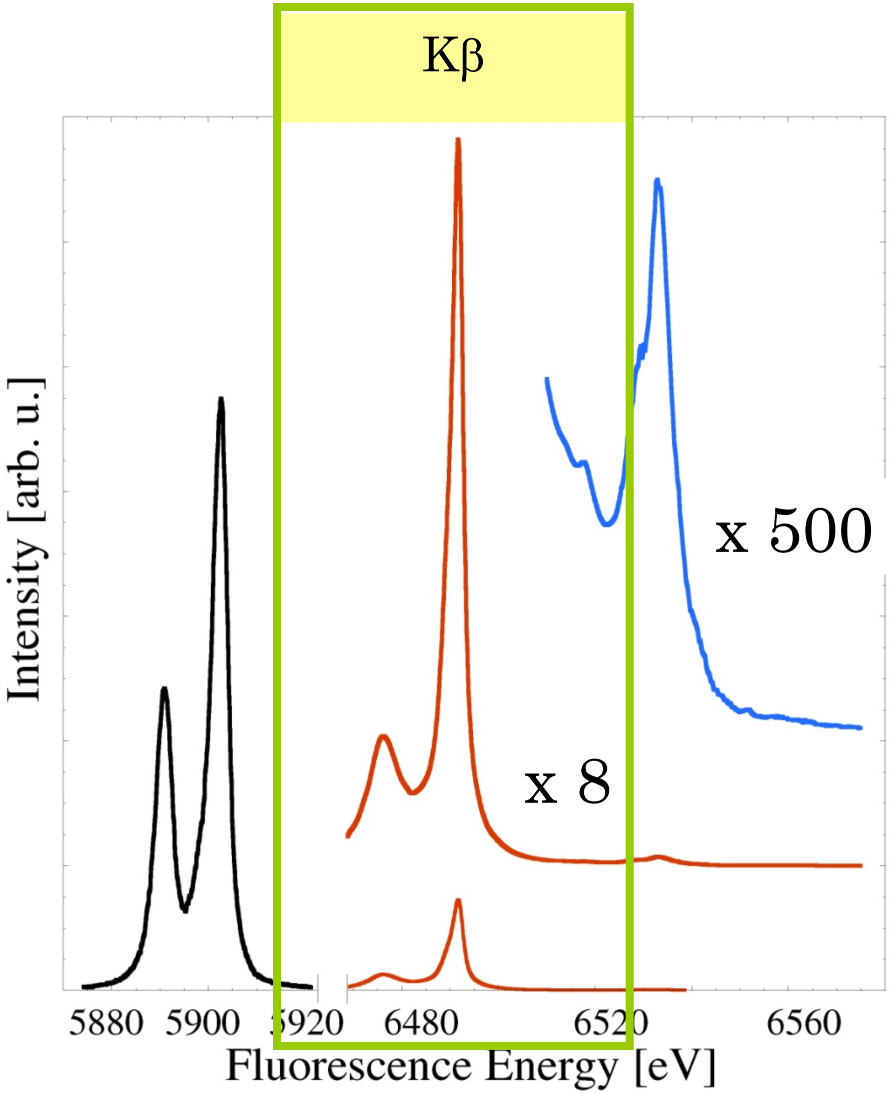

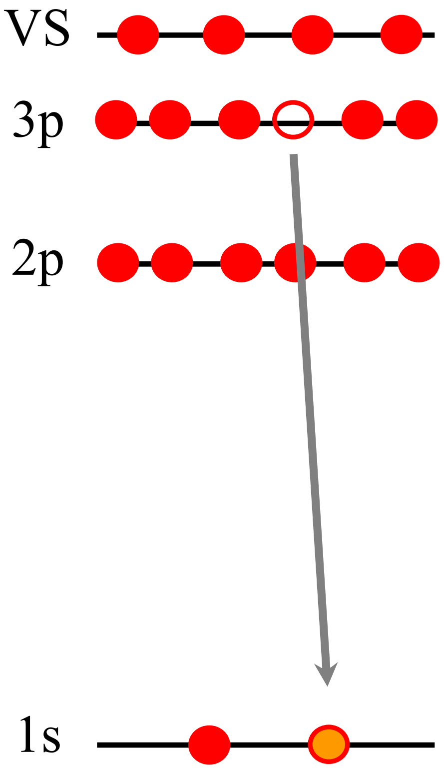

Kβ spectroscopy in 1959

JOURNAL OF THE PHYSICAL SOCIETY OF JAPAN, Vol. 14, No. 12, DECEMBER 1959

The X-ray Non-diagram Lines *Kβ′* of Some Compounds of the Iron Group

By Kenjiro TSUTSUMI
Department of Physics, Faculty of Science, Osaka University

(Received August 1, 1959)

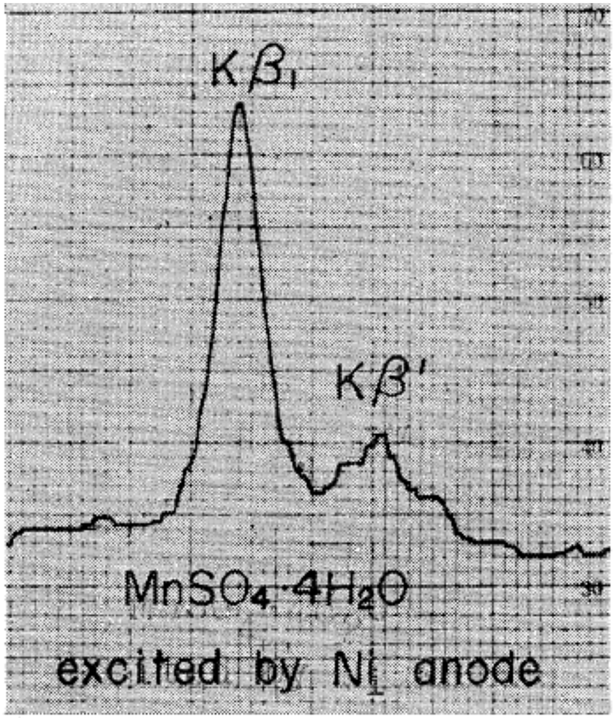

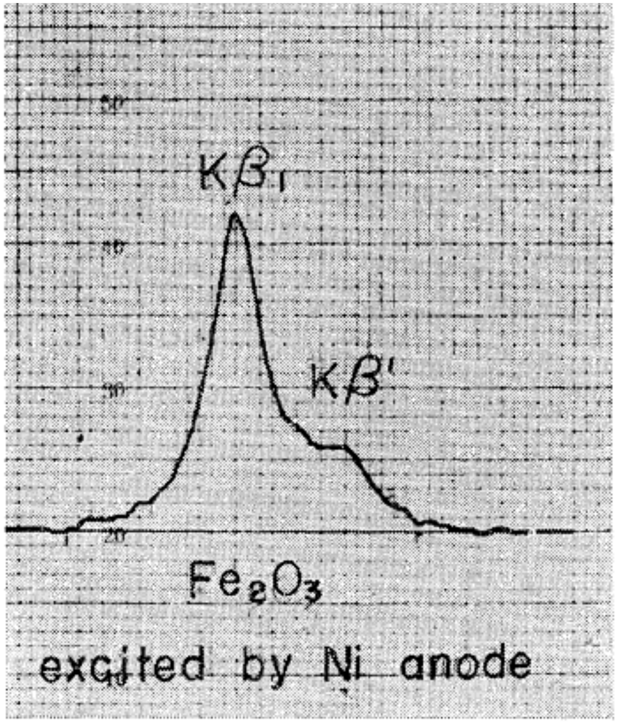

Multiplets and core holes

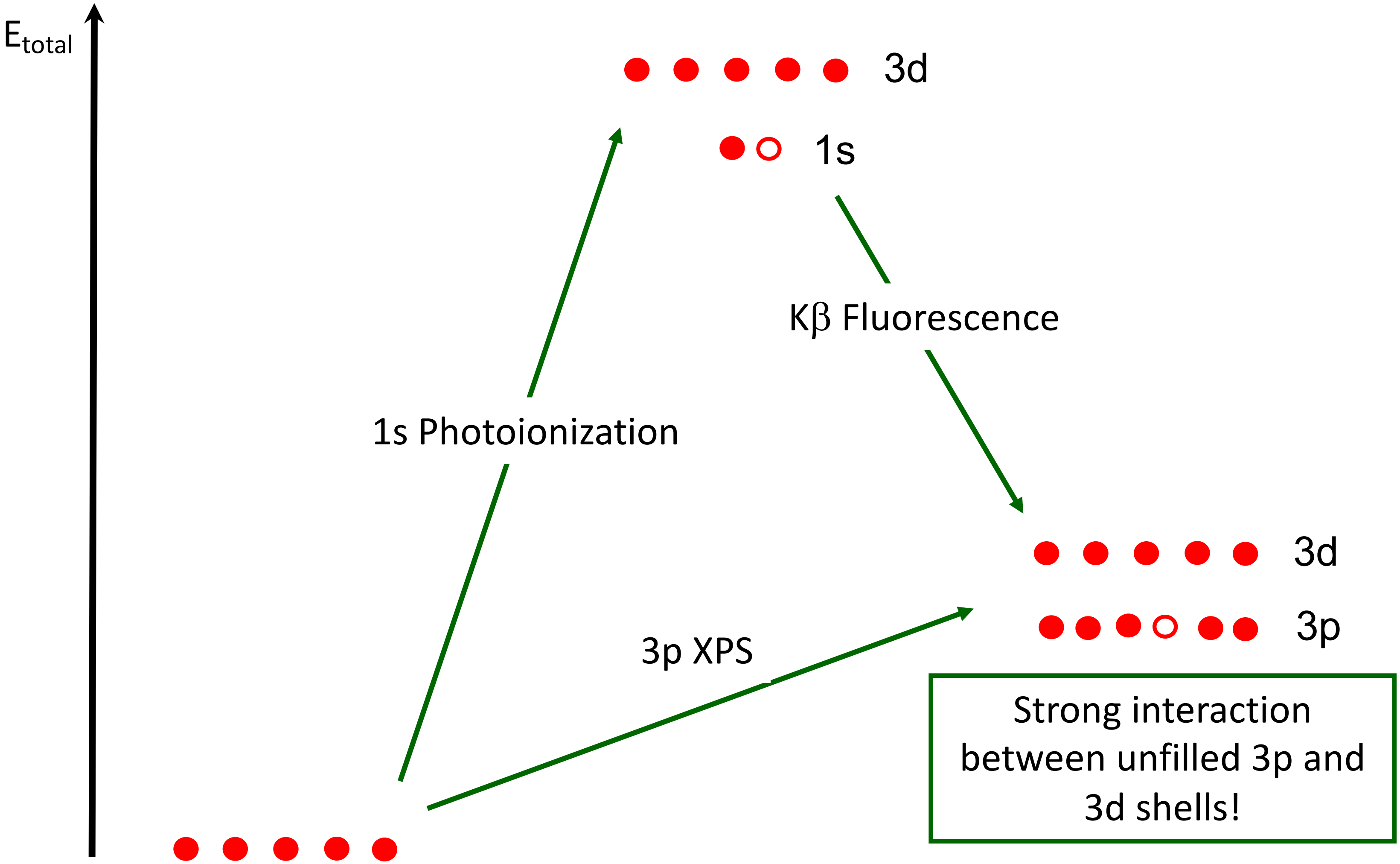

Strong interaction between unfilled 3p and 3d shells!

XES measures the electron-electron interactions in the final state!

Multiplets and core holes

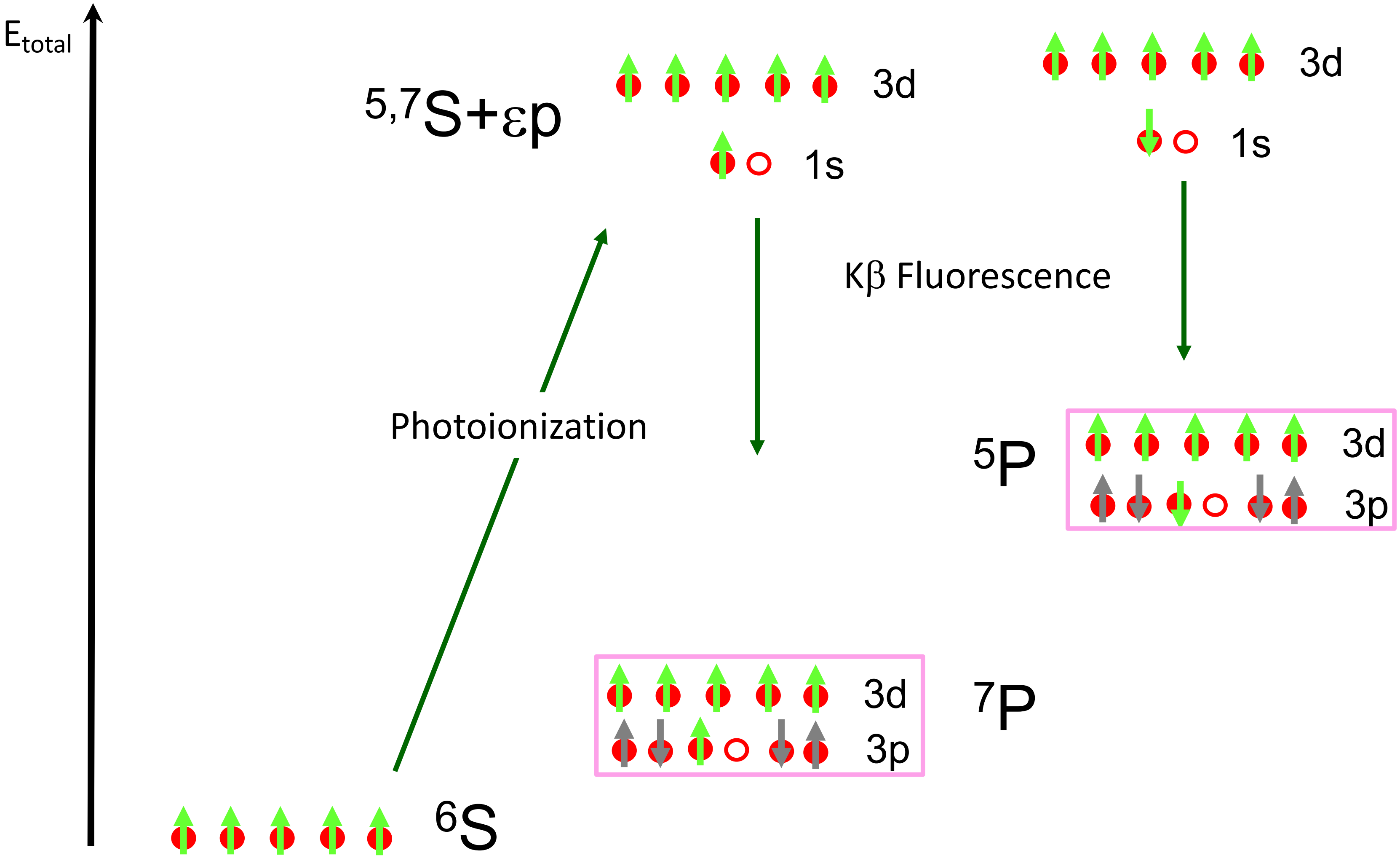

E_{total}

$^{5,7}S+\varepsilon p$

3d

1s

3d

1s

Kβ Fluorescence

Photoionization

^5P

3d

3p

3d

3p

^7P

^6S

XES measures the electron-electron interactions in the final state! The strong (3p,3d) exchange interaction splits the final states into ^5P and ^7P.

Spin-selectivity in the Kβ line

LS coupling works pretty well but the shoulder in the spectrum cannot be explained.

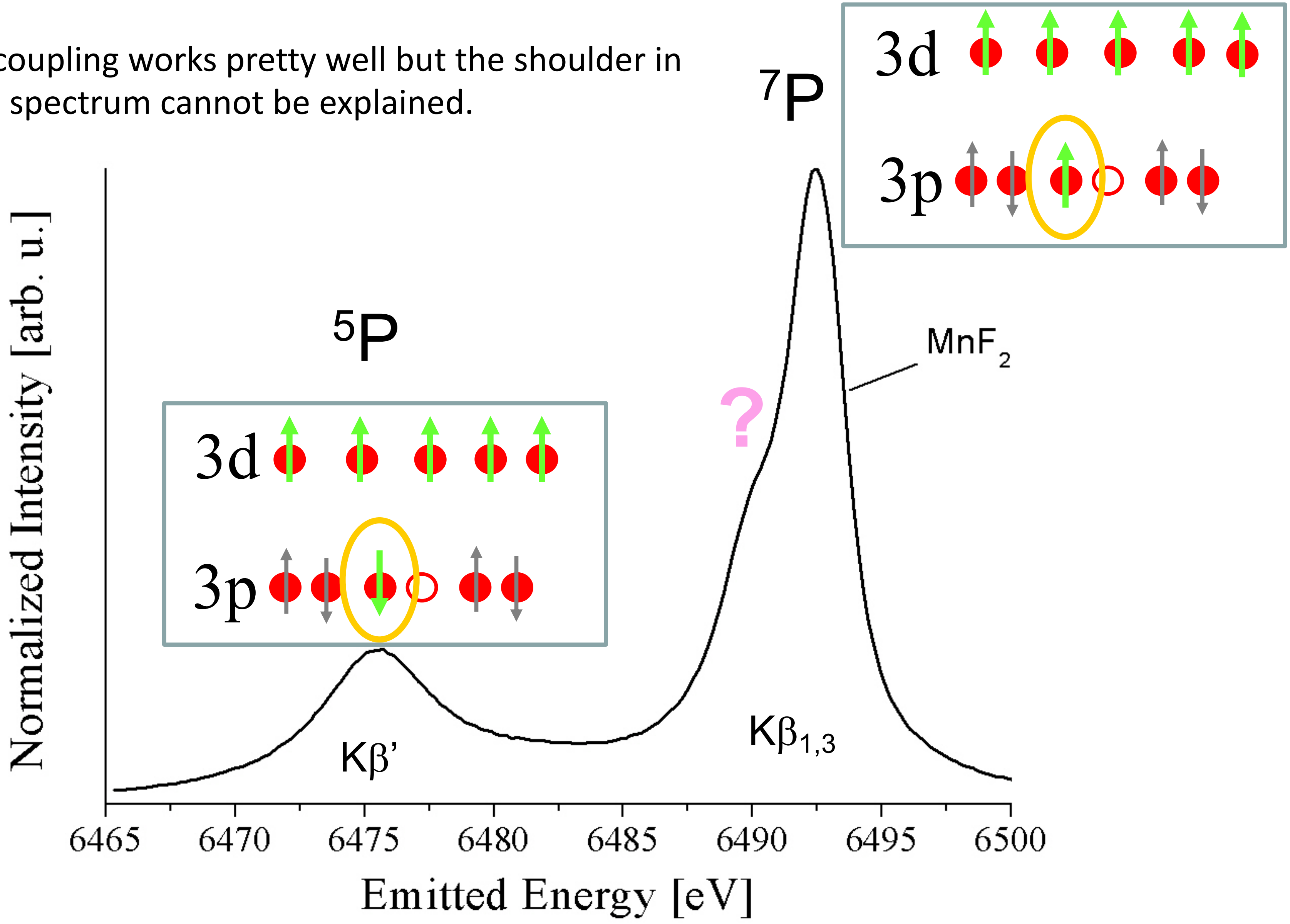

Multi-electron excitation in the Mn Kβ line

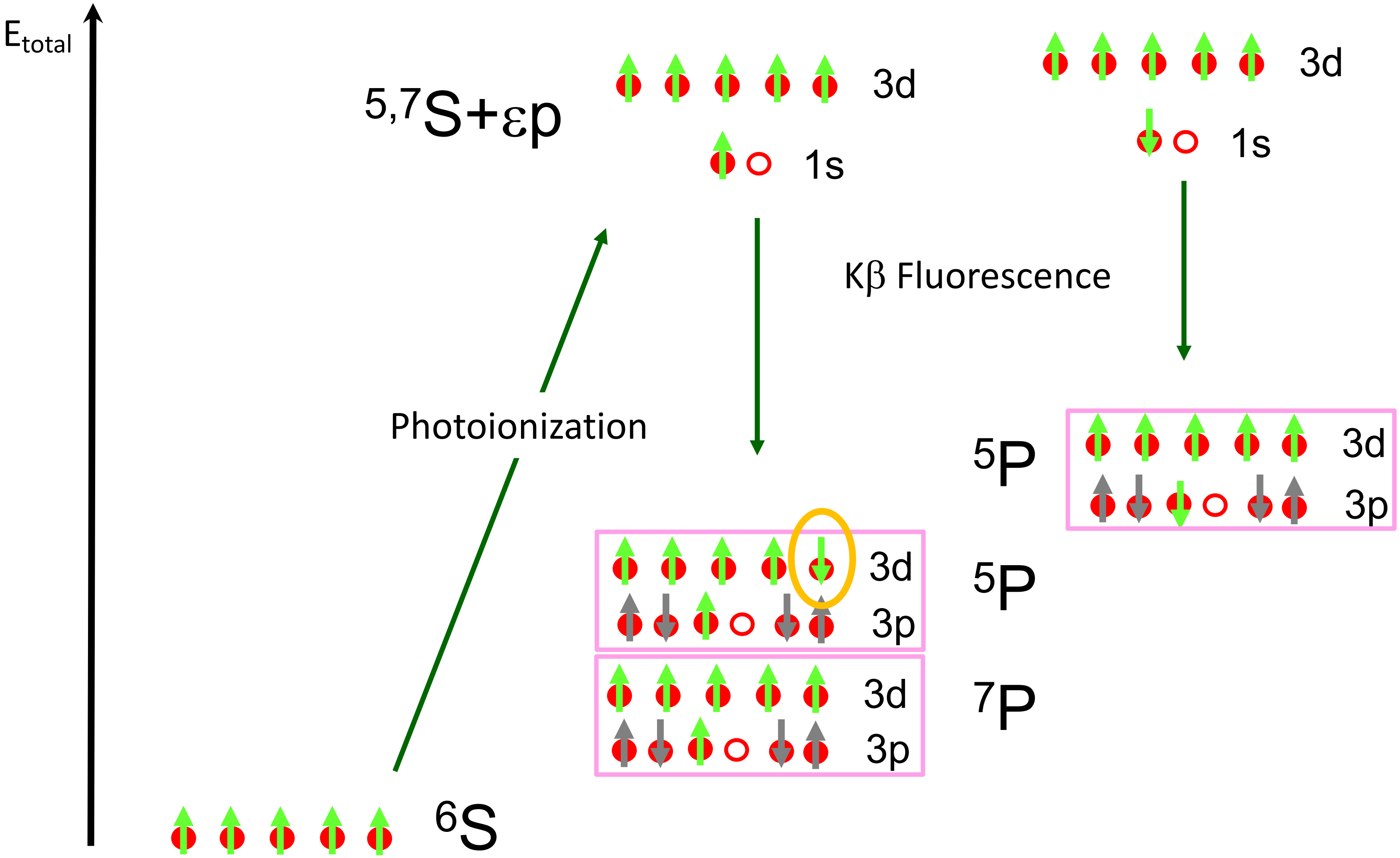

Spin flip in 3d shell induced by the strong (3p,3d) interaction. This can be referred to as "multi-electron" transition because more than one electron changes its quantum numbers. The selection rules for the total spin are maintained ($^{5,7}P$ are final states).

Spin-selectivity in the Kβ line

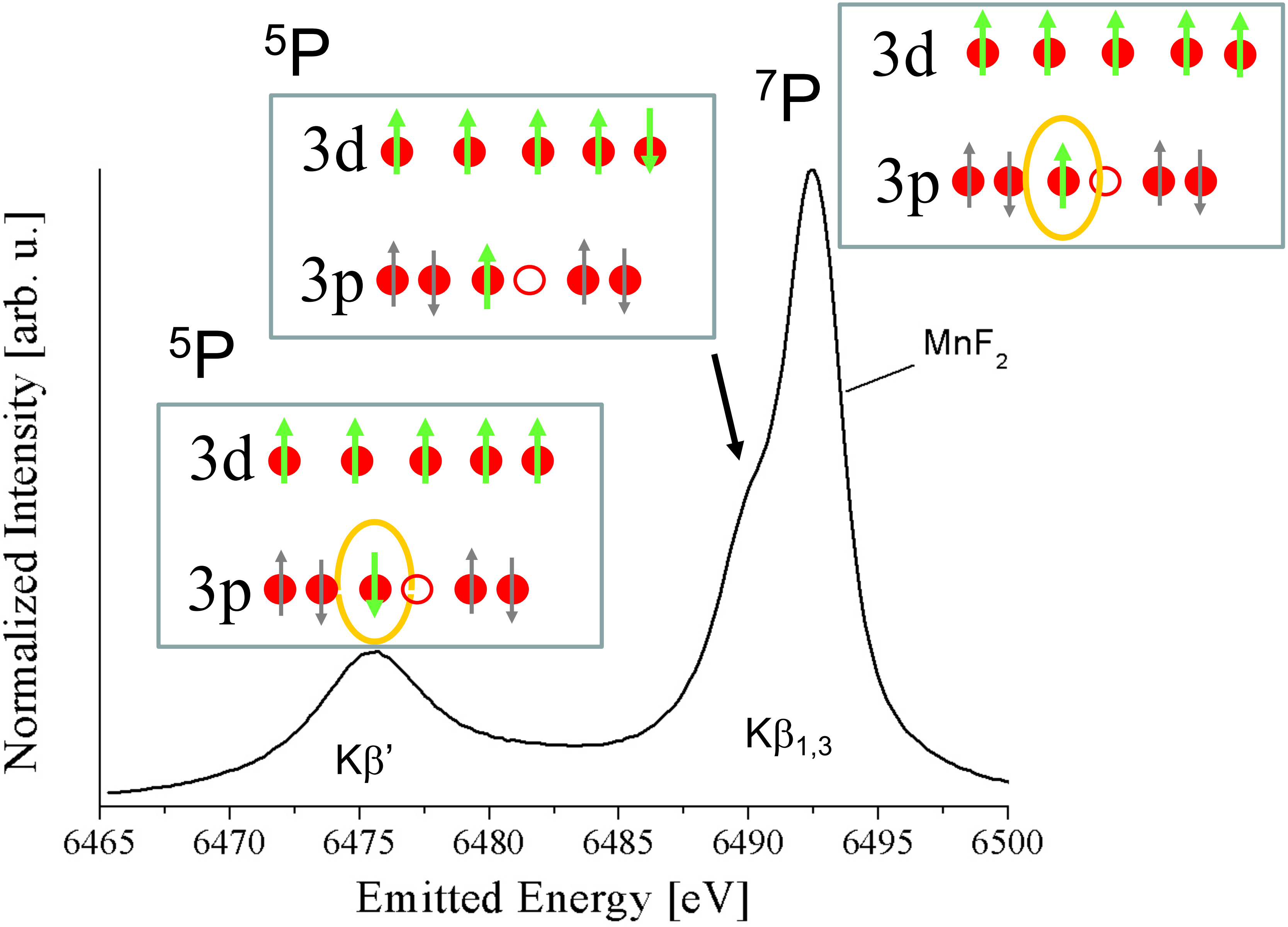

The exchange interaction

The K fluorescence lines in 3d transition metals are very sensitive to the spin in the valence shell. This holds for Kβ and Kα but the effect is 2-3 weaker for Kα (see slide with Slater integrals in lecture 12/02/2019). As the spin changes with a change of oxidation state, the lines are sensitive to the oxidation state.

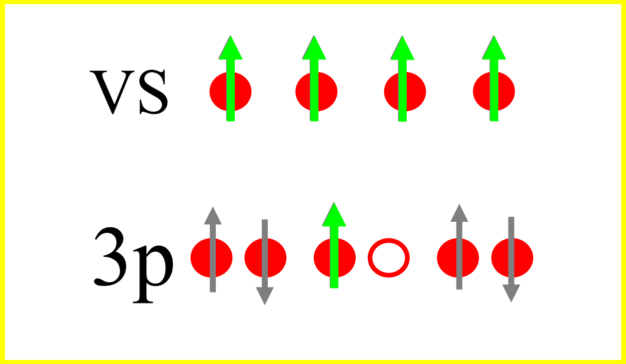

Acts only between electrons with parallel spins and lowers the total Energy

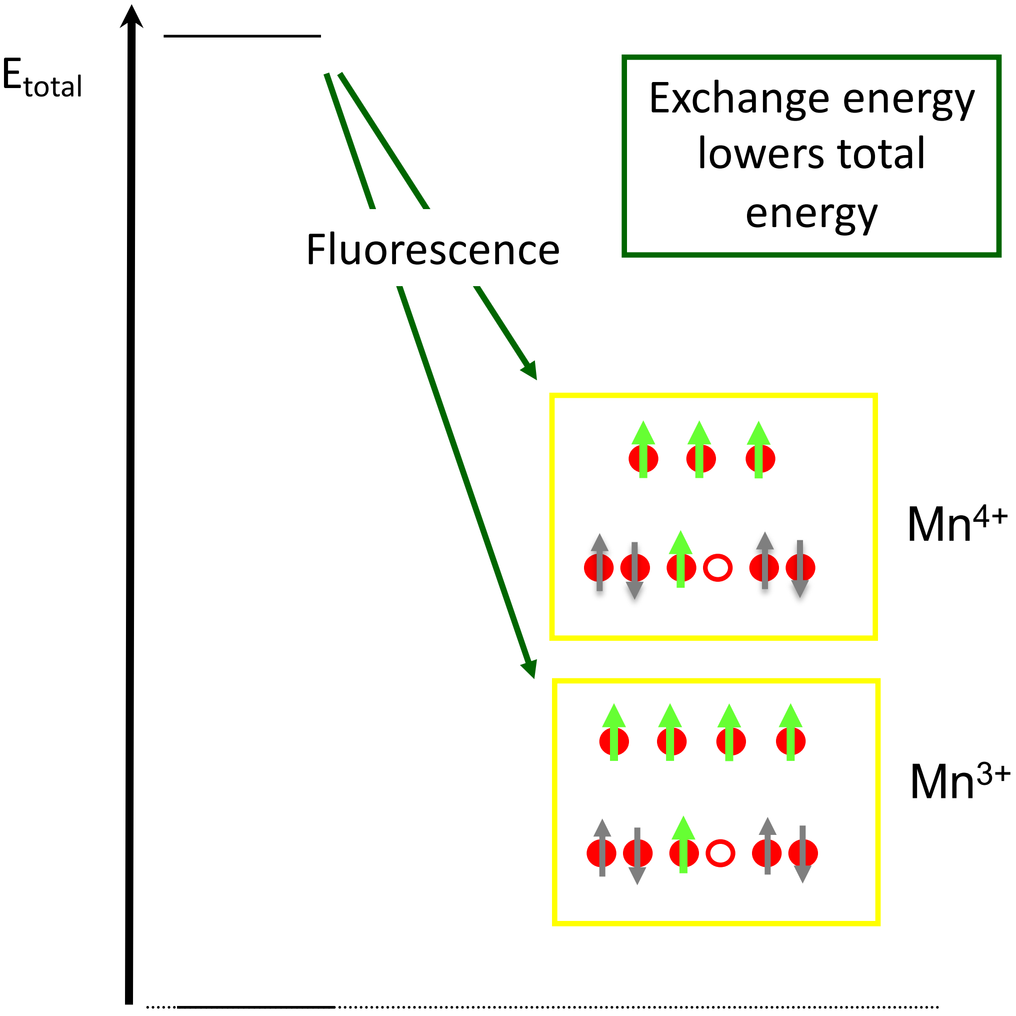

Exchange energy lowers total energy

Chemical sensitivity of Kβ Emission

Screening effect very small (unlike Sulfur – see below).
(3p,3d) interactions are dominating.

MnF_4: S=3/2

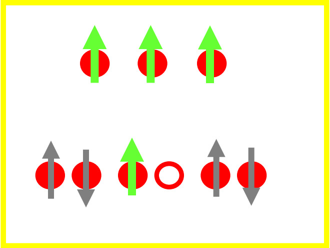

MnF_3: S=2

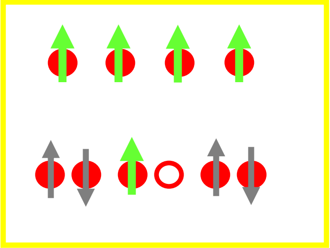

MnF_2: S=5/2

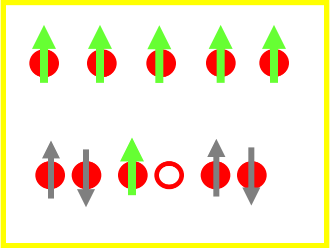

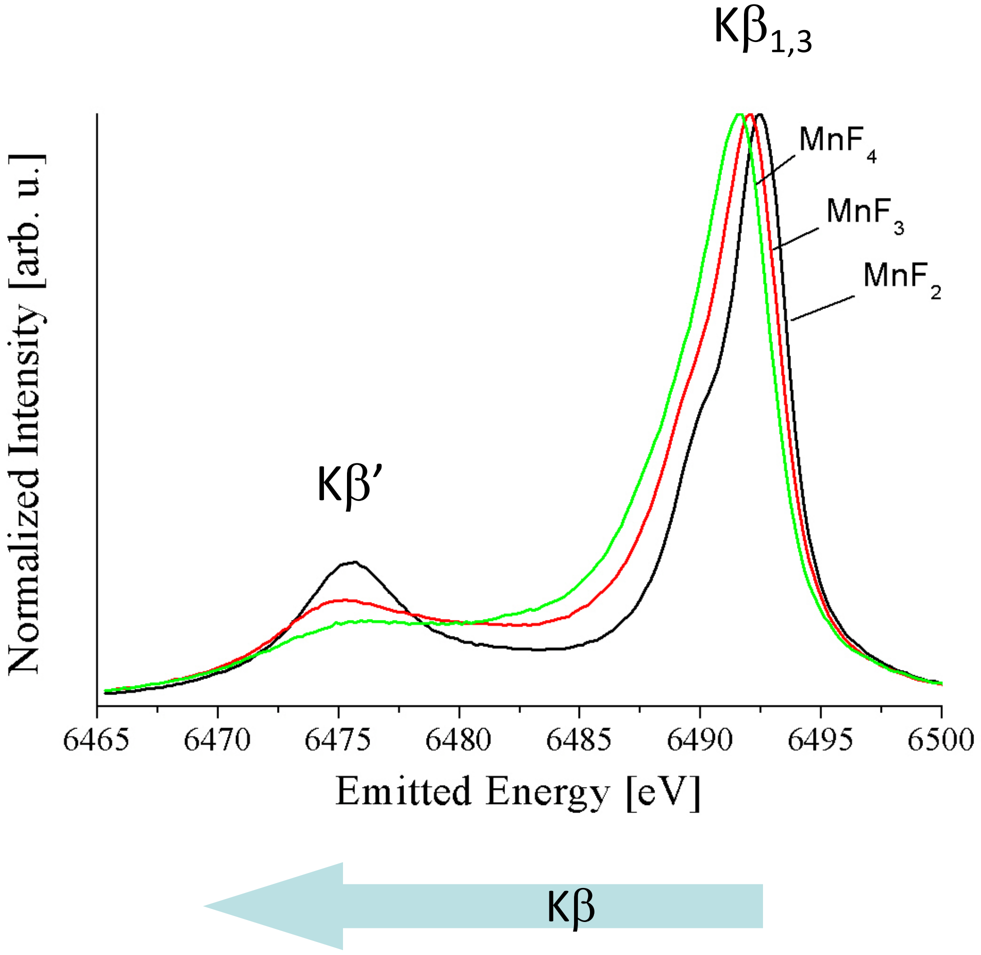

Wang et al. Phys. Rev. B 56, 4553 (1997)

Kβ XES and 3p XPS

Identical final state configuration:
$3p^5 3d^5$

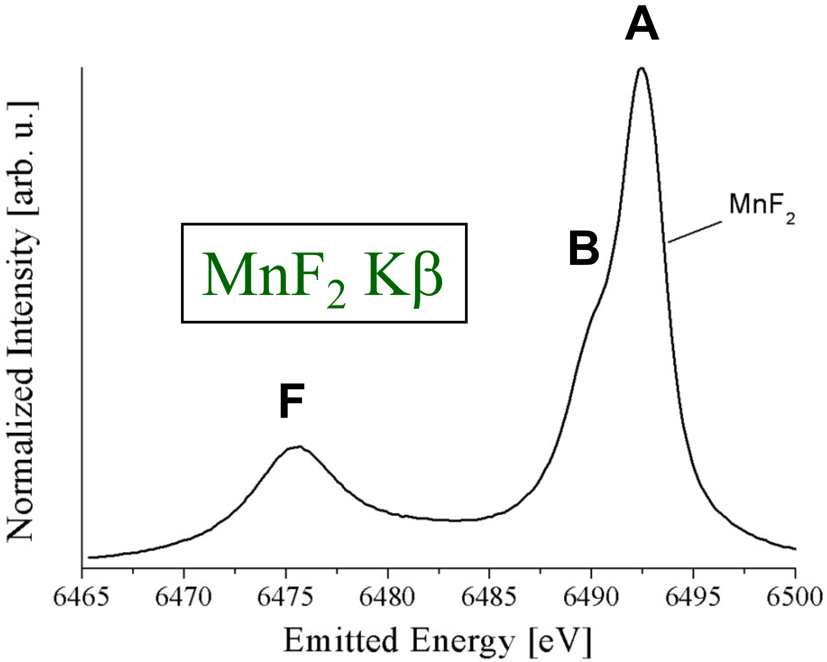

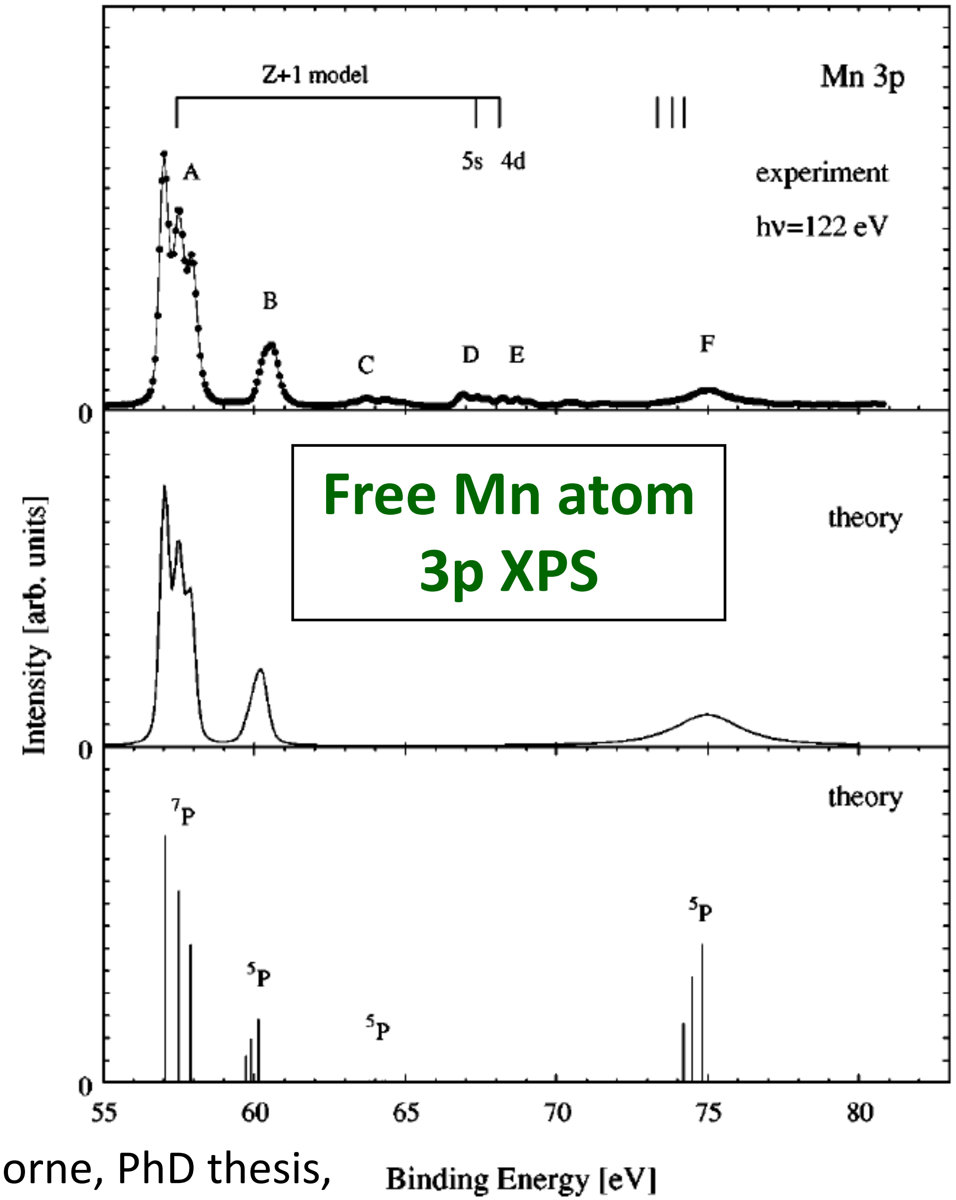

Experiments on free metal atoms confirm the interpretation in terms of intra-atomic interactions

A. von dem Borne, PhD thesis,
Hamburg university, 1997

Kβ XES and 3p XPS

Identical final state configuration:
$3p^5 3d^5$

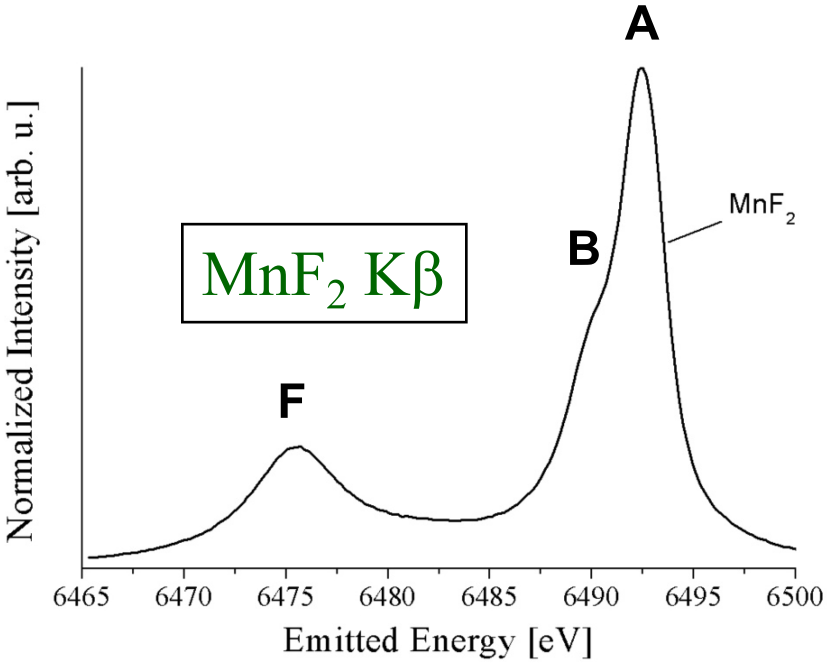

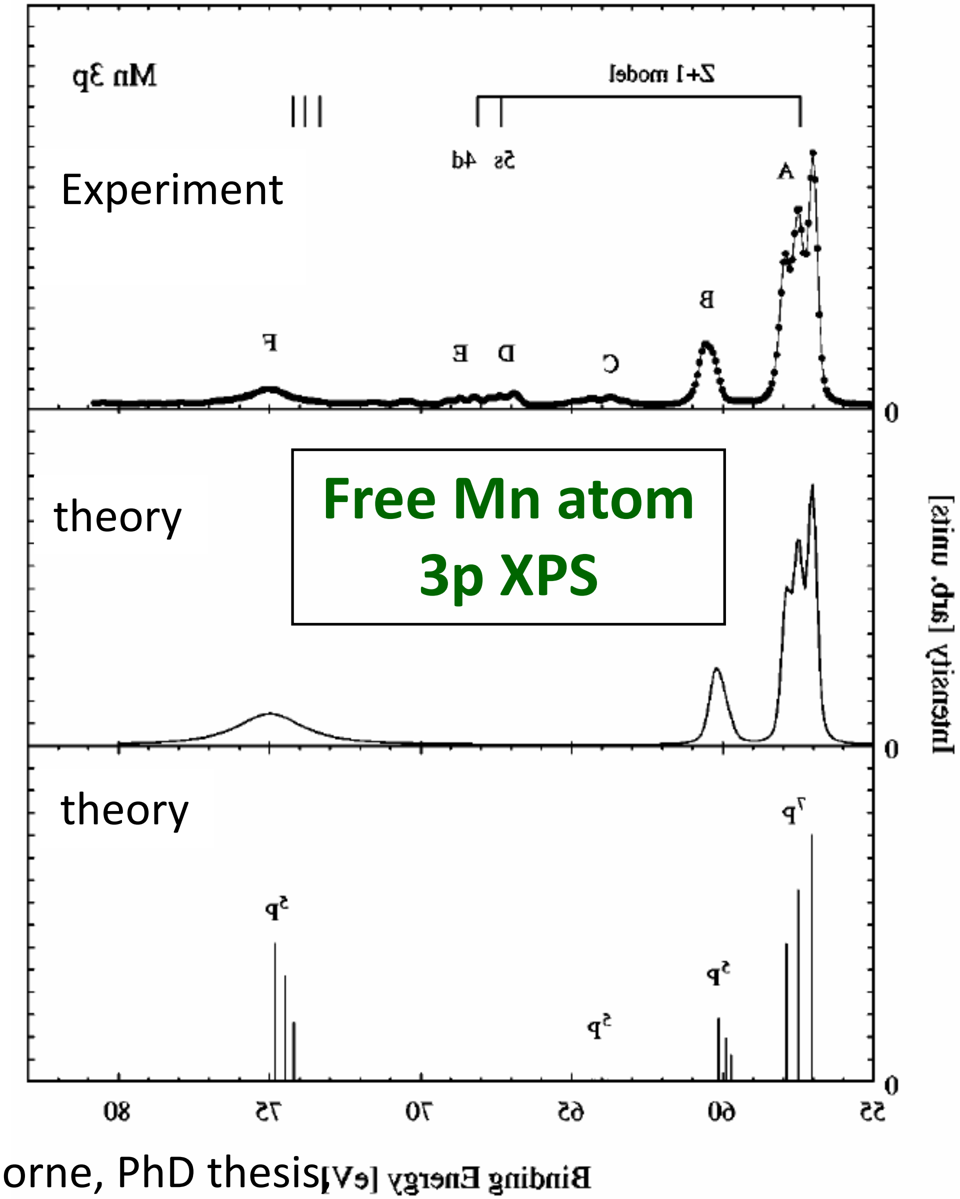

Experiments on free metal atoms confirm the interpretation in terms of intra-atomic interactions

A. von dem Borne, PhD thesis
Hamburg university, 1997

Effect of covalency on the Kβ line in 3d transition metals

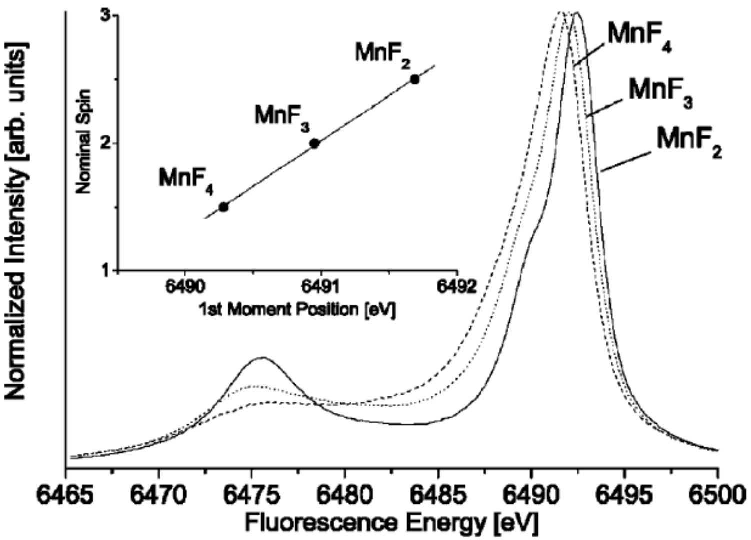

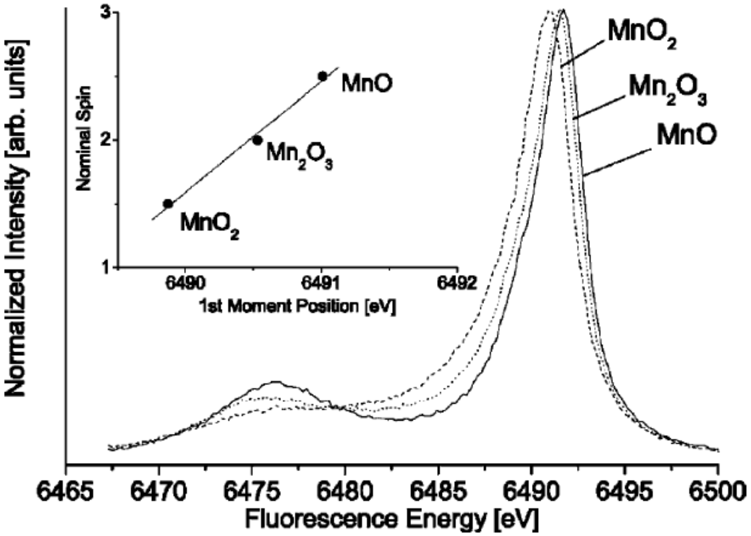

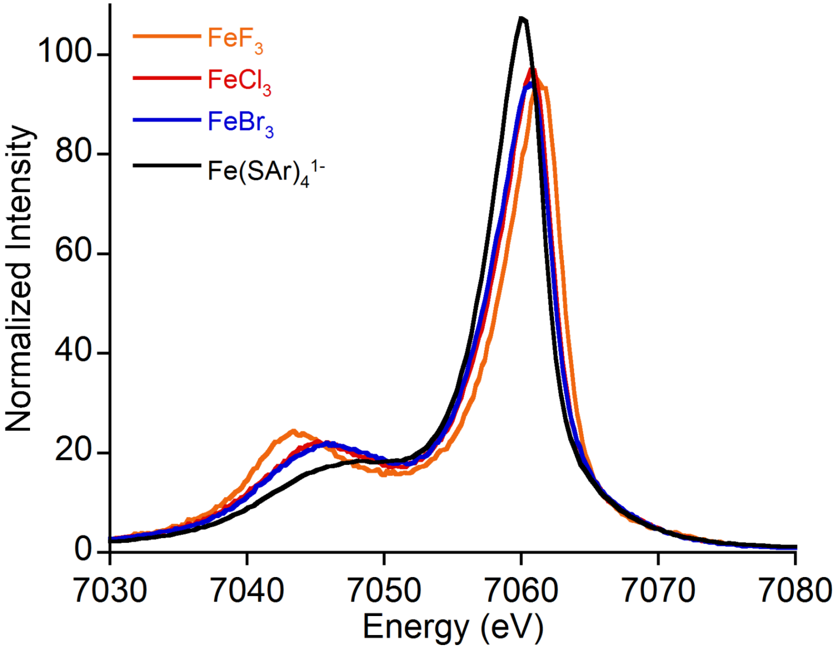

Covalency influences Kβ spectral shape.

Covalency can be considered by

- Scaling of the electron-electron interaction: Empirically or using DFT (see Pollock et al. JACS 136 (2014) 9453-9463)
- Configuration interaction calculation

Glatzel and Bergmann Cord. Chem. Rev. 249 (2005) 65-95

Kβ Emission in the Charge Transfer Model

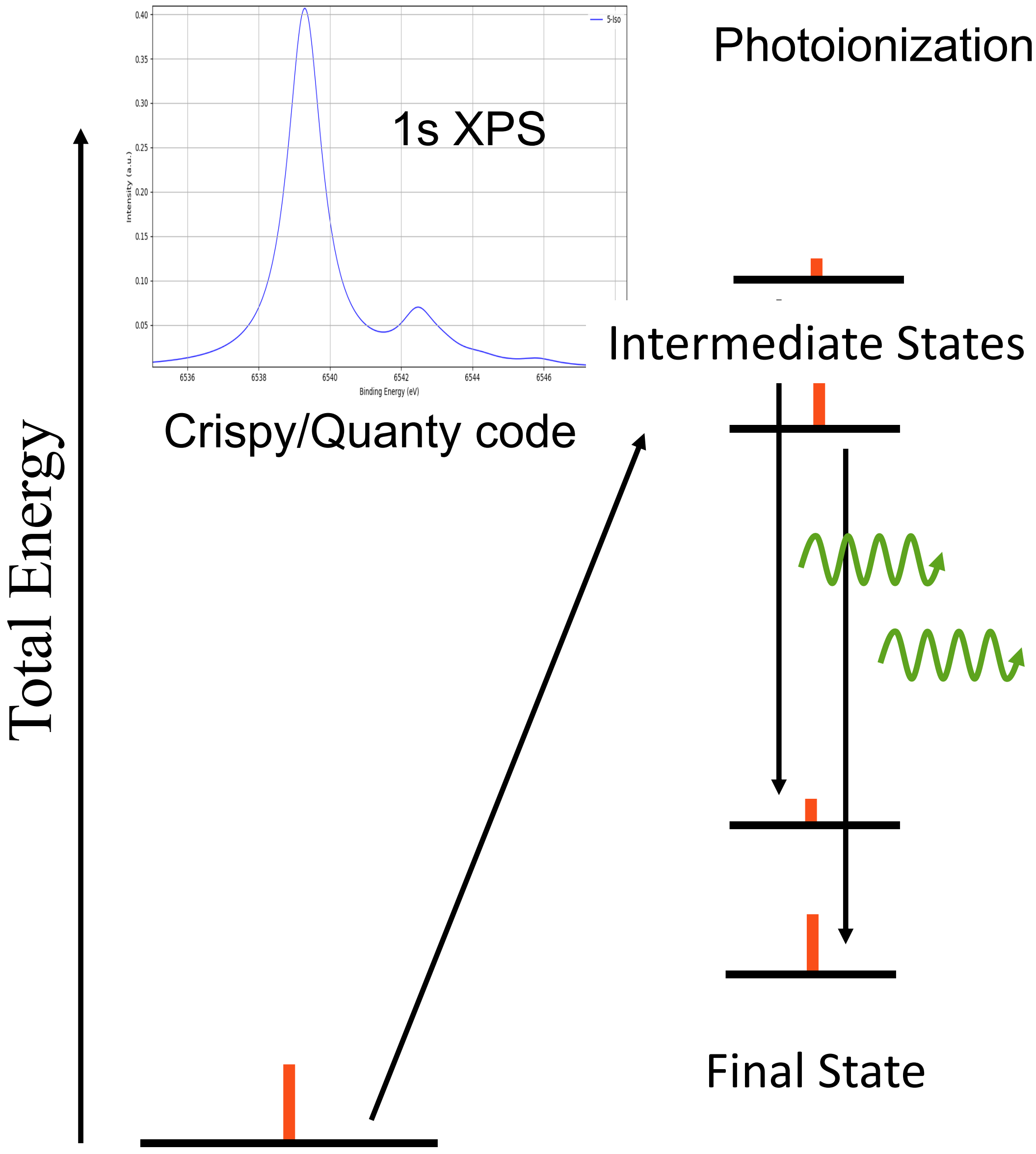

1s XPS

Crispy/Quanty code

Total Energy

Intermediate States

Final State

Ground State

Photoionization creates a range of excited states

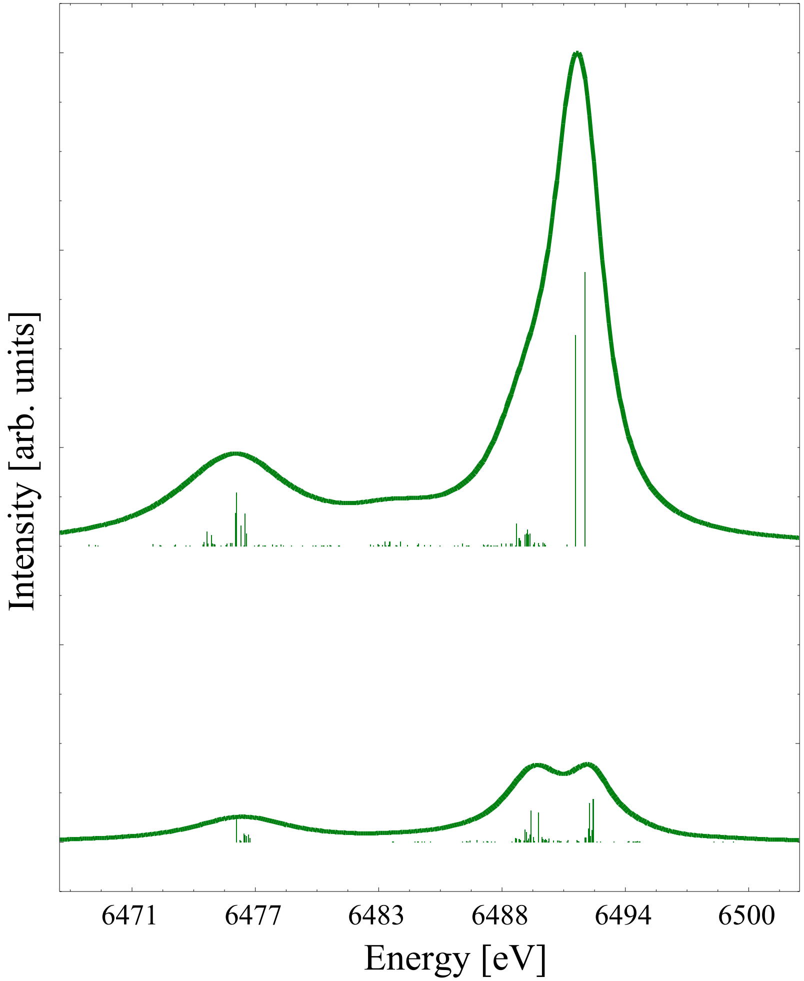

Term dependent lifetime broadening.

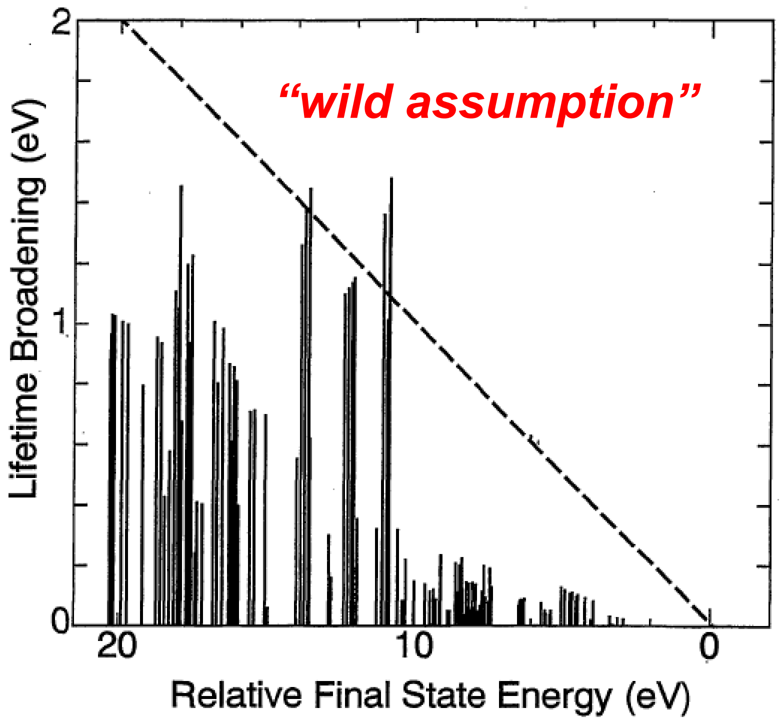

Taguchi, Uozumi, Kotani
J. Phys. Soc. Japan **66** 247 (1997)

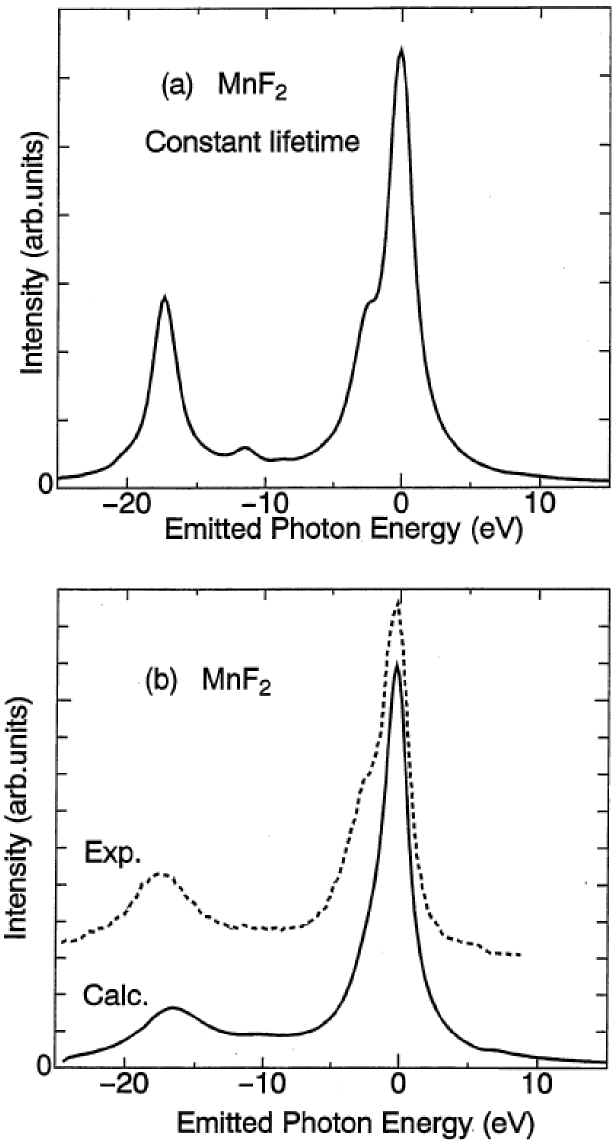

In order to analyze fine details of the K fluorescence lines in 3d TM, the final state lifetime has to be calculated

Kβ lines in Mn compounds

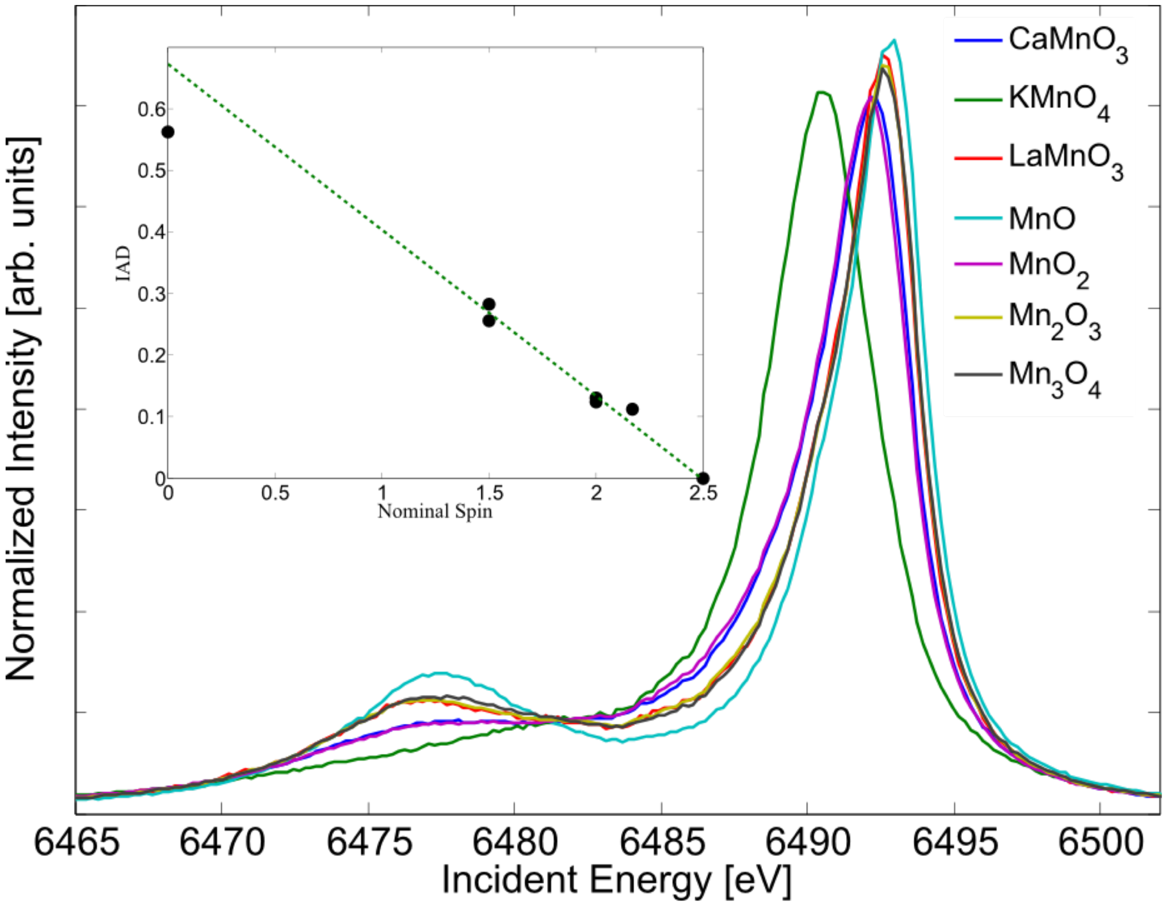

Non-resonant Kβ XES in earth science (Badro et al.), biology (Bergmann et al.), materials science (Rueff et al.), Ultra-fast spin transitions (Vanko et al.)

Mn-Mg$_k$ complexes in GaN

Magnetic anisotropy (SQUID)

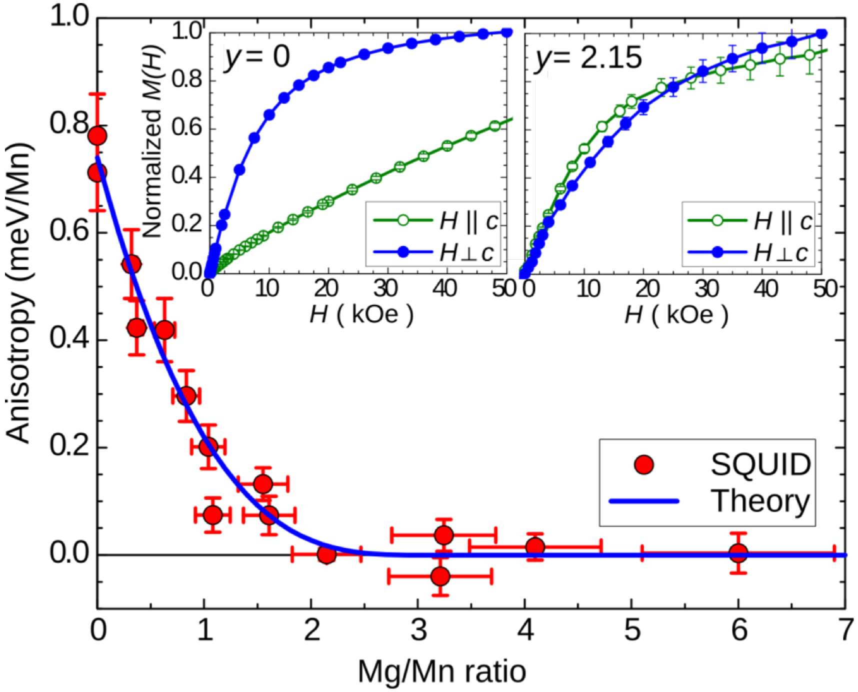

EXAFS and DFT

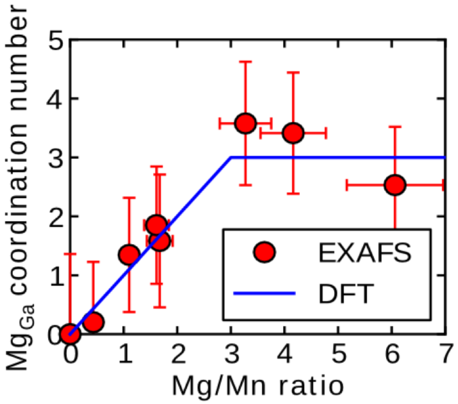

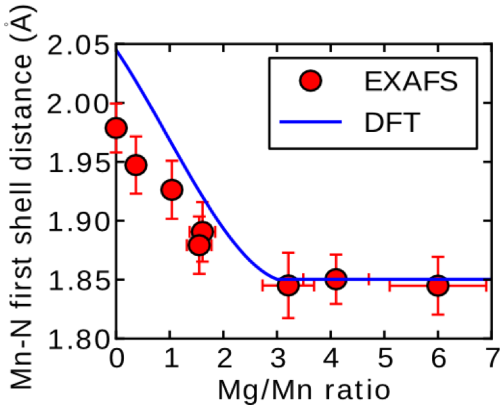

Functional impurities in wide-gap semiconductors: spin/charge control

Mn in GaN as active center for IR PL
Co-doping with Mg increases PL – why?

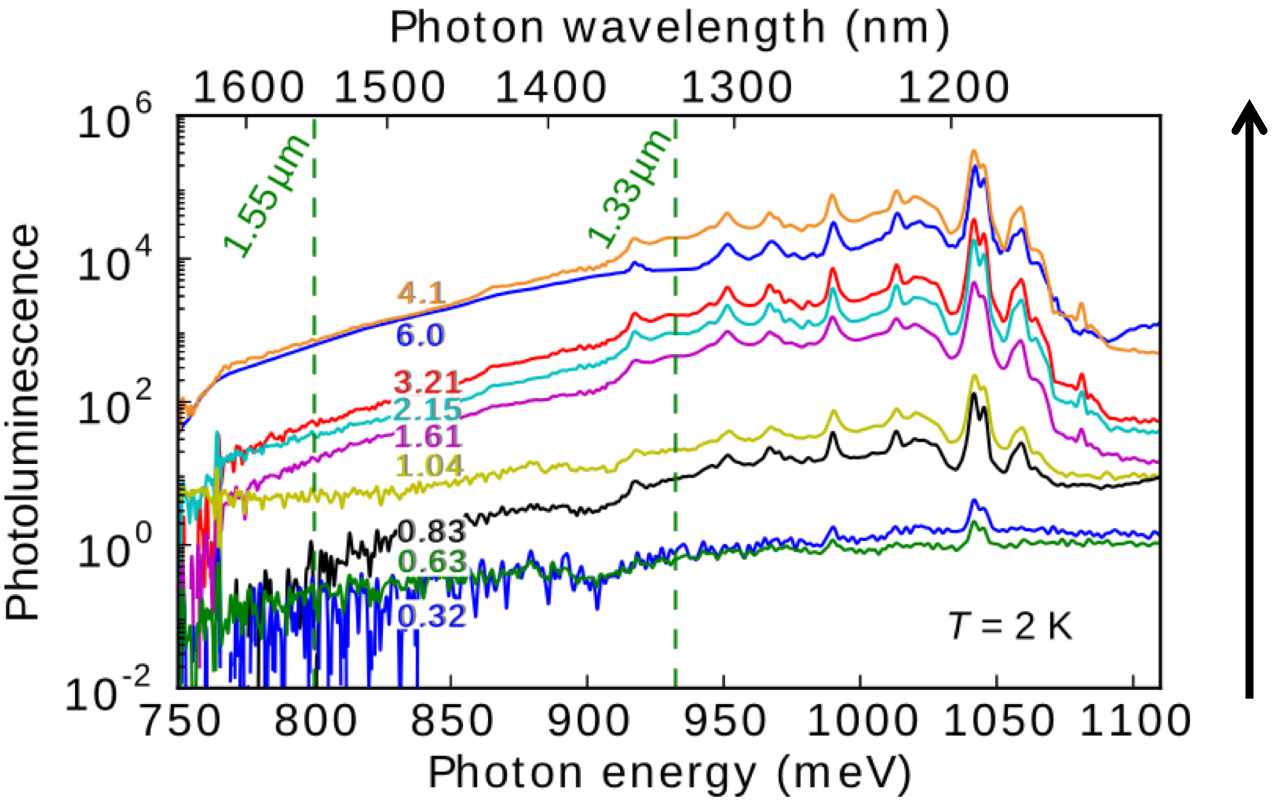

$$y = \frac{Mg}{Mn}$$

Mn-Mg pairs in GaN

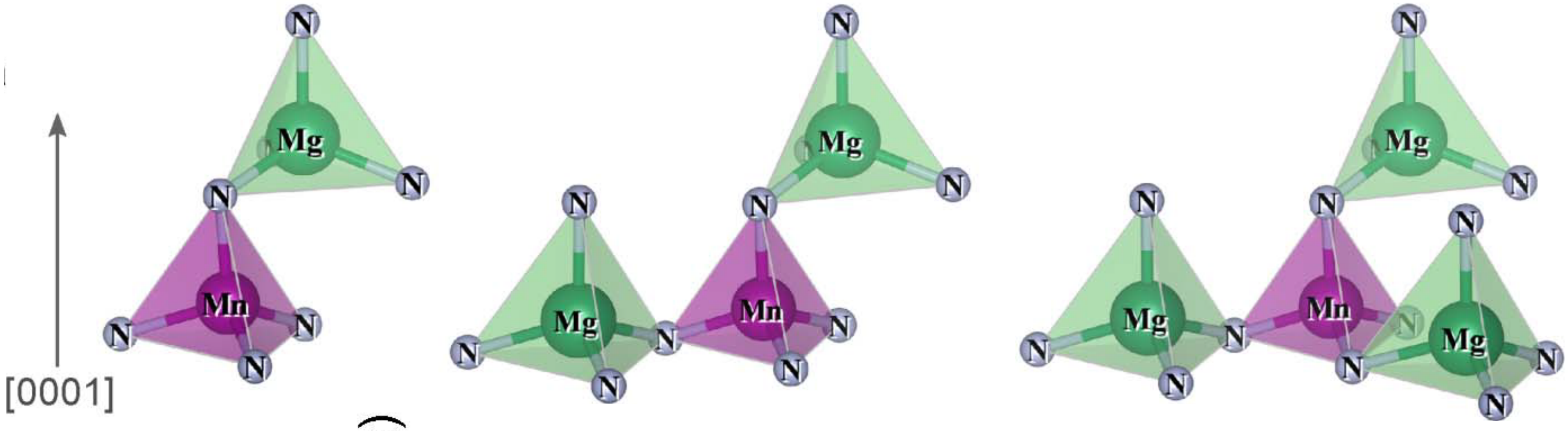

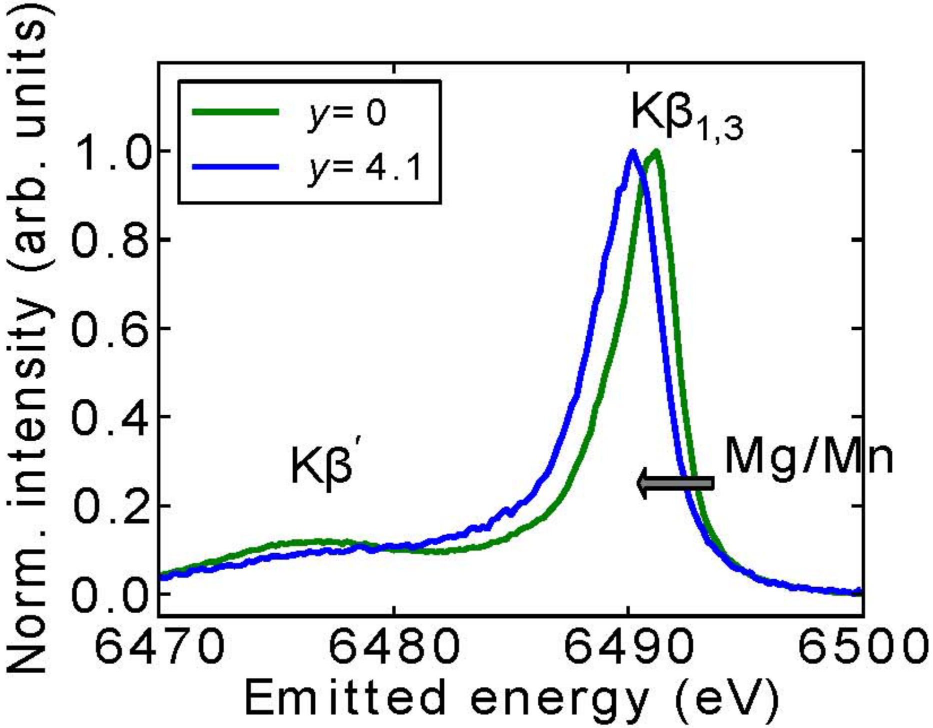

Th. Devillers, M. Rovezzi, *et al.* Scientific Reports 2 722 (2012)

Density functional theory spin densities

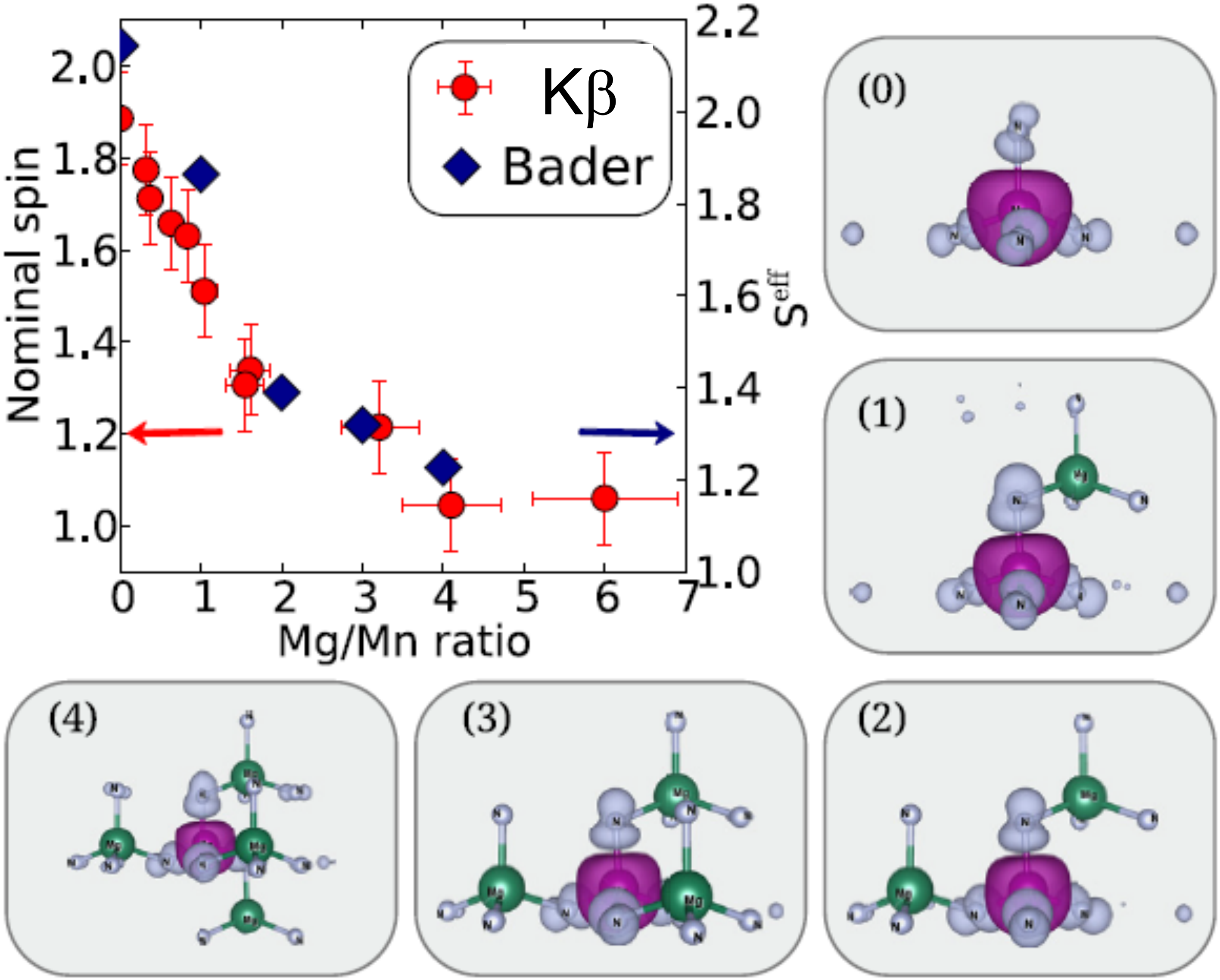

Th. Devillers, M. Rovezzi, *et al.* Scientific Reports 2 722 (2012)

If a leaf can do it, we can do it too!

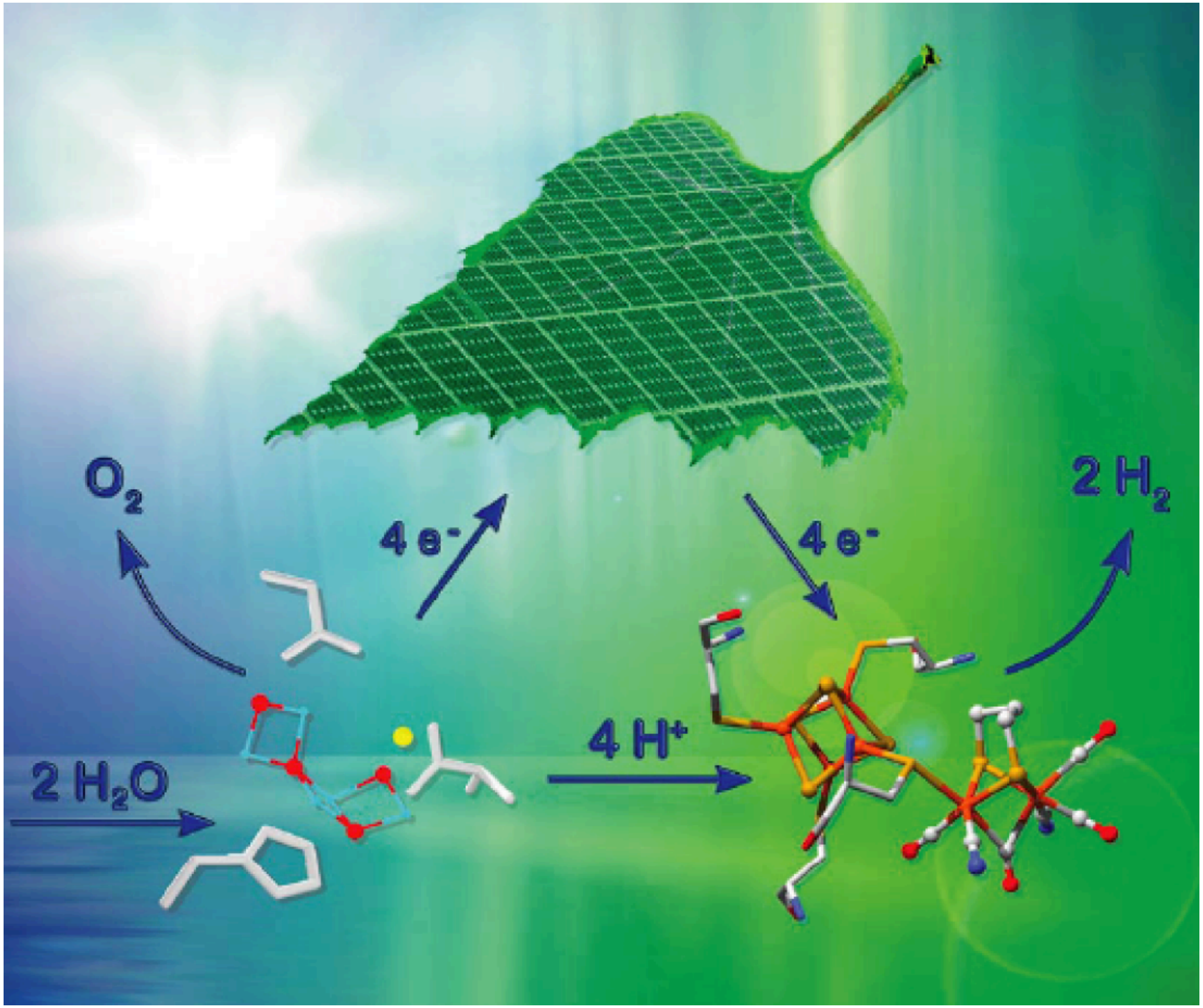

Lubitz and Messinger, Energy and Environmental Science, 2008

Kβ as a diagnostic tool to support XRD

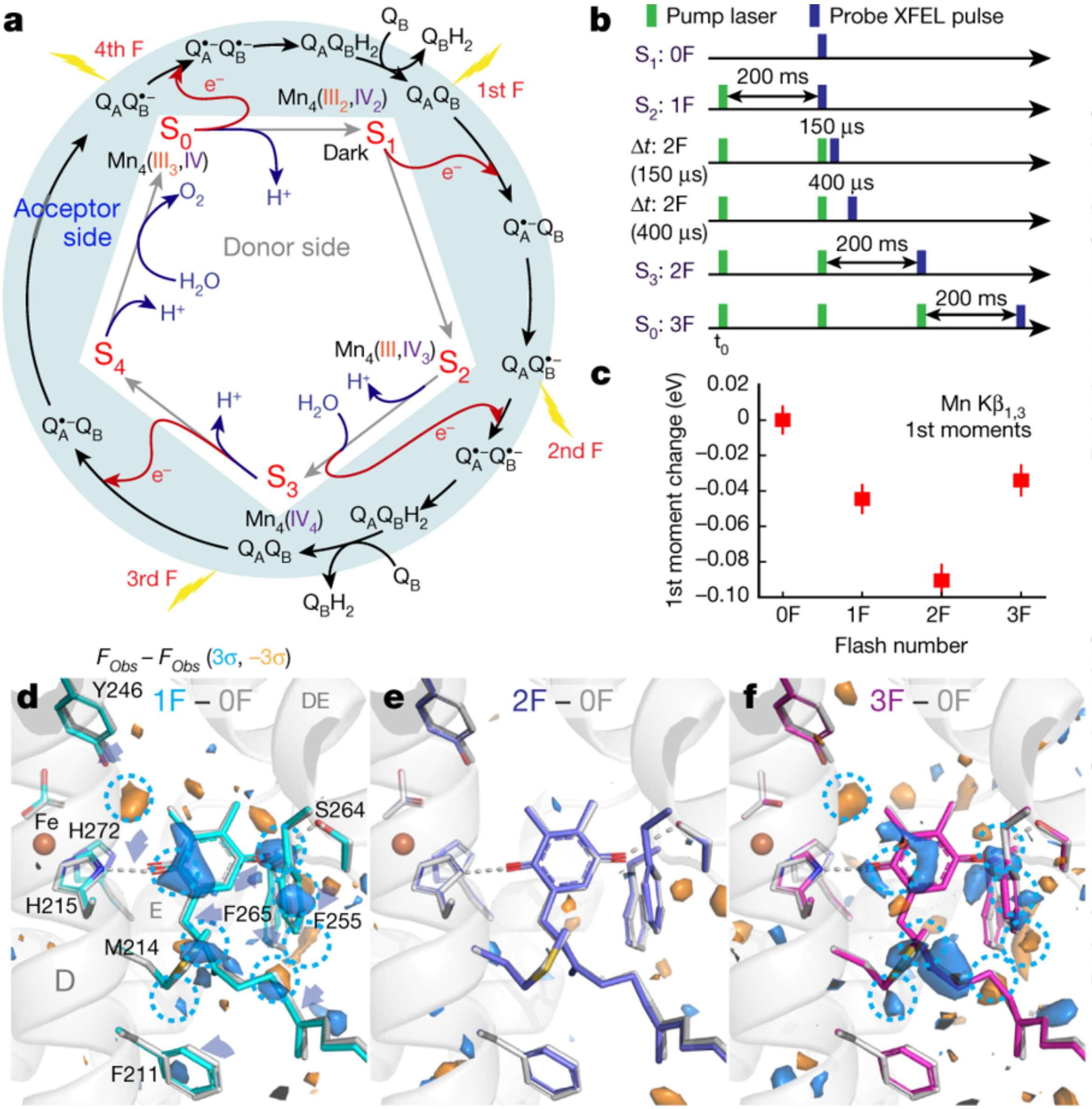

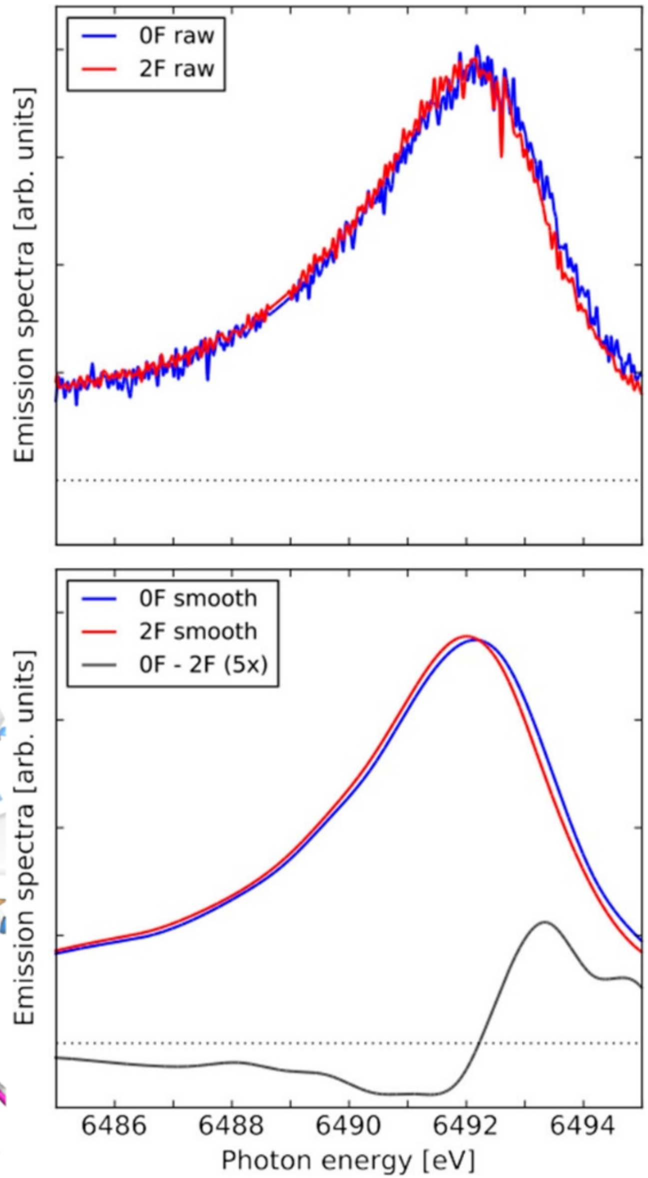

Kern et al. *Nature* **563** 421–425 (2018)

XAS and XES in a layered Mn perovskite

The $La_{1-x}Sr_{1+x}MnO_4$ series: doping dependence

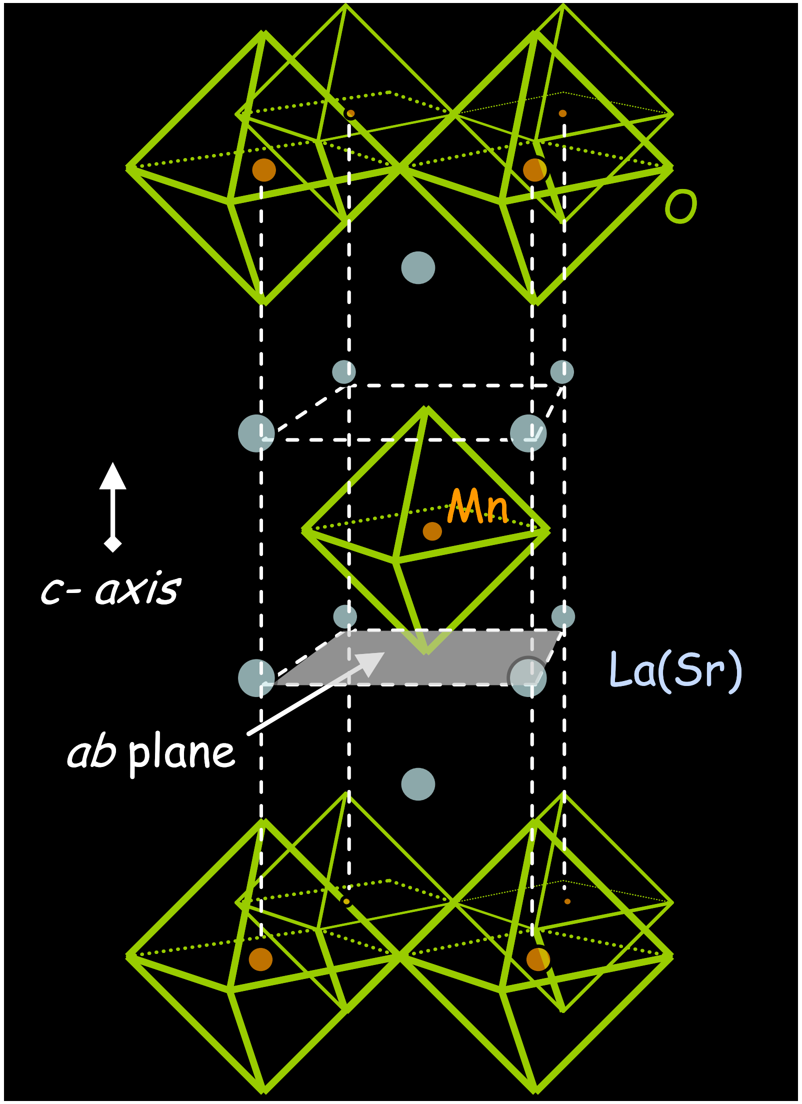

XAS and XES in a layered Mn perovskite

The $La_{1-x}Sr_{1+x}MnO_4$ series: doping dependence

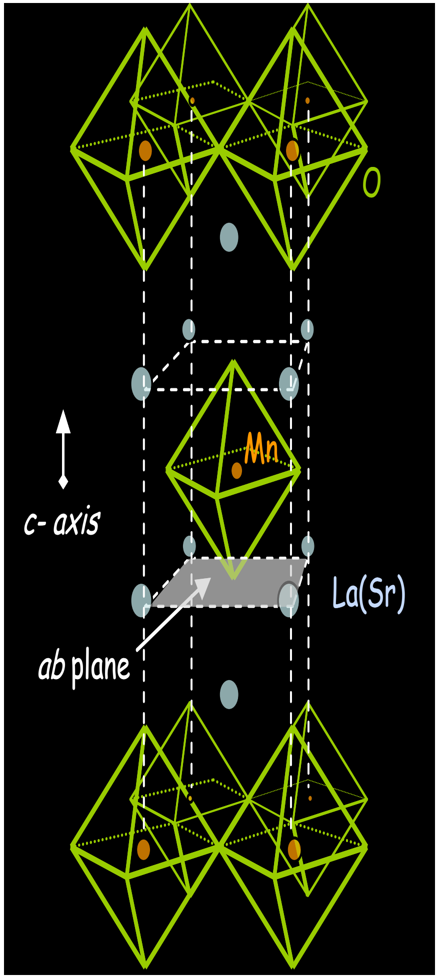

MnO_6 local **anisotropy** is large and inversely proportional to hole content

	N	r (Mn-O) (Å)	
$LaSrMnO_4$	4	1.90(1)	x=0
	2	2.27(3)	
$La_{0.7}Sr_{1.3}MnO_4$	4	1.92(1)	x=0.3
	2	2.05(2)	
$La_{0.5}Sr_{1.5}MnO_4$	4	1.92(1)	x=0.5
	2	1.98(1)	

J. Herrero-Martín et al, Phys. Rev. B **72**, 085106 (2005)

XAS and XES in a layered Mn perovskite

The $La_{1-x}Sr_{1+x}MnO_4$ series: doping dependence

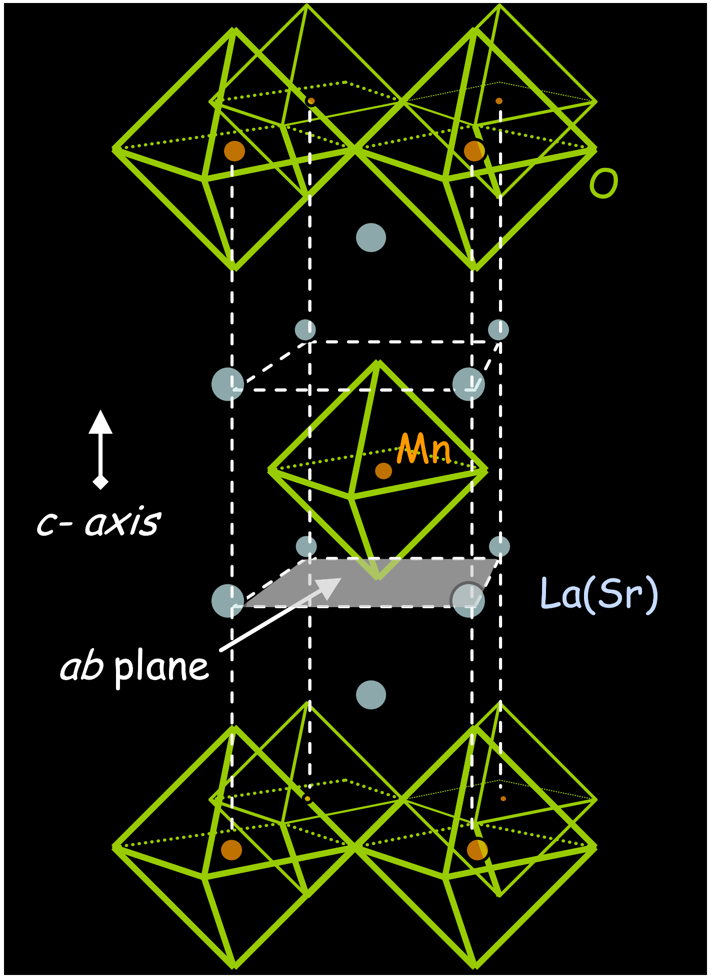

MnO_6 local **anisotropy** is large and inversely proportional to hole content

	N	r (Mn-O) (Å)	
$LaSrMnO_4$	4	1.90(1)	x=0
	2	2.27(3)	
$La_{0.7}Sr_{1.3}MnO_4$	4	1.92(1)	x=0.3
	2	2.05(2)	
$La_{0.5}Sr_{1.5}MnO_4$	4	$\boxed{1.92(1)}$	x=0.5
	2	$\boxed{1.98(1)}$	

J. Herrero-Martín et al, Phys. Rev. B **72**, 085106 (2005)

XAS and XES in a layered Mn perovskite

The La$_{1-x}$Sr$_{1+x}$MnO$_4$ series: doping dependence in powders

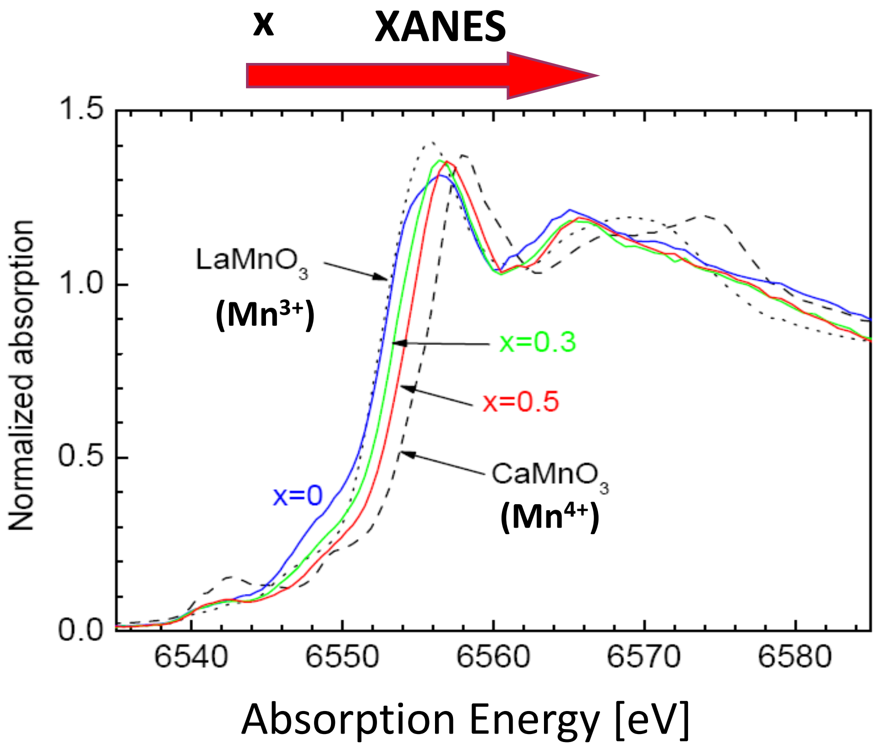

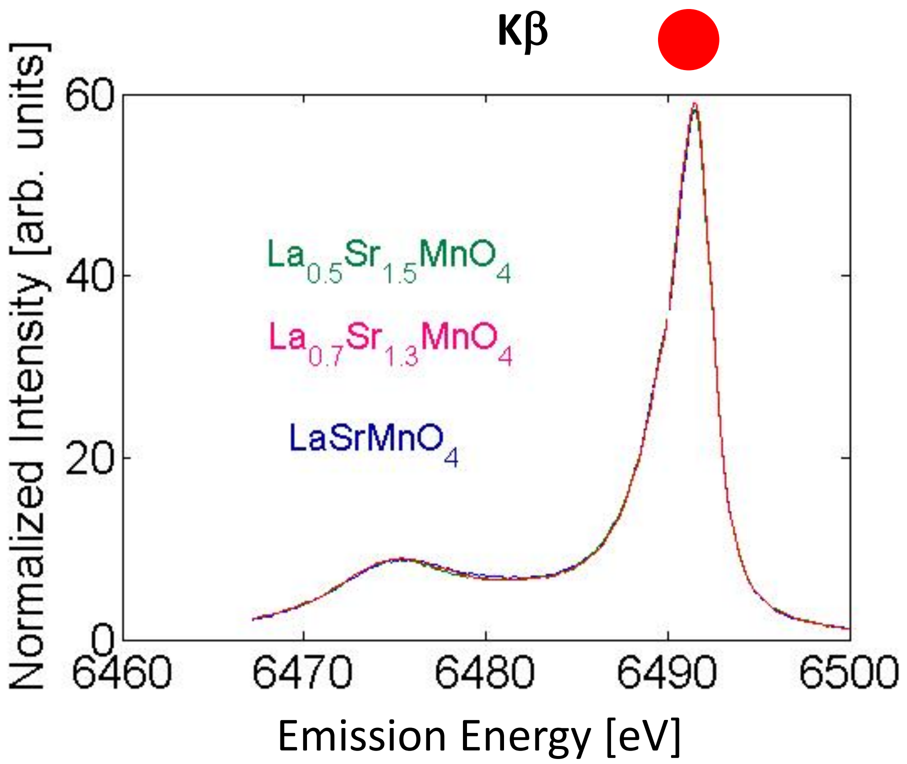

Replace La^{3+} by Sr^{2+} ⟶ Formally: Mn^{3+} → Mn$^{3.5+}$

XANES changes, Kβ invariant.

XANES shift due to structural changes! Angle-integrated electron density unchanged.

Linear Dichroism in XES

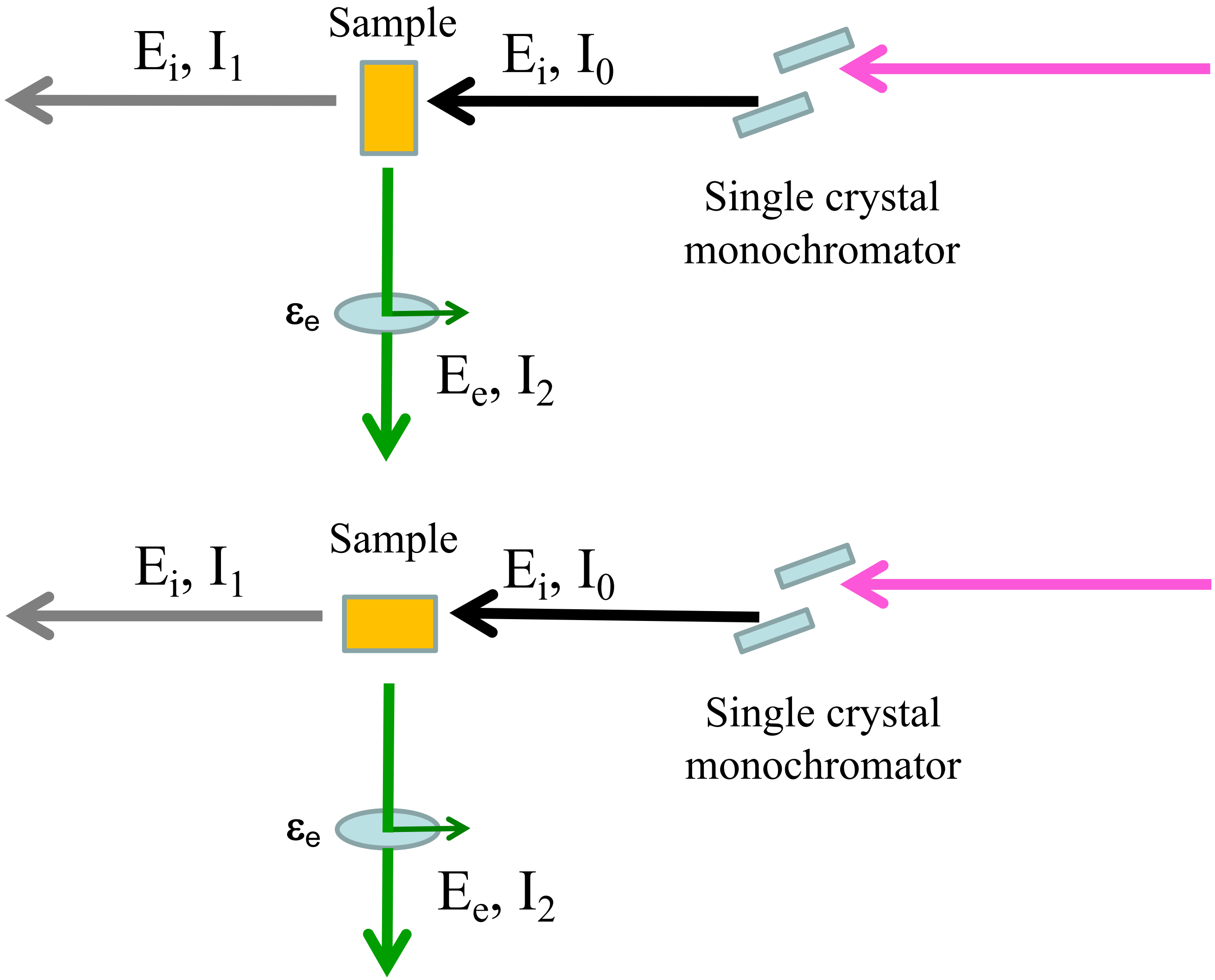

Even without polarization analysis in the emission a dichroism can be observed because of the transversal character of electro-magnetic radiation (one component is always missing).

Kβ Linear Dichroism in D_{4h} symmetry

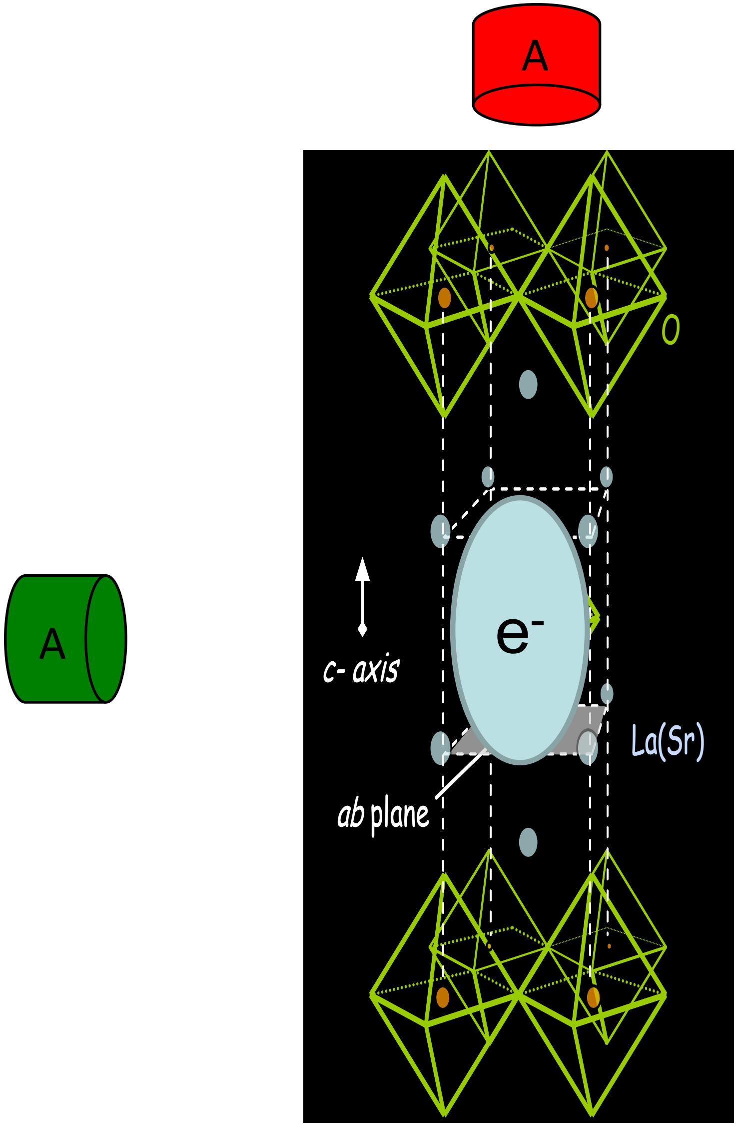

Single Crystal

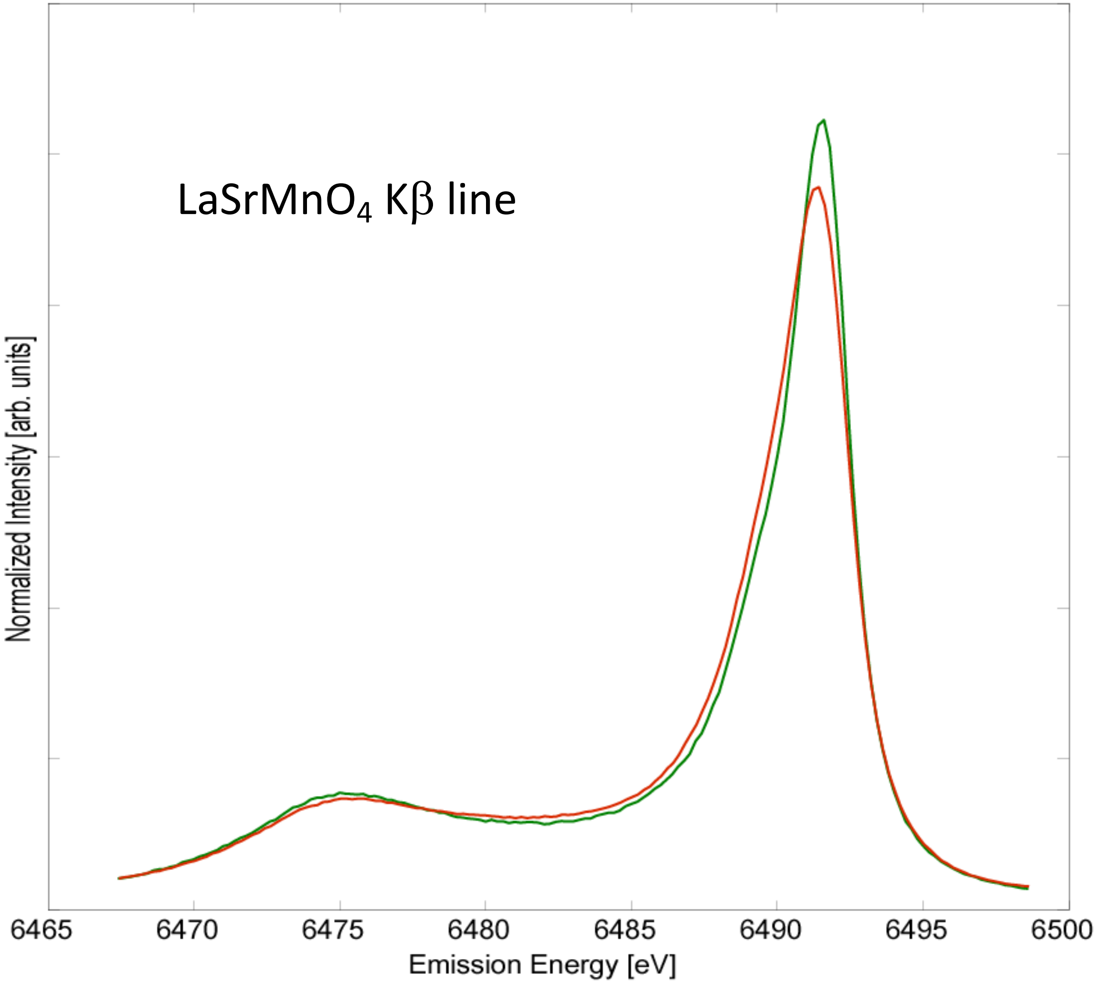

Kβ LD sensitive to anisotropic valence electron distribution

Linear Dichroism in $La_{1-x}Sr_{1+x}MnO4$

Anisotropic distribution of spin density

Physical Review B (2010) **82:** 075112

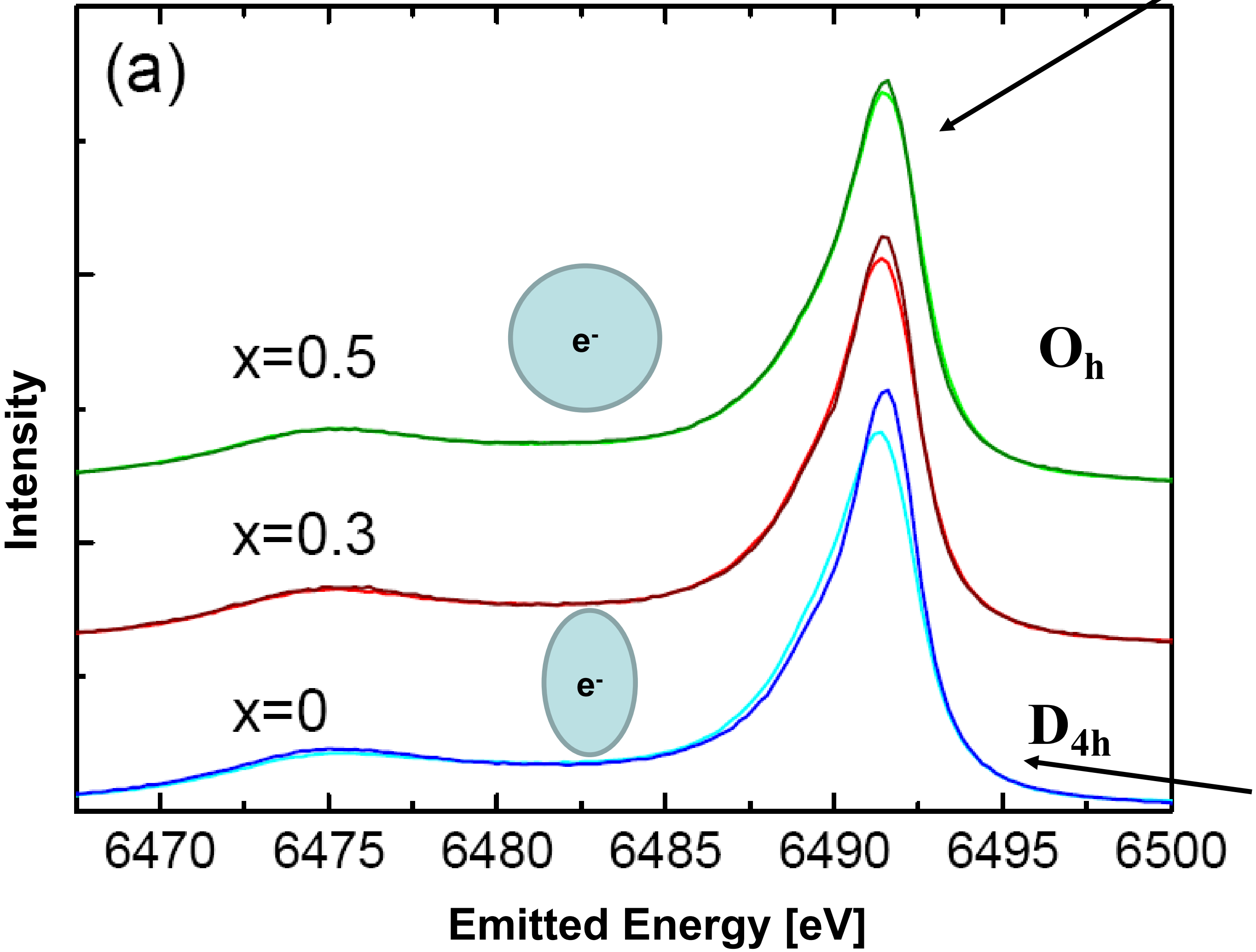

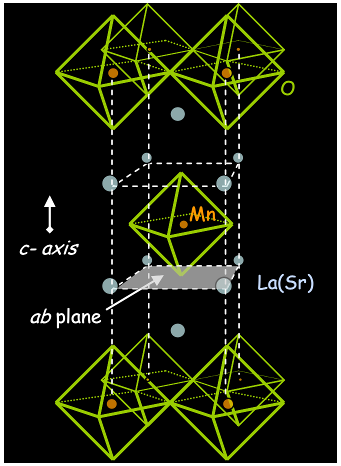

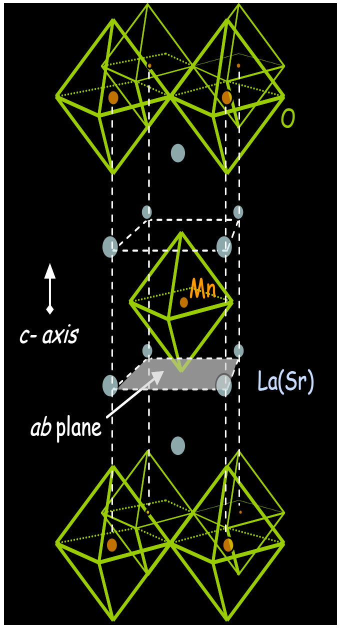

Valence-to-core (vtc or v2c) emission lines

The K fluorescence lines in 3d transition metals

Valence to core (v2c)

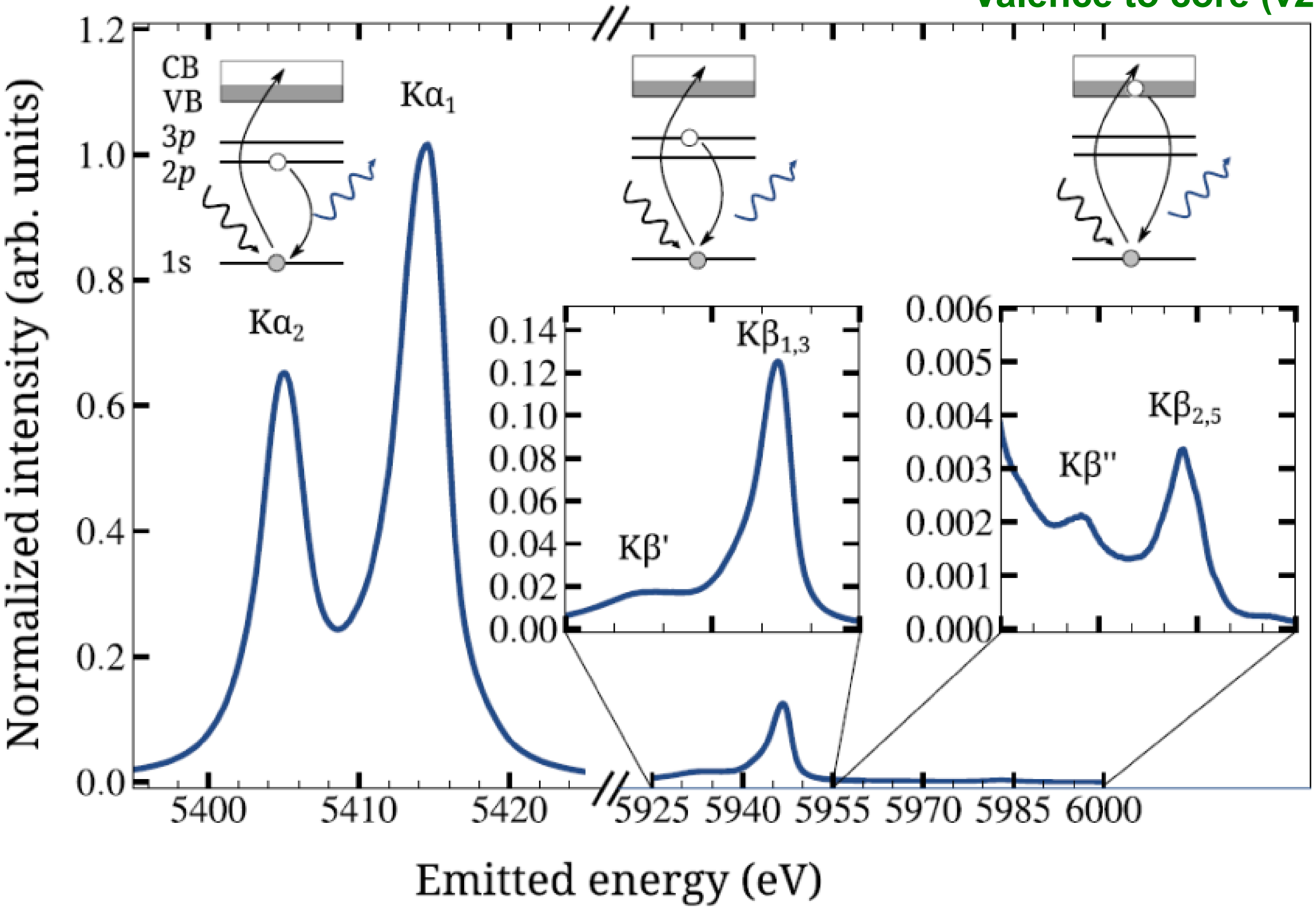

XES and XAS: Complementary Techniques

Mn(V)N

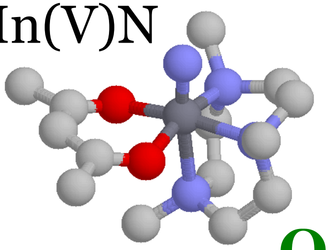

Fermi Energy

Occupied states

Unoccupied states

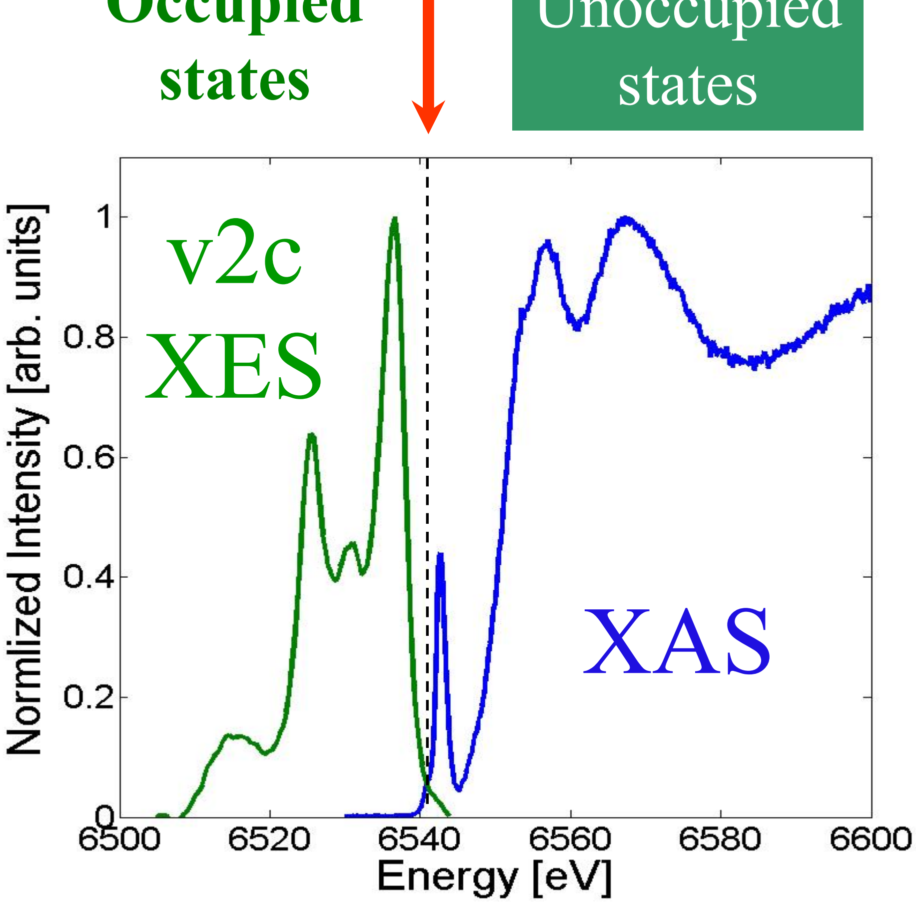

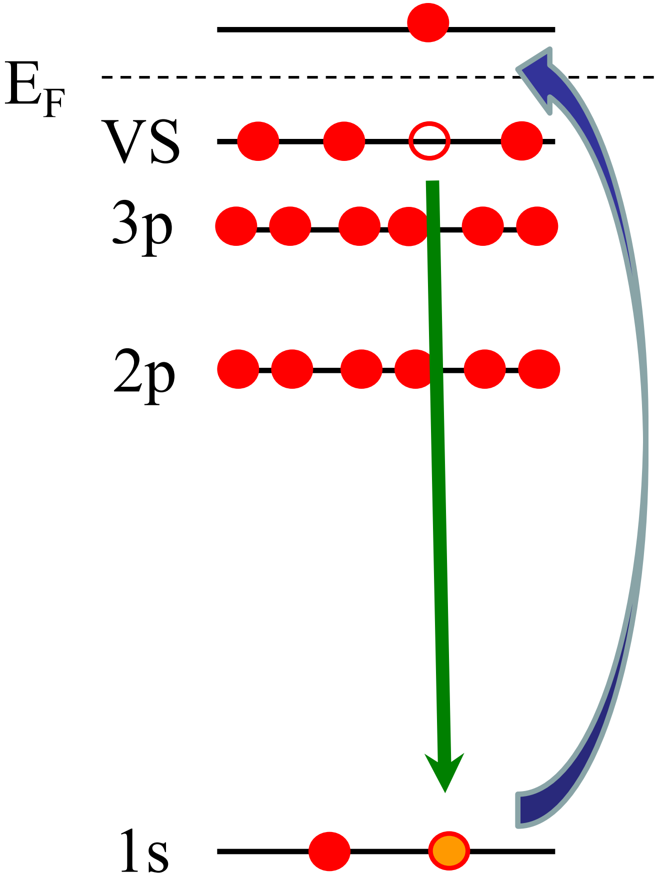

Orbital mixing – Molecular orbitals

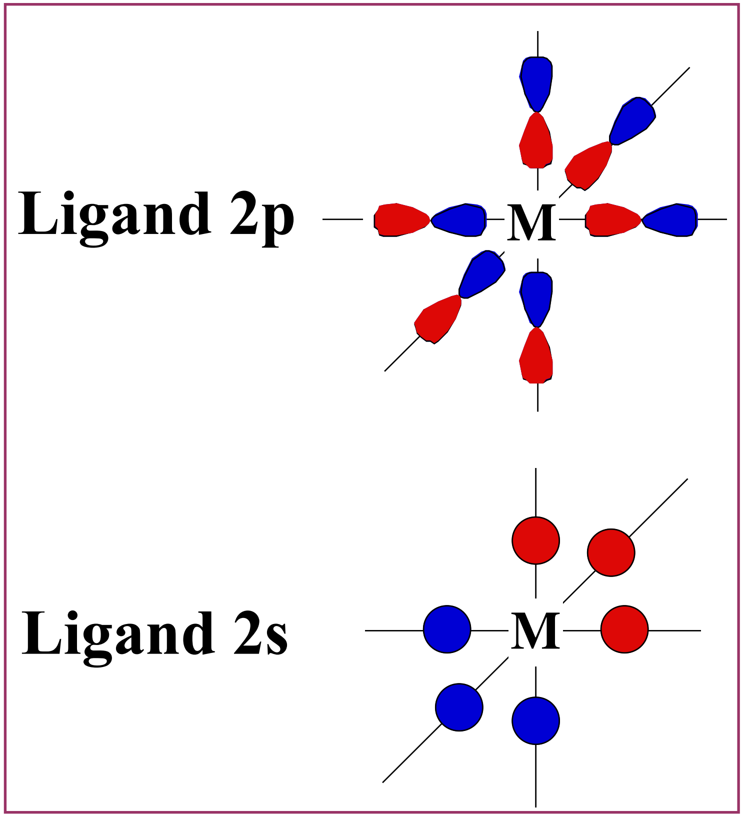

t_{1u} symmetry with respect to metal center

The electronic states in matter have the symmetry of the system.

Within a one-electron picture, this applies to the valence orbitals.

Using a “linear combination of atomic orbitals” approach, we can picture the valence orbitals as sums of atomic orbitals.

NOTE: Any point group symmetry (including SO(3) for atomic orbitals is relative to a point, i.e. a center.

An example, s-orbitals on ligands may have p-like symmetry when choosing the metal as center

Molecular orbitals of a 3d TM complex in Oh

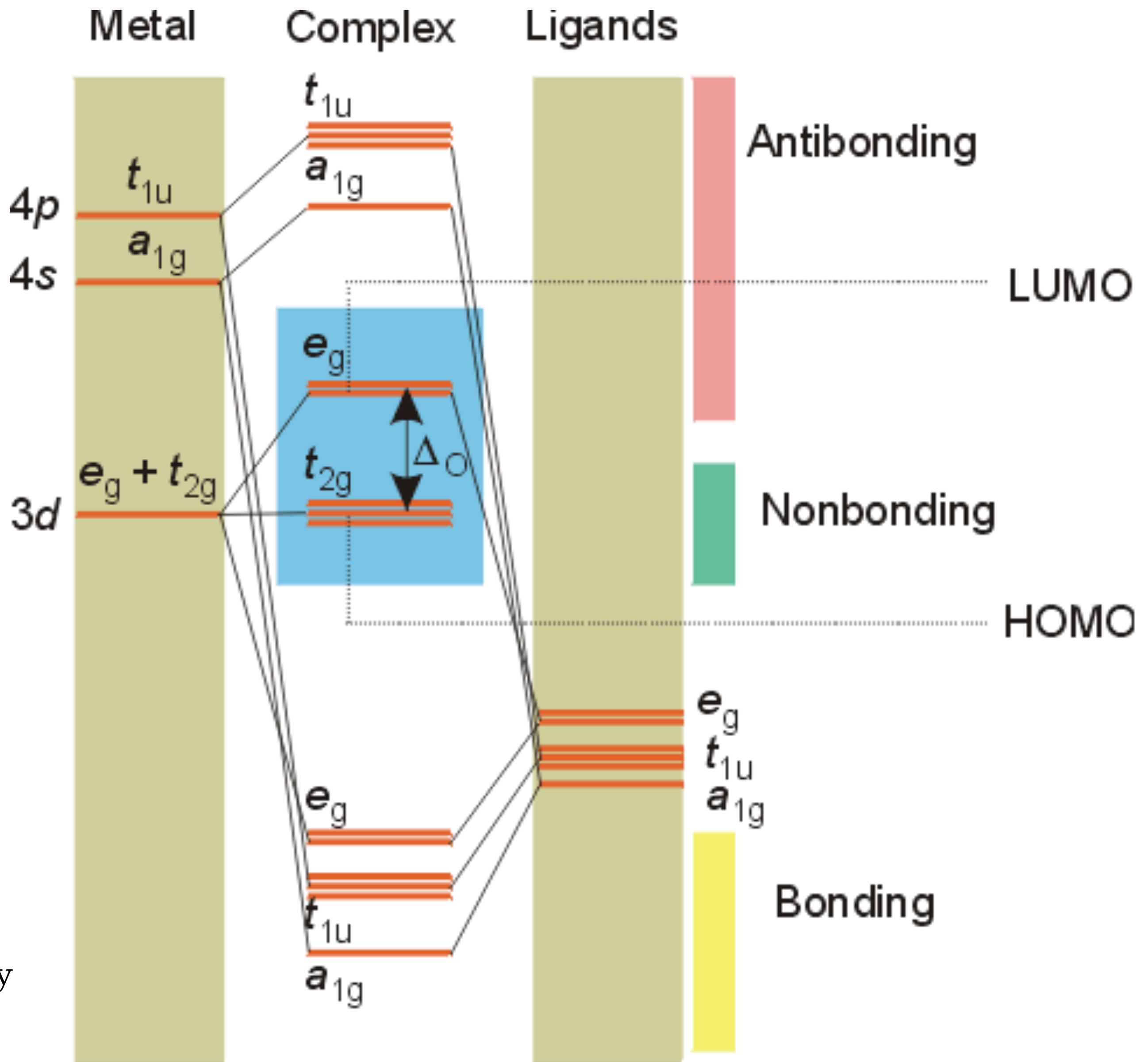

A 1s vacancy will be filled by electrons in the t_{1u} bonding orbitals.

Fine structure of valence-to-core emission lines

Mainly sensitive to orbitals that are centered on ligands.

Transitions from:

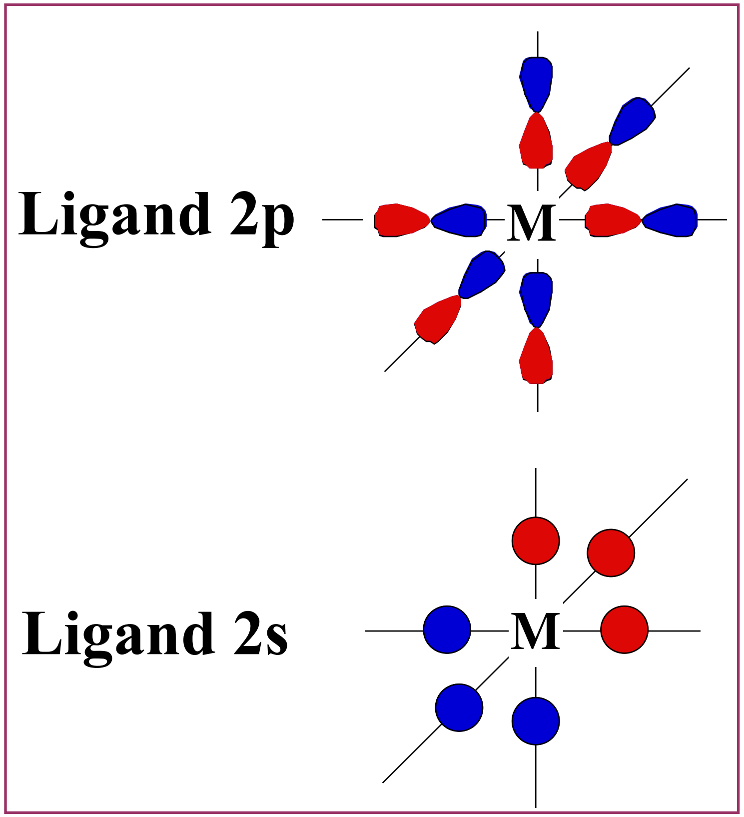

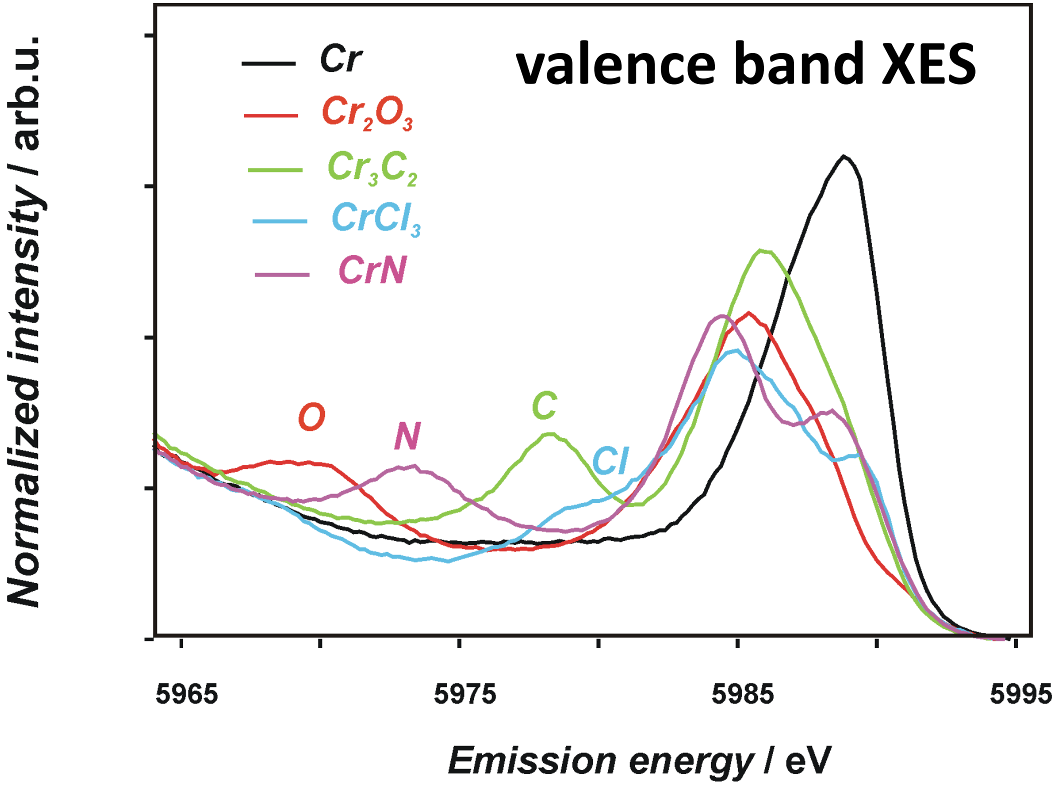

t_{1u} symmetry with respect to metal center

U. Bergmann, Chem. Phys. Lett. 302 119–124 (1999)
V.A. Safonov et al., J. Phys. Chem. B 110 23192 (2006)
O.V. Safonova et al. / Electrochimica Acta *56 145 (2010)*

Photoelectron spectroscopy and XES

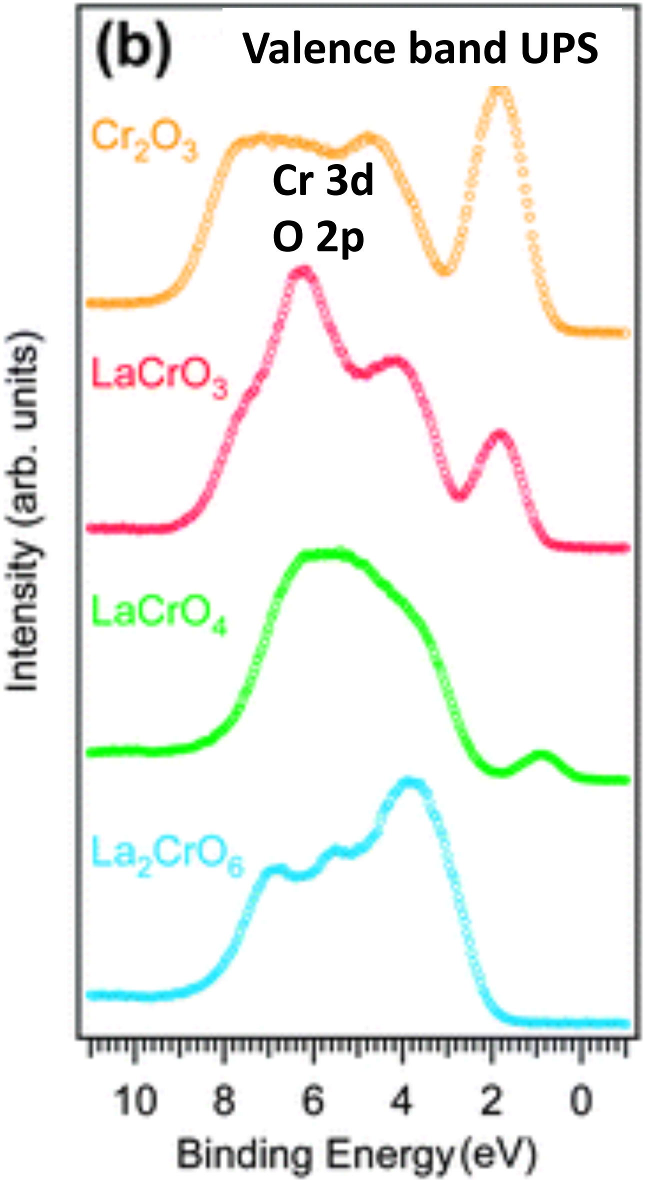

Same electron levels are probed.

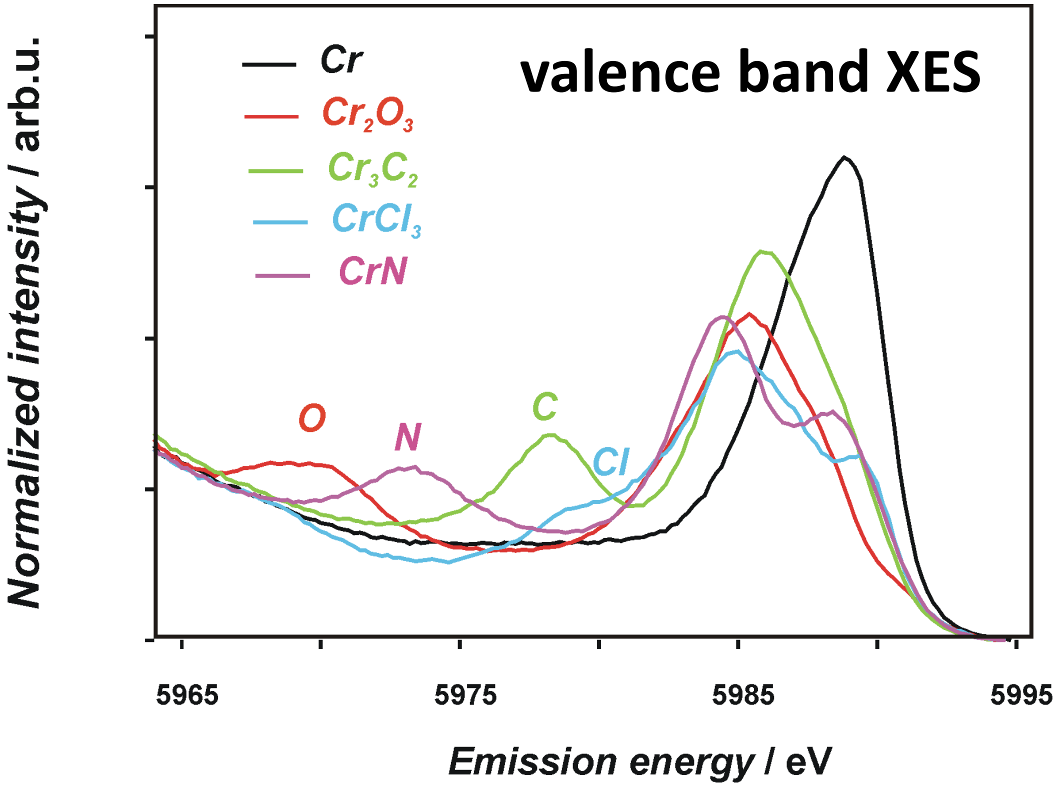

J. Mater. Chem. C, 2013,1, 4527-4535

Element-selectivity in XES greatly facilitates interpretation of spectra

Electrochemical Chrome Plating

Process best started from Cr(VI)

→ Toxic !!

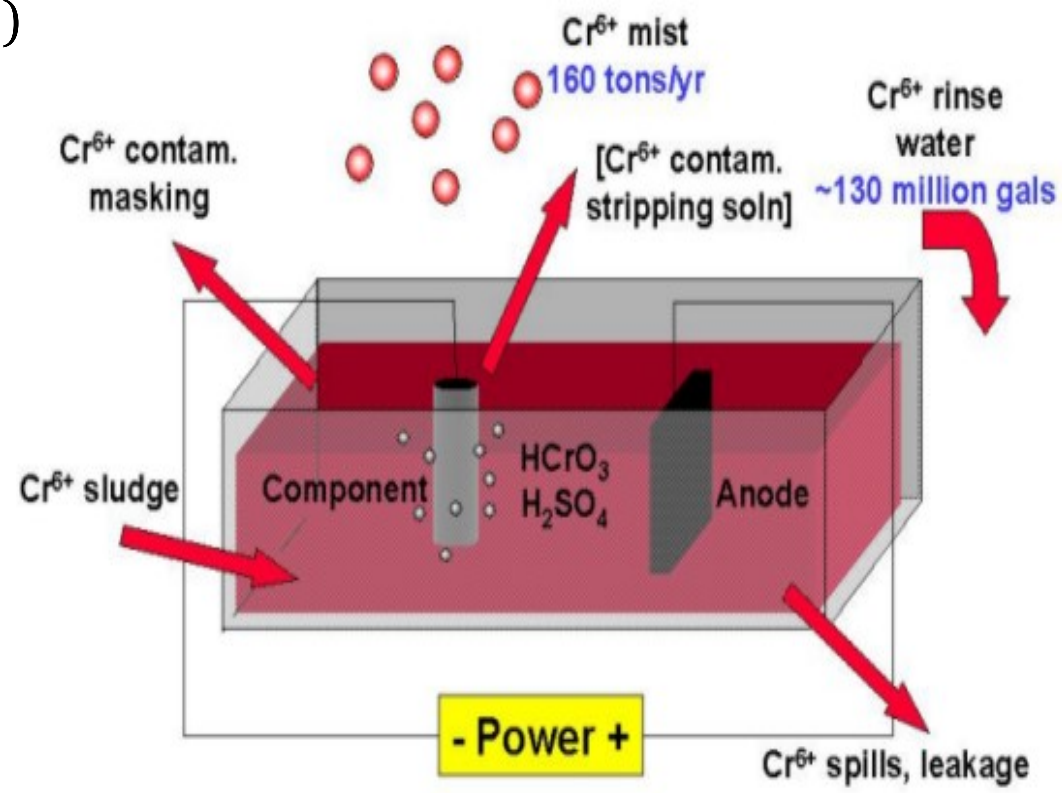

Replace Cr(VI) with Cr (III)
+ organic substances

How does Cr(III) behave chemically in electrolytes with organic substances?
In what chemical state is Cr electroplated ?

Valence-to-Core XES of electroplated Cr in organic electrolyte

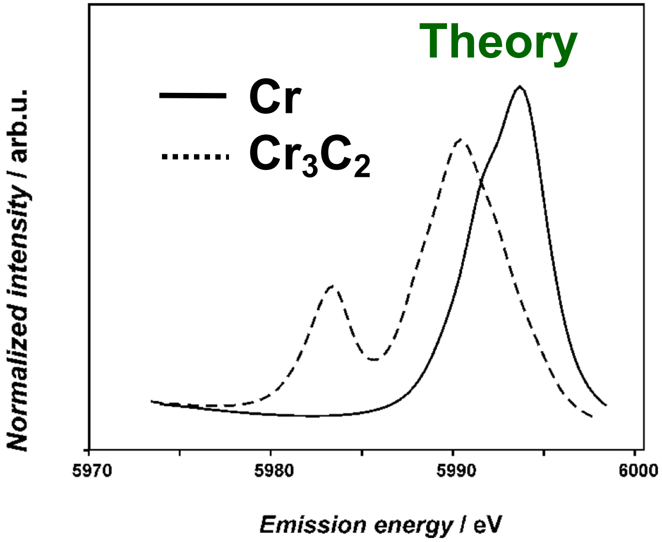

- ☐ Formation of Cr_3C_2 in nanocrystalline Cr Coatings

- ☐ No O ligand found

Safonov et al., J. Phys. Chem. B 110 23192 (2006)

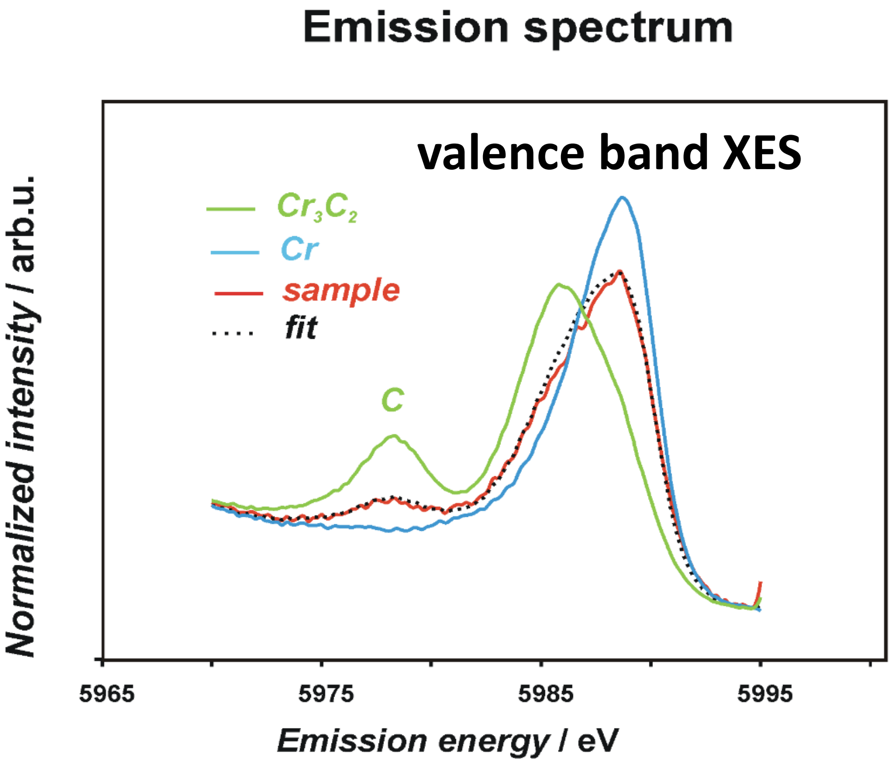

Sample: nanocrystalline Cr thin film deposited electrochemically from organic solution

29% Cr_3C_2 and 71% Cr

Calculation of vtc XES

Ground state DFT calculations work surprisingly well.

$$I(E_i) \propto |\langle \Psi_{1s} | \hat{\boldsymbol{\varepsilon}} \cdot \boldsymbol{r} | \varphi_{MO} \rangle|^2$$

This approach neglects:

- Multi-electron excitations
- The core hole potential

Some codes for inner-shell spectroscopy with XES:

- ORCA by Frank Neese (MPI Muelheim)
- FDMNES by Yves Joly (CNRS Grenoble)
- StoBe (Lars Petterson, Klaus Hermann, Stockholm/Berliln)
- FEFF (John Rehr, Washington)

Valence-to-Core XES of Mn^{2+} in Solution

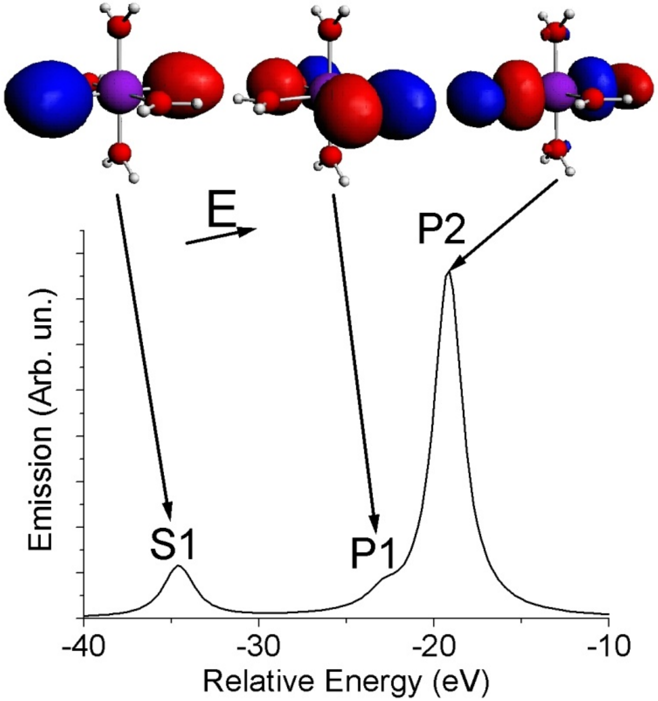

Mn^{2+} in solution

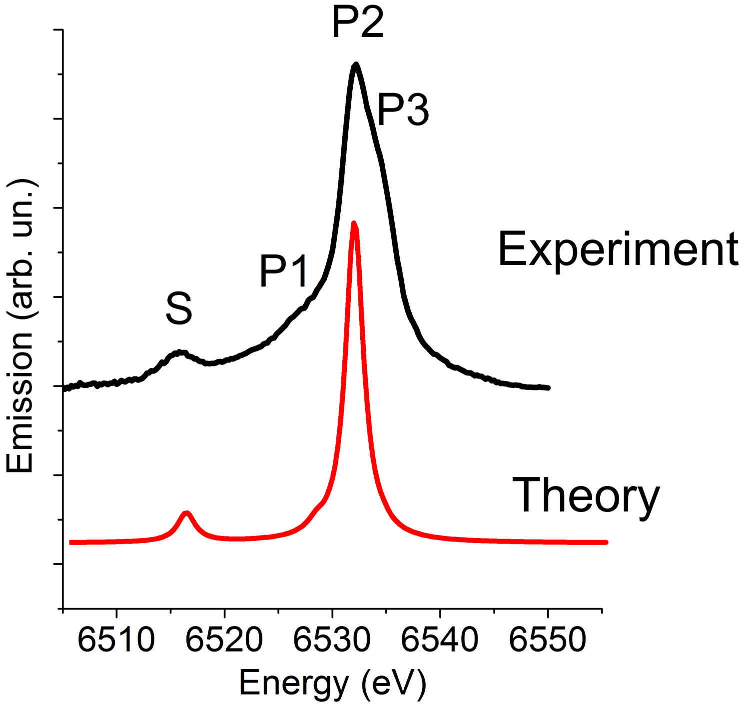

P1 and P3 probably due to dynamical disorder and distant H_2O molecules.

Smolentsev et al. JACS **131** 12451 (2009)

Detection of Ligand Protonation

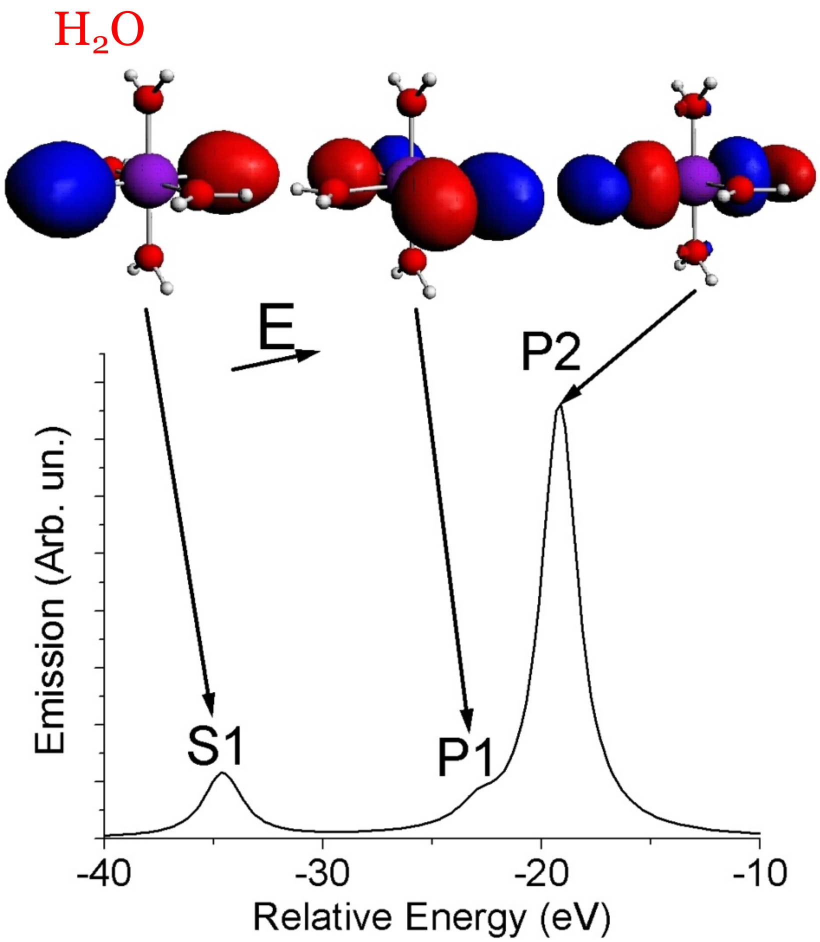

$[Mn(H_2O)_6]^{2+}$

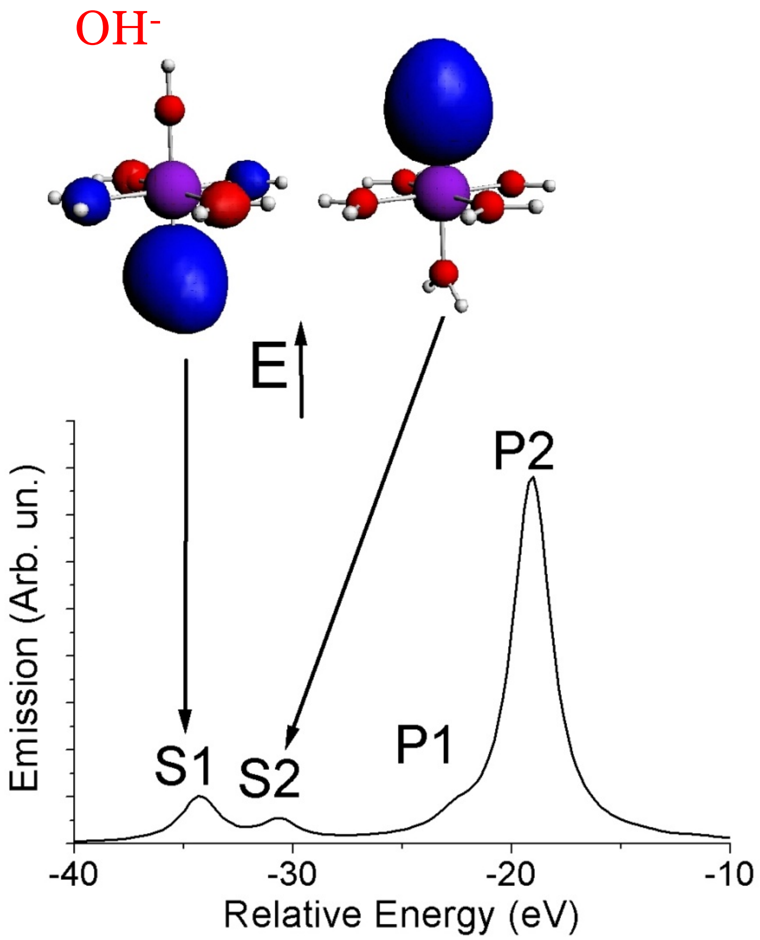

$[Mn(H_2O)_5OH]^{+}$

$$I(E_i) \propto |\langle \Psi_{1s} | \hat{\boldsymbol{\varepsilon}} \cdot \boldsymbol{r} | \varphi_{MO} \rangle|^2$$

Smolentsev et al. JACS **131** 12451 (2009)

Ligand Protonation in a Zn coordination complex

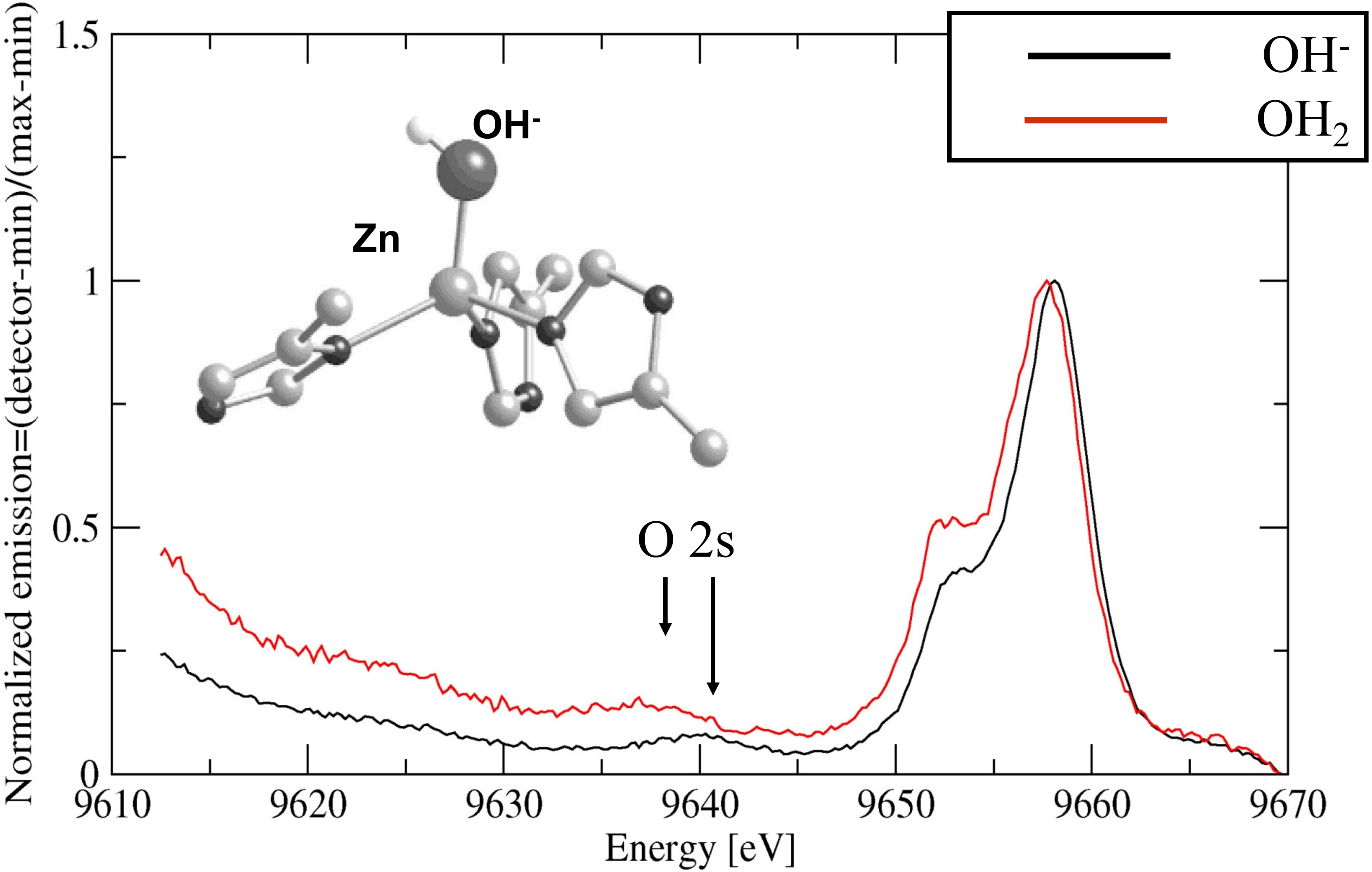

Pennerhahn et al., unpublished

Degree of ligand protonation

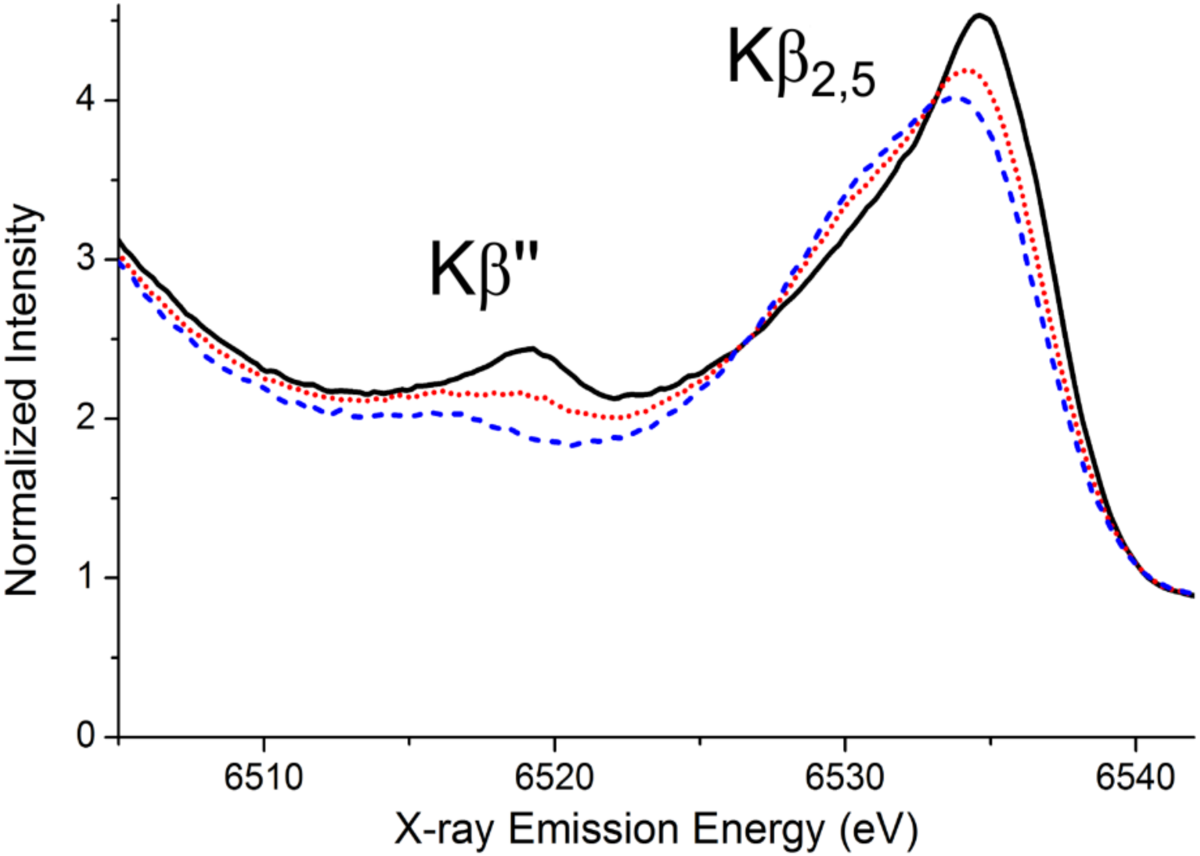

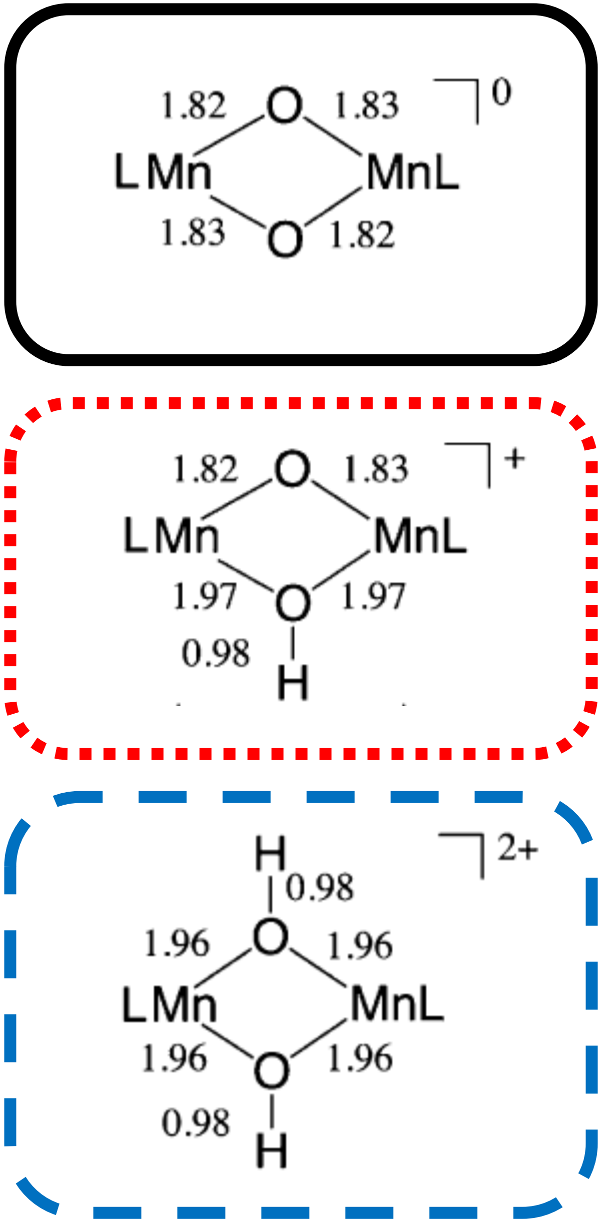

Lassalle-Kaiser et al., Inorg. Chem. 2013, 52, 12915–12922

vtc in metalloproteins: understanding nitrogen fixation ($N_2 \rightarrow NH_3$)

Nitrogenase FeMoco

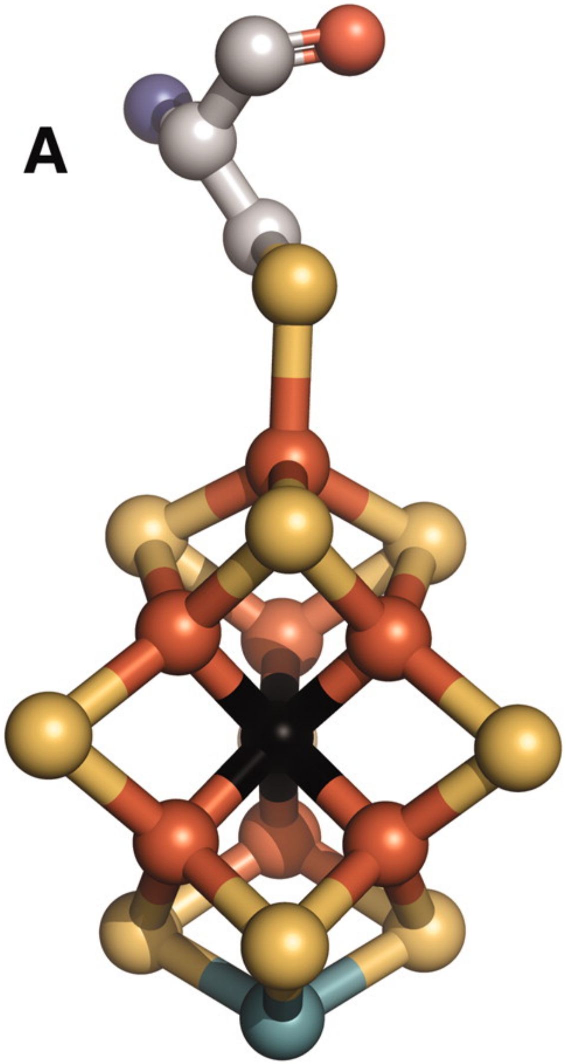

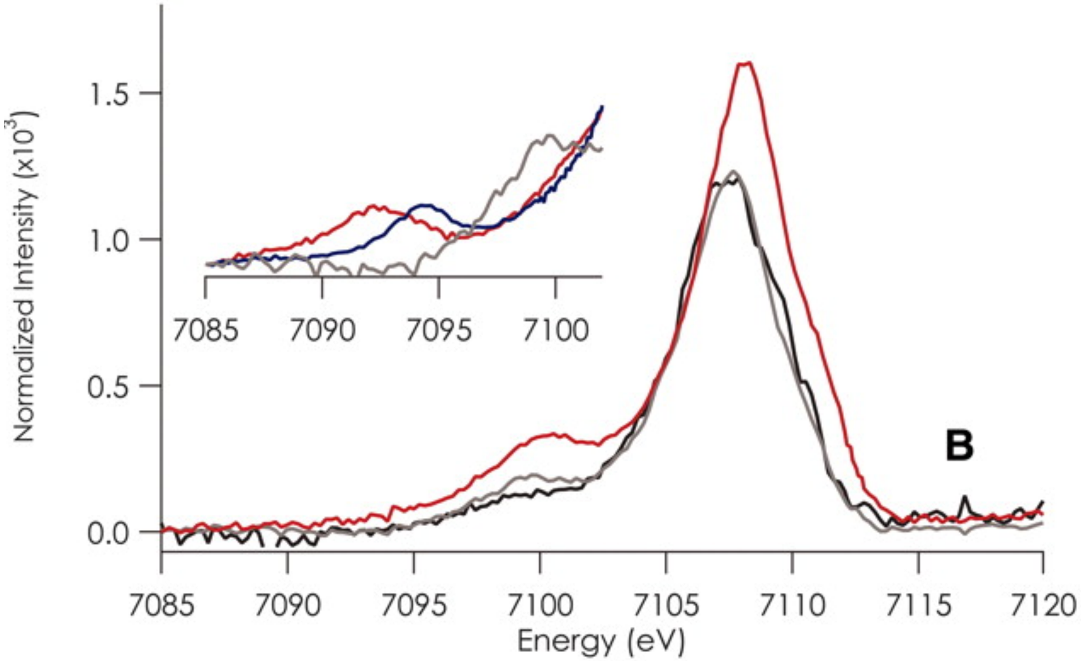

(B) Comparison of the normalized V2C XES data for FeMoc (red), the MoFe protein (gray), and the ΔnifB MoFe protei (black). (Inset) V2C satellite region for Fe_2O_3 (red), Fe_3N (blue), and MoFe protein (gray).

Lancaster et al., Science **334** 974 (2011)

Orange, Fe; yellow, S; light blue, Mo; black, C^{4-}, N^{3-}, or O^{2-}; dark blue, nitrogen; gray, carbon.

Titanium in Silicate – TS-1

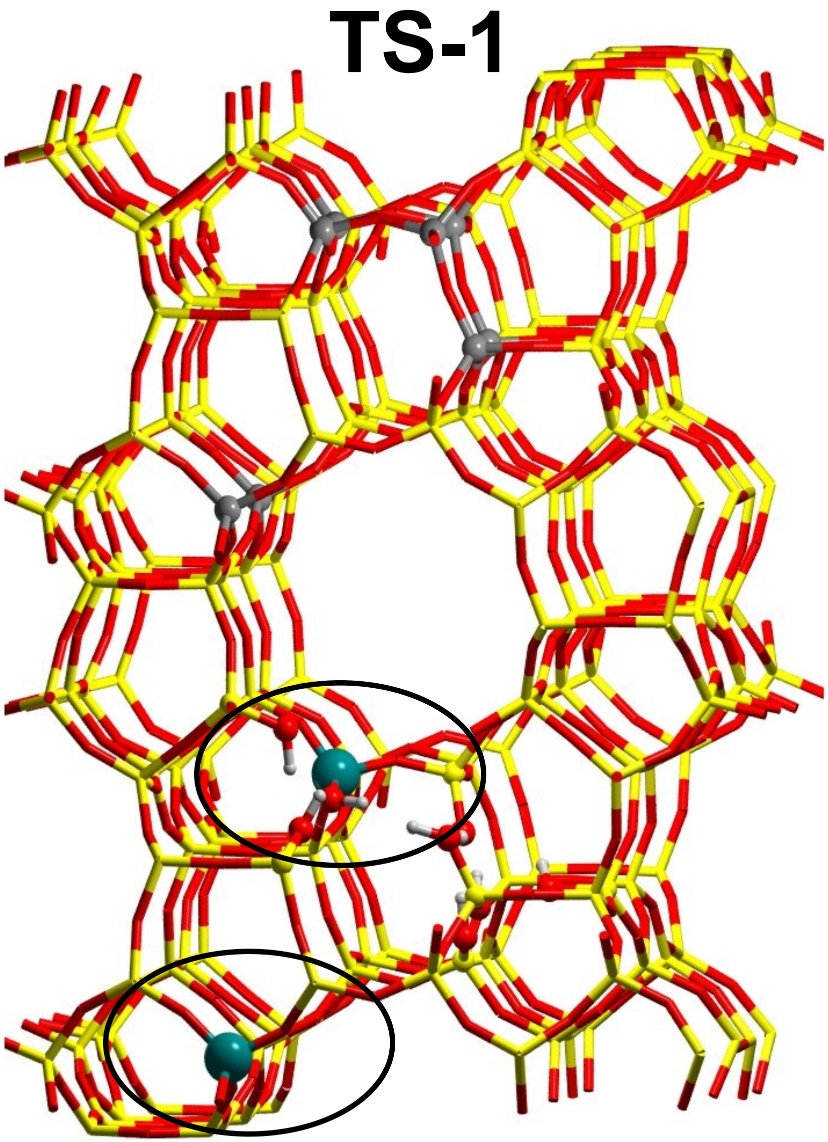

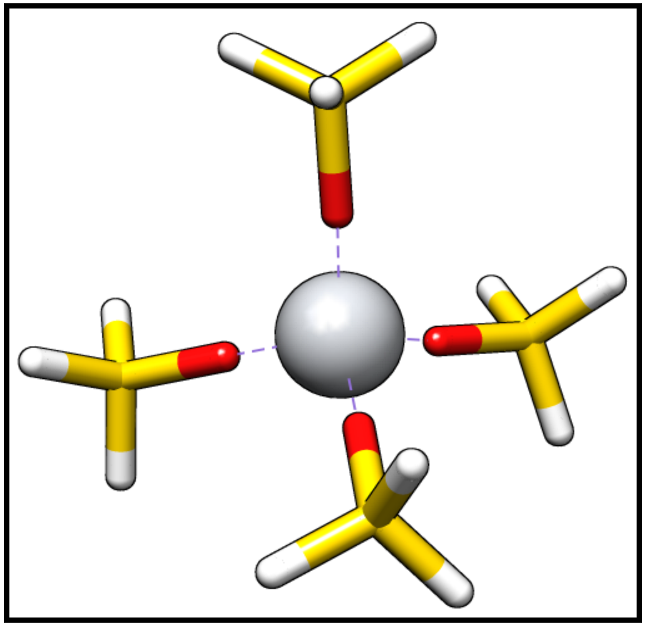

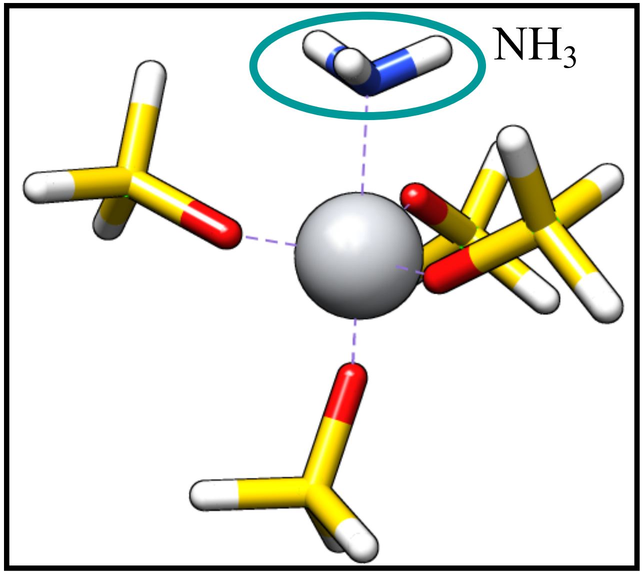

DFT calculations of vtc XES of Ti in TS-1

De-gased

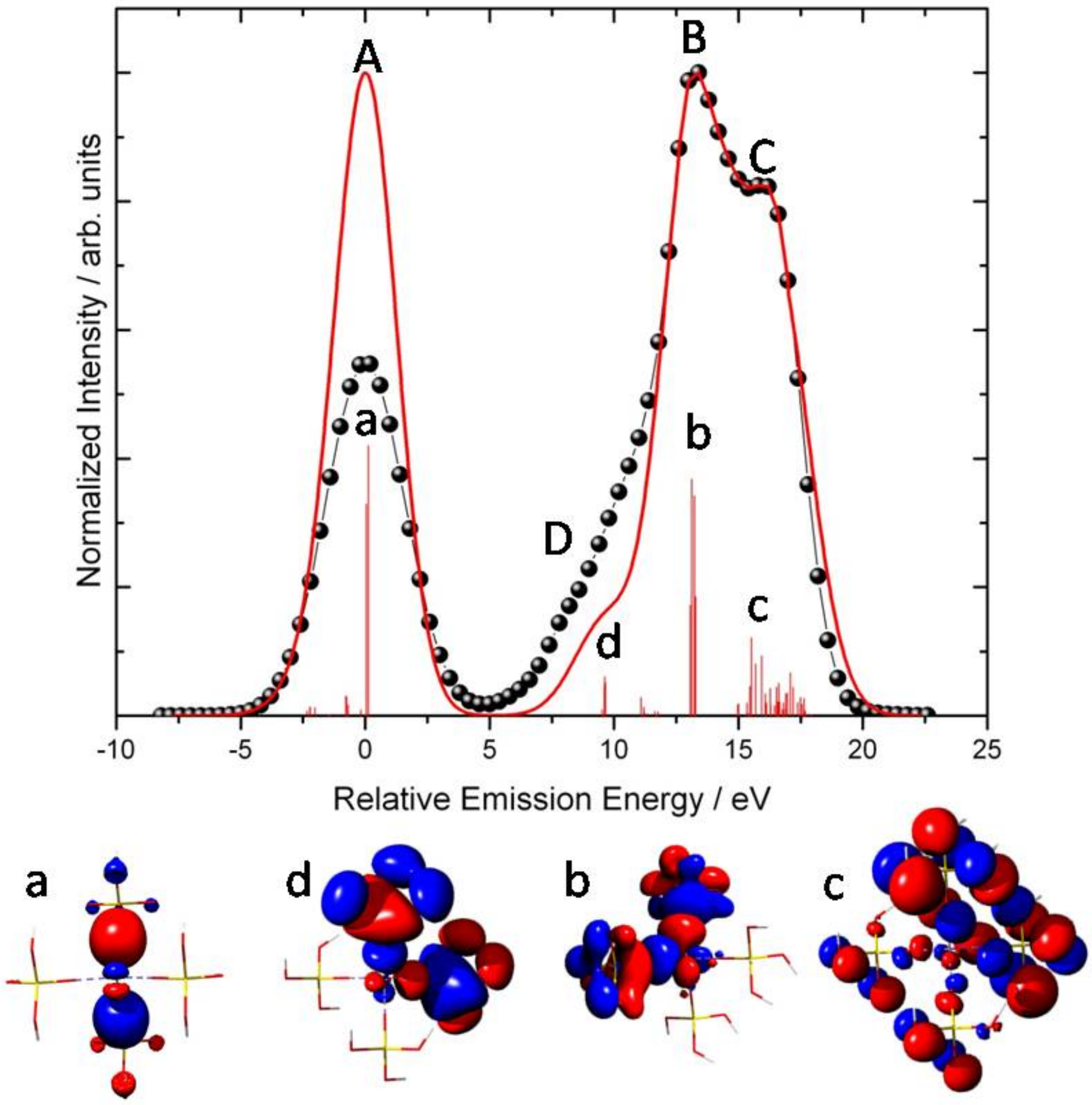

Phys. Chem. Chem. Phys., 2011, **13, 19409–19419**

Different chemical sensitivities in S Kα and v2c

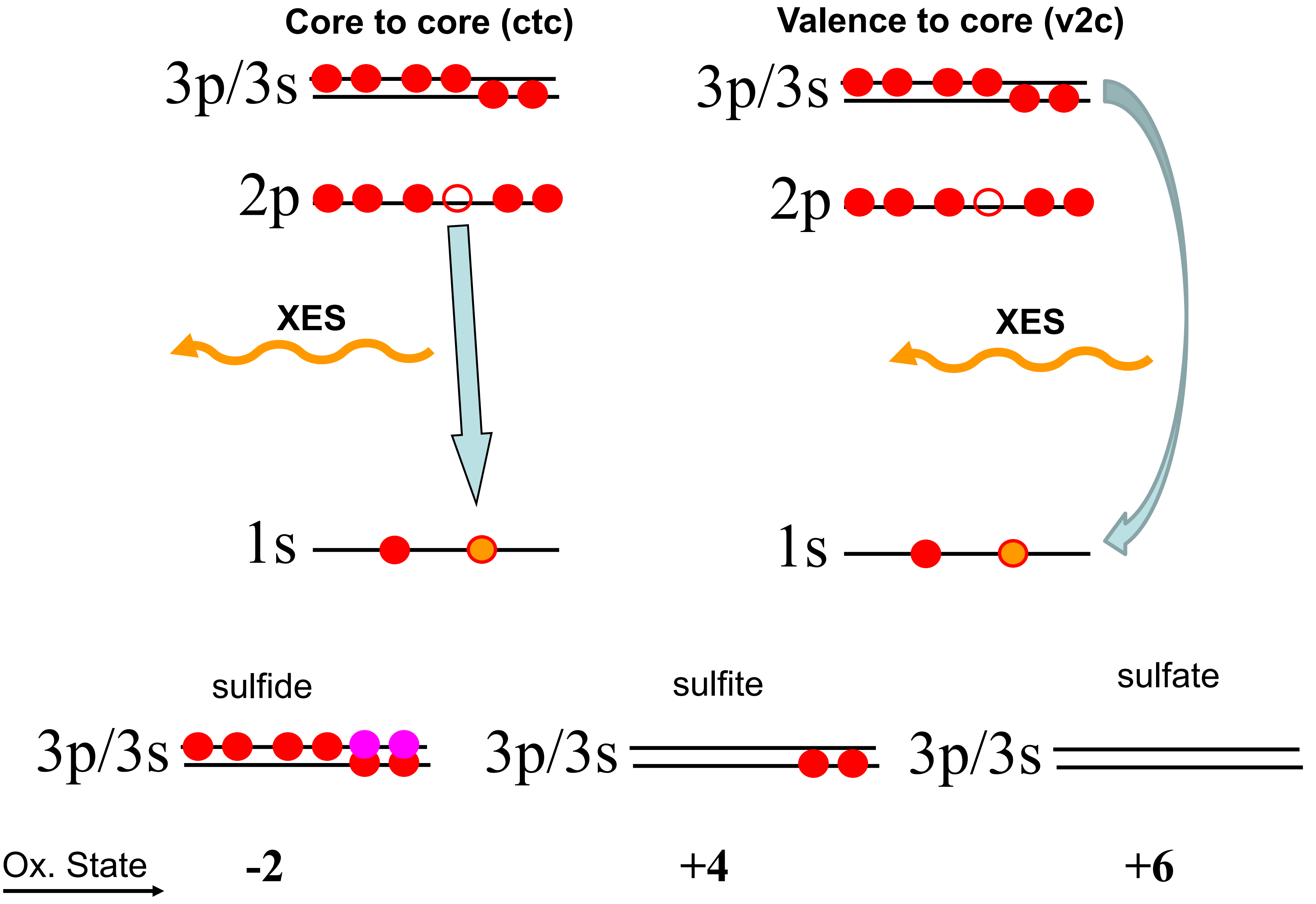

Core to core (ctc)

3p/3s

2p

XES

1s

Valence to core (v2c)

3p/3s

2p

XES

1s

sulfide

3p/3s

sulfite

3p/3s

sulfate

3p/3s

Ox. State

-2

+4

+6

Valence Shell Molecular Orbitals

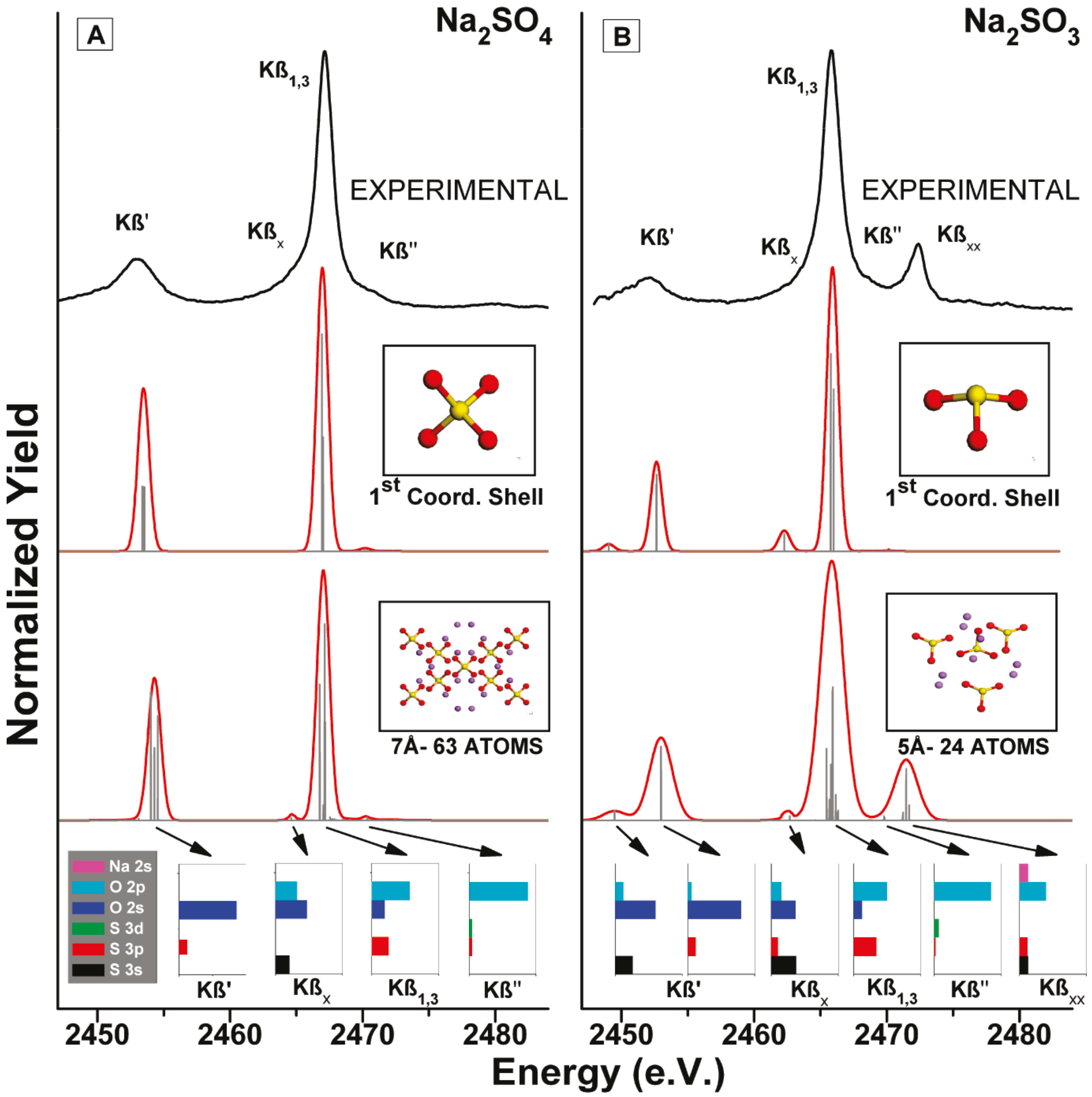

Valence-to-core XES in S compounds with DFT calculations using different cluster sizes.

The atomic contributions to the molecular orbitals are give.

Inorg. Chem. 2010, 49, 6468–6473

Resonant inelastic X-ray scattering

Interaction of X-rays with matter

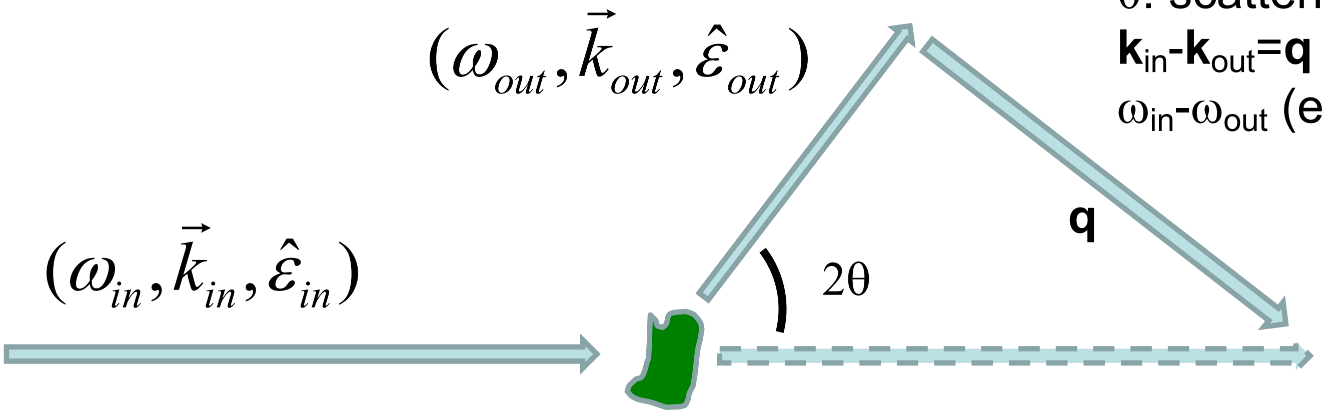

θ: scattering angle
$\mathbf{k}_{in}$-$\mathbf{k}_{out}$=$\mathbf{q}$ (momentum transfer)
ω_{in}-ω_{out} (energy transfer)

Describe photon with vector field:

$$\boldsymbol{A}(z,t) = A_0(\boldsymbol{\varepsilon}_x e^{i(kz-\omega t)} + \boldsymbol{\varepsilon}_x e^{-i(kz-\omega t)})$$

Treat the interaction of **A** with sample within perturbation theory.
We neglect interaction of the magnetic field with the electron spin (magnetic scattering).

In first order, a term in $\mathbf{A}^2$ is retained.

In second order, a term in $\mathbf{A}\cdot\mathbf{p}$ is retained.

Two scattering terms

The perturbative contributions to the scattering amplitude can be shown as ‘Feynman’ diagrams:

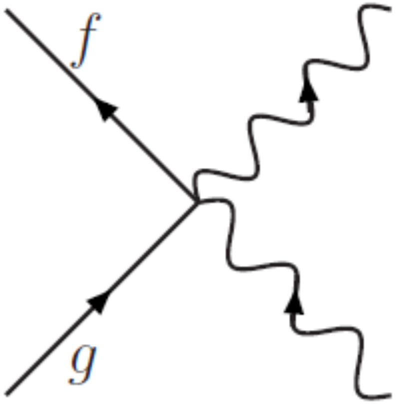

$$\vec{A}^2$$

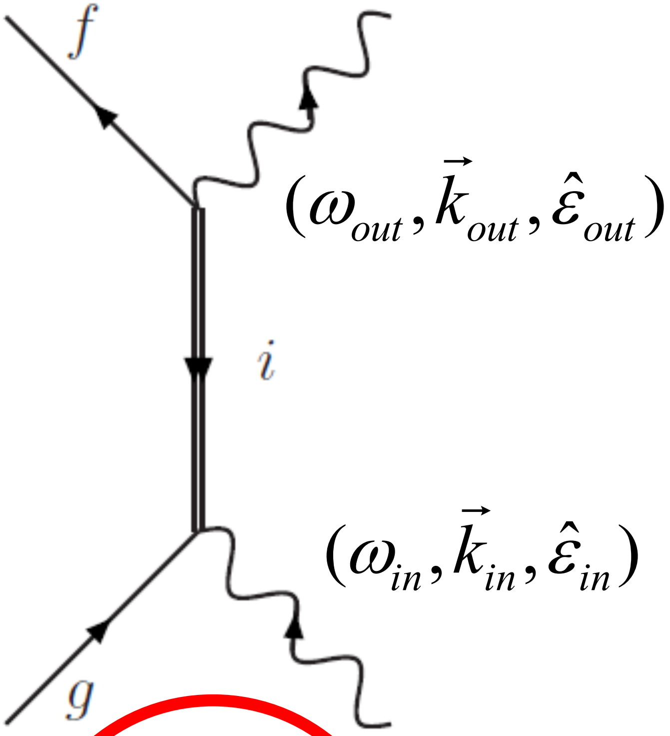

$$\vec{p} \cdot \vec{A}$$

What is a resonance?

One may think of using the definition that all **p·A** processes are resonant. However, that would cover EXAFS and even XPS.

Often, resonances are defined as excitations close to an absorption edge. But what is special about a resonance?

Two aspects are important:

1) A “resonance” shows a distinct (isolated) change in transition rate. This may be indicated by a peak in the density of states.

2) The scattering process is coherent, that means the phase of the scattered photon is preserved and we can observed interference effects.

Energy diagram in photon-in/photon-out spectroscopy

$$F^{KH}(\omega_{in},\omega_{out}) = \frac{\omega_{out}}{\omega_{in}} \sum_f \left| \sum_n \frac{\langle f | \hat{O}'^{\dagger} | n \rangle \langle n | \hat{O} | g \rangle}{E_n - E_g - \hbar\omega_{in} - i\Gamma_n} \right|^2 \delta\left(E_f - E_g - \hbar(\omega_{in} - \omega_{out})\right)$$

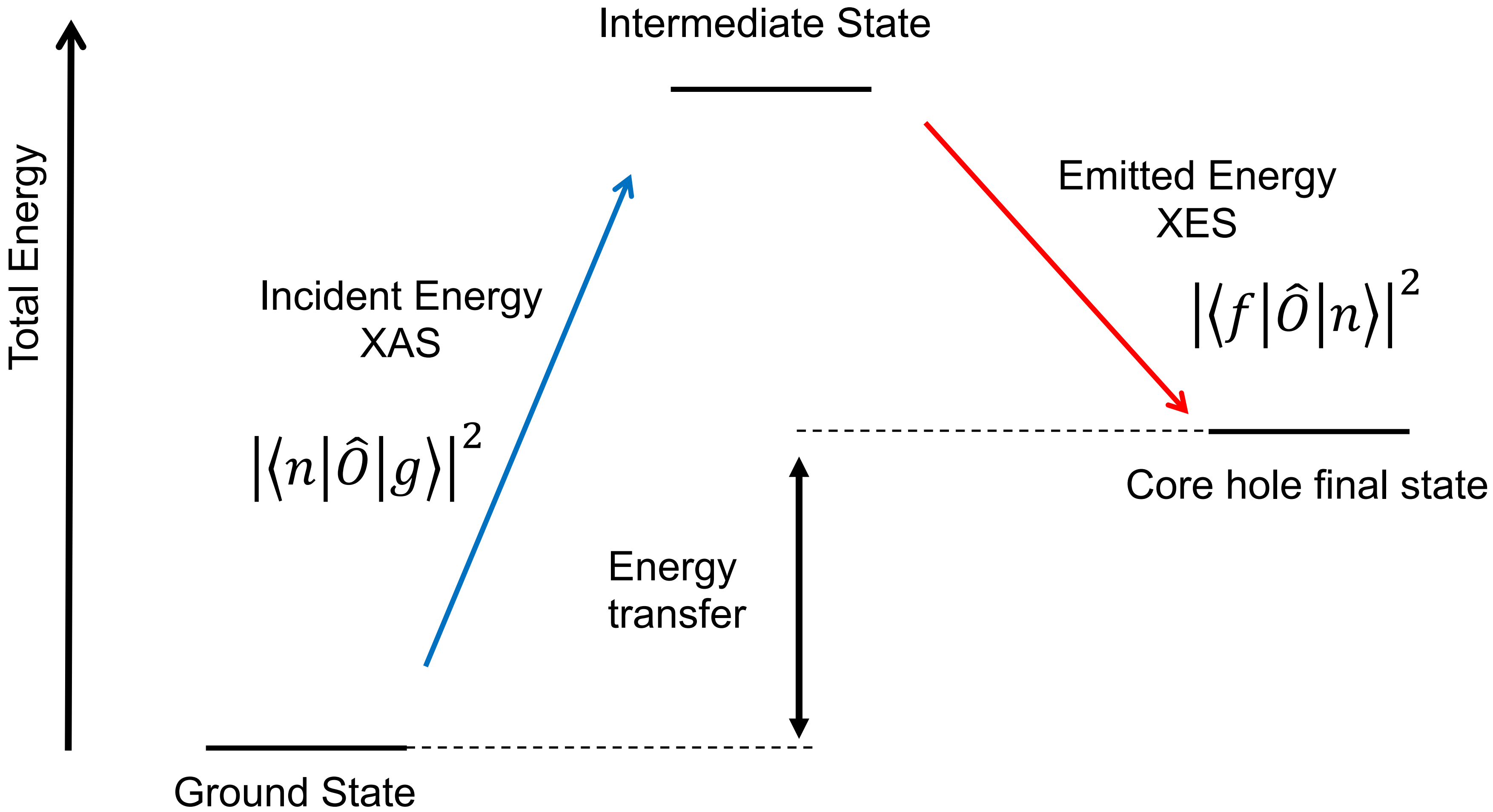

Intermediate State

Total Energy

Emitted Energy
XES

$$\left|\langle f | \hat{O} | n \rangle\right|^2$$

Incident Energy
XAS

$$\left|\langle n | \hat{O} | g \rangle\right|^2$$

Core hole final state

Energy
transfer

Ground State

Energy diagram in photon-in/photon-out spectroscopy

$$F^{KH}(\omega_{in},\omega_{out}) = \frac{\omega_{out}}{\omega_{in}} \sum_f \left| \sum_n \frac{\langle f|\hat{O}'^{\dagger}|n\rangle\langle n|\hat{O}|g\rangle}{E_n - E_g - \hbar\omega_{in} - i\Gamma_n} \right|^2 \delta\left(E_f - E_g - \hbar(\omega_{in} - \omega_{out})\right)$$

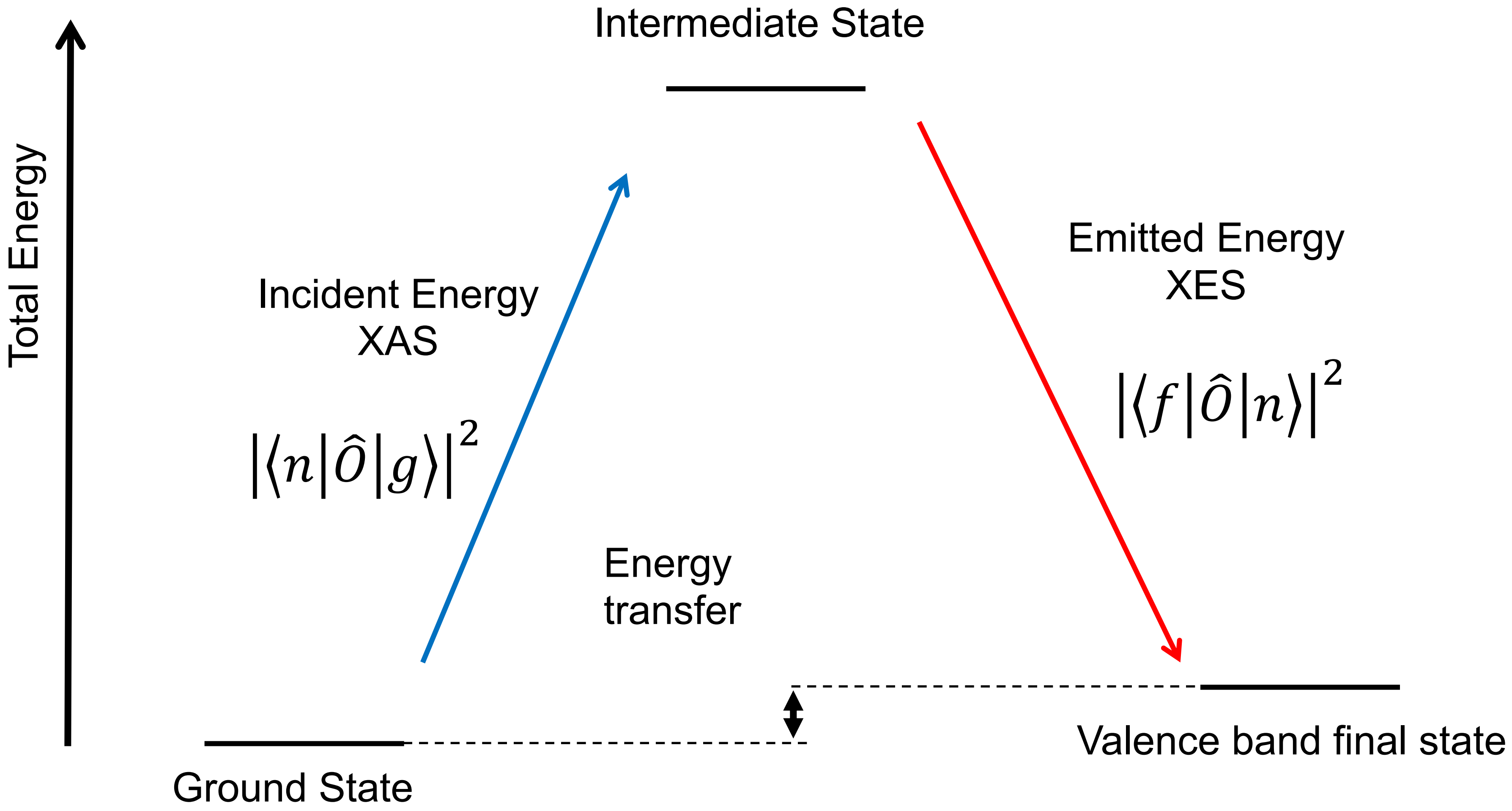

Intermediate State

Total Energy

Incident Energy
XAS

$|\langle n|\hat{O}|g\rangle|^2$

Emitted Energy
XES

$|\langle f|\hat{O}|n\rangle|^2$

Energy
transfer

Valence band final state

Ground State

Different kinds of RIXS

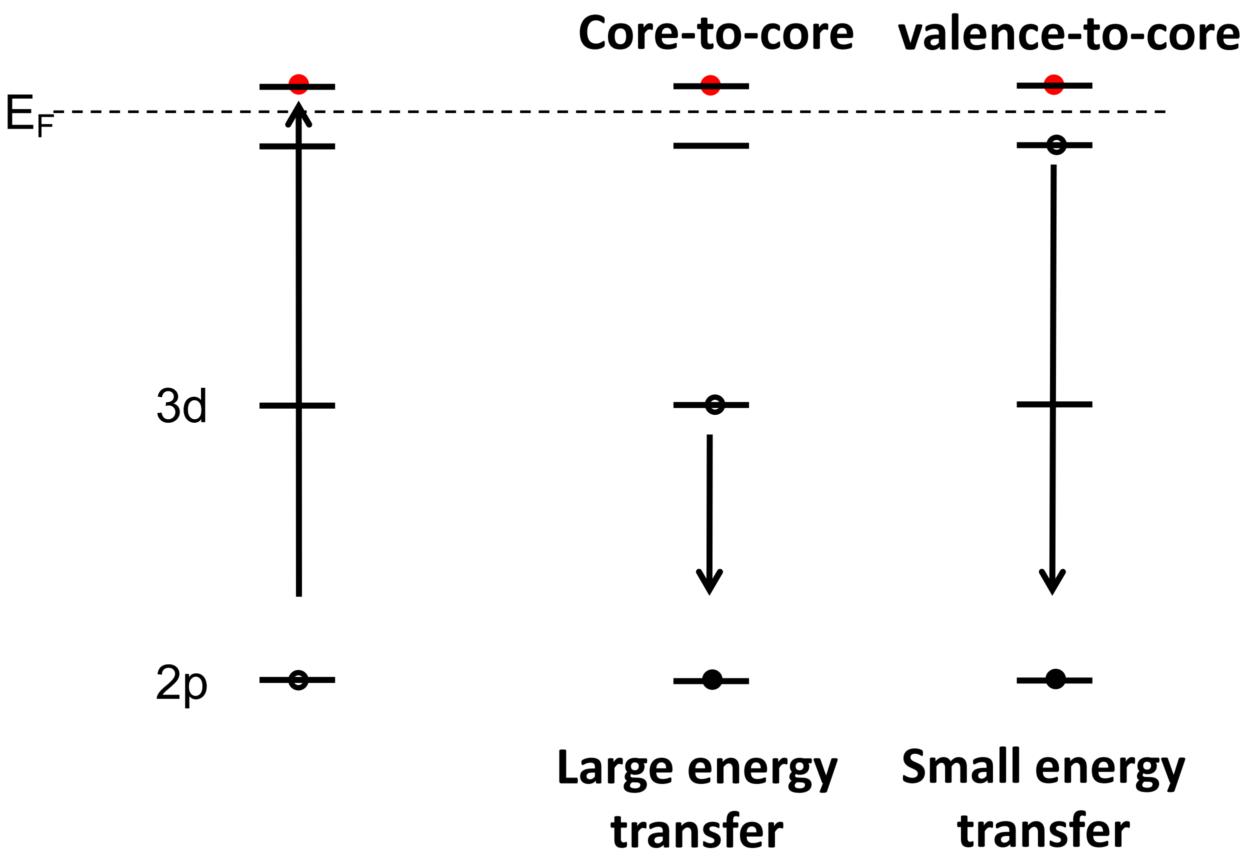

Core-to-core **valence-to-core**

E_F

3d

2p

Large energy transfer

Small energy transfer

The scheme above shows the RIXS process in a one-electron picture. Note that the final state in valence-to-core RIXS could also be observed in optical spectroscopy.

Inelastic X-ray scattering

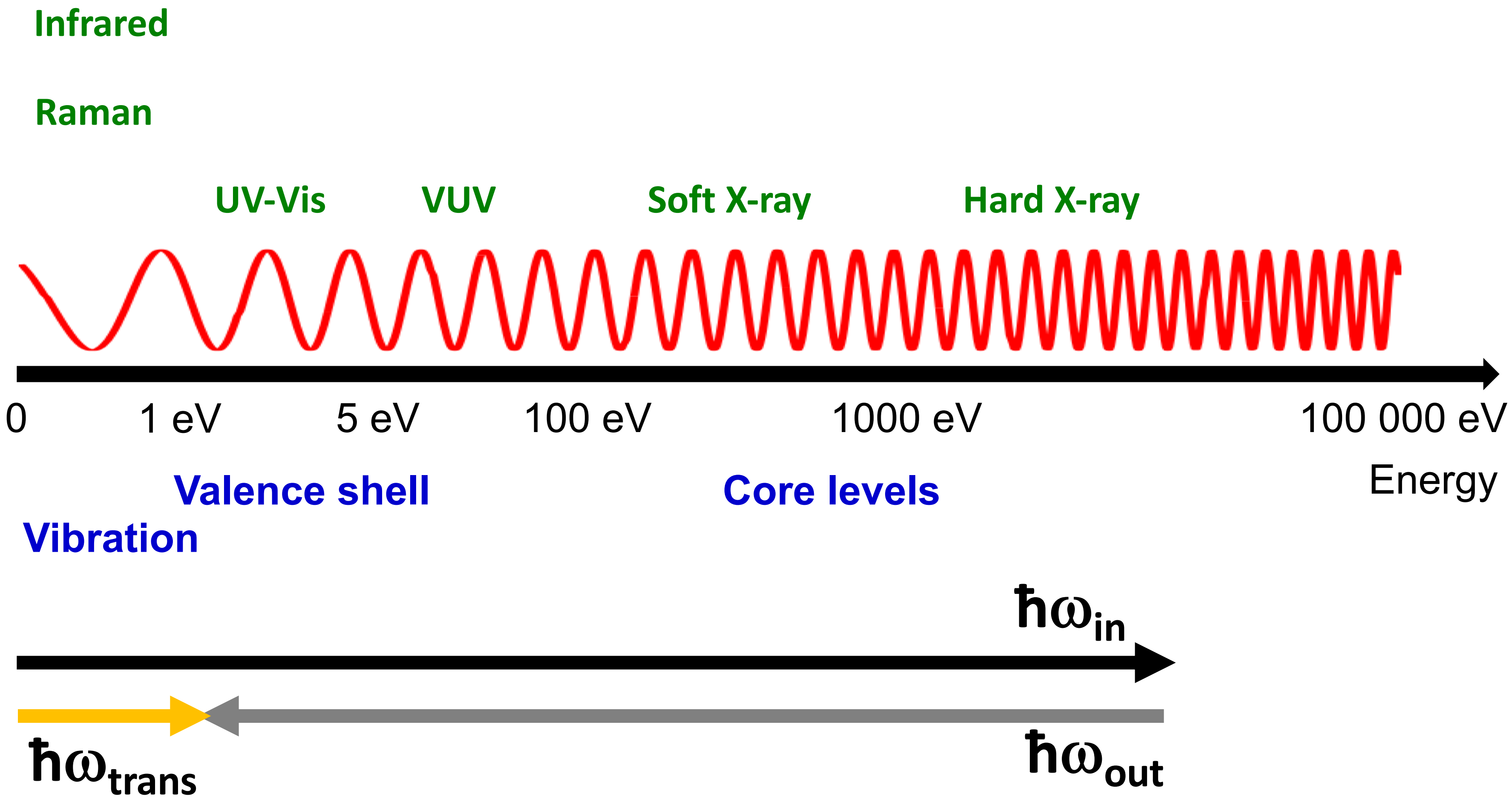

Infrared

Raman

UV-Vis **VUV** **Soft X-ray** **Hard X-ray**

0 1 eV 5 eV 100 eV 1000 eV 100 000 eV

Energy

Valence shell **Core levels**

Vibration

$\hbar\omega_{in}$

$\hbar\omega_{trans}$

$\hbar\omega_{out}$

X-ray scattering allows studying low energy excitations element-selectively!

Photon-in/photon-out spectroscopy

Inelastic X-ray scattering

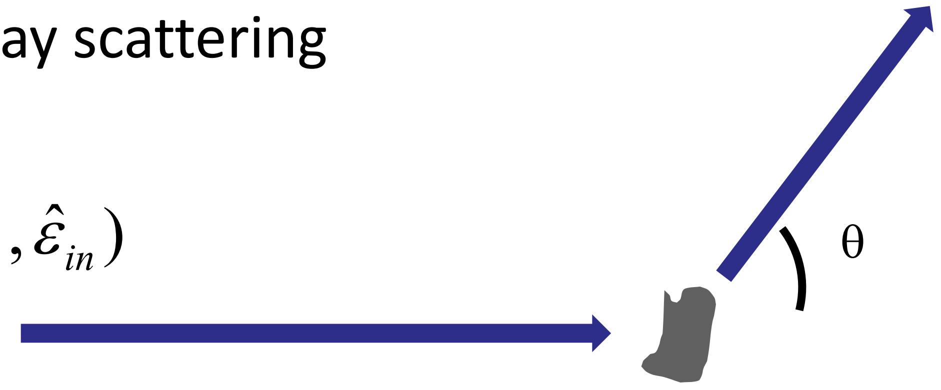

$(E_{in}, \vec{k}_{in}, \hat{\varepsilon}_{in})$

$(E_{out}, \vec{k}_{out}, \hat{\varepsilon}_{out})$

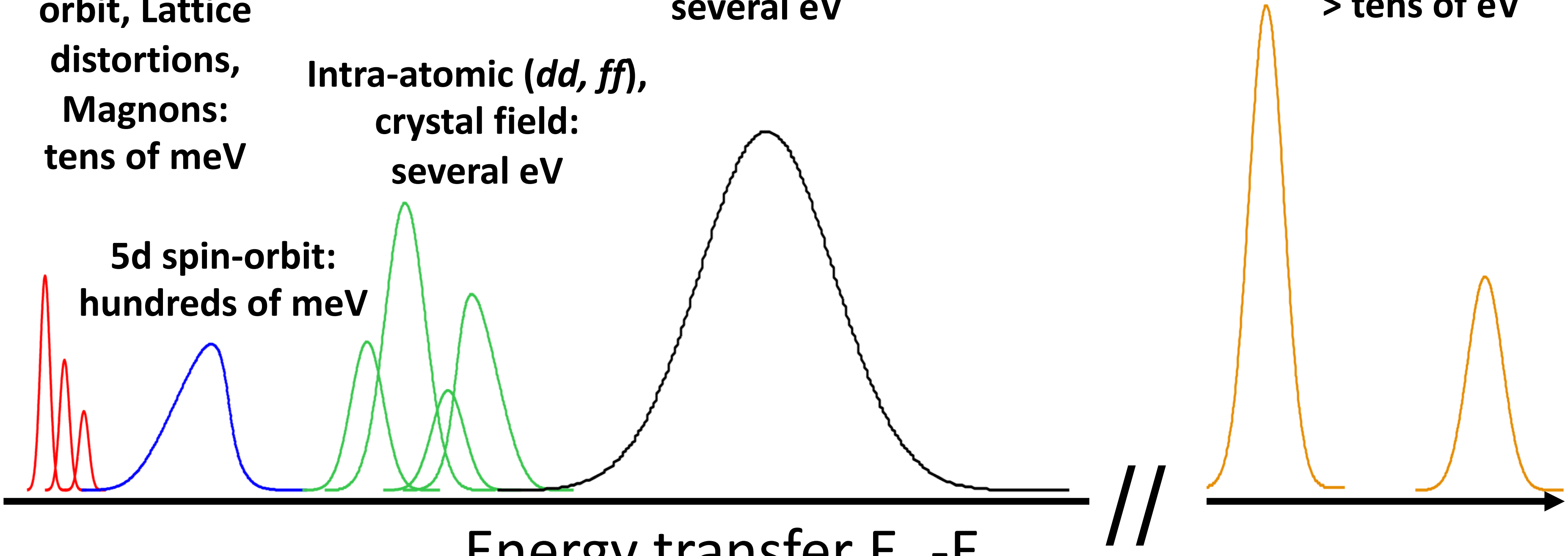

Phonons, 3d spin-orbit, Lattice distortions, Magnons: tens of meV

5d spin-orbit: hundreds of meV

Intra-atomic (*dd, ff*), crystal field: several eV

***Charge transfer*: several eV**

***Core levels*: > tens of eV**

Energy transfer E_{in}-E_{out}

Photon-in/photon-out spectroscopy at the ESRF

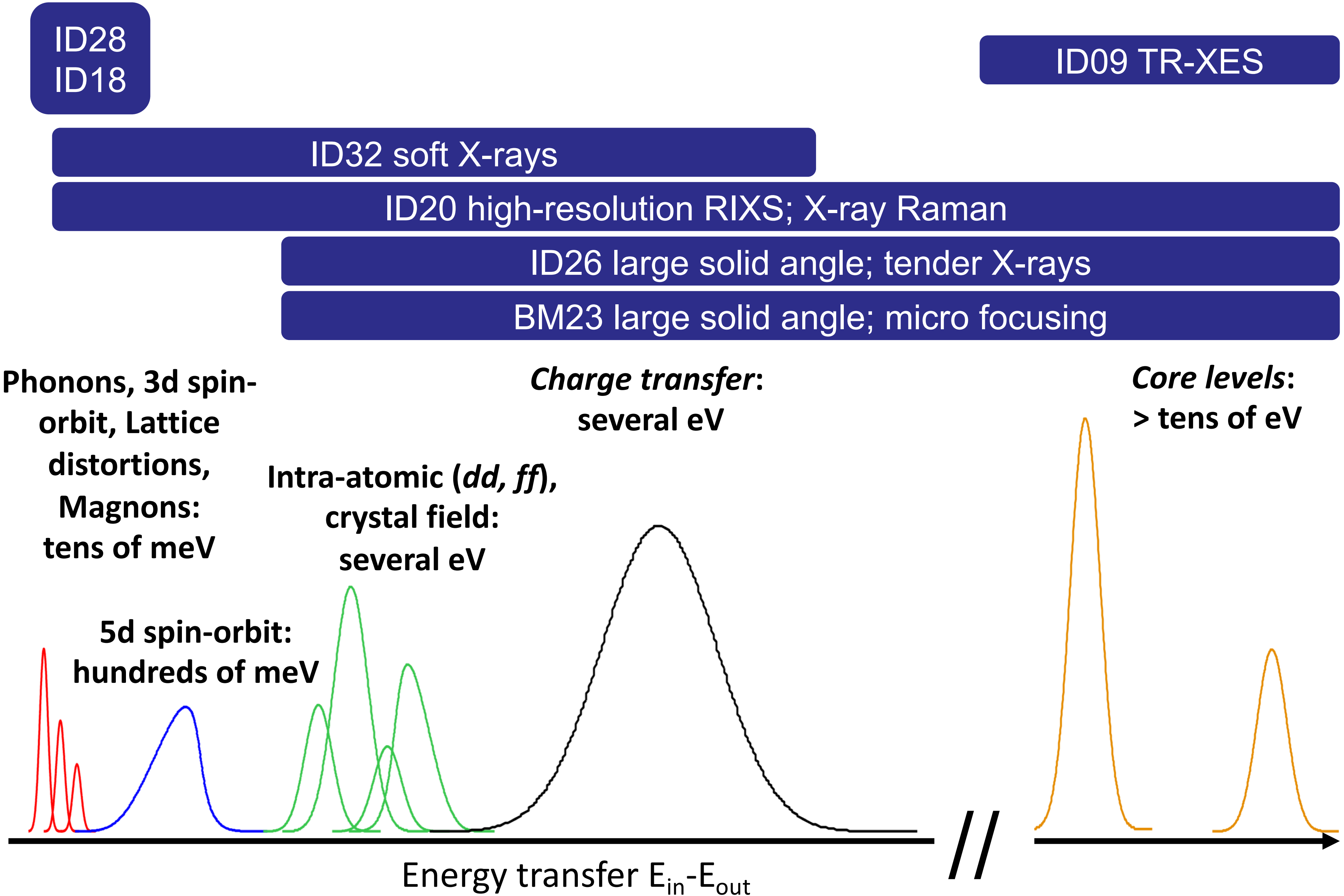

ID28
ID18

ID09 TR-XES

ID32 soft X-rays

ID20 high-resolution RIXS; X-ray Raman

ID26 large solid angle; tender X-rays

BM23 large solid angle; micro focusing

Phonons, 3d spin-orbit, Lattice distortions, Magnons: tens of meV

5d spin-orbit: hundreds of meV

Intra-atomic (*dd, ff*), crystal field: several eV

***Charge transfer*: several eV**

***Core levels*: > tens of eV**

Energy transfer E_{in}-E_{out}

Hard X-ray Photon-in/Photon-out spectroscopy

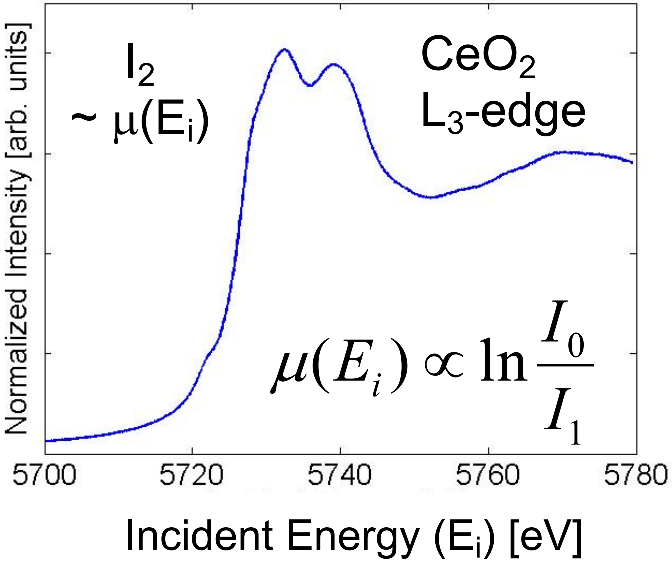

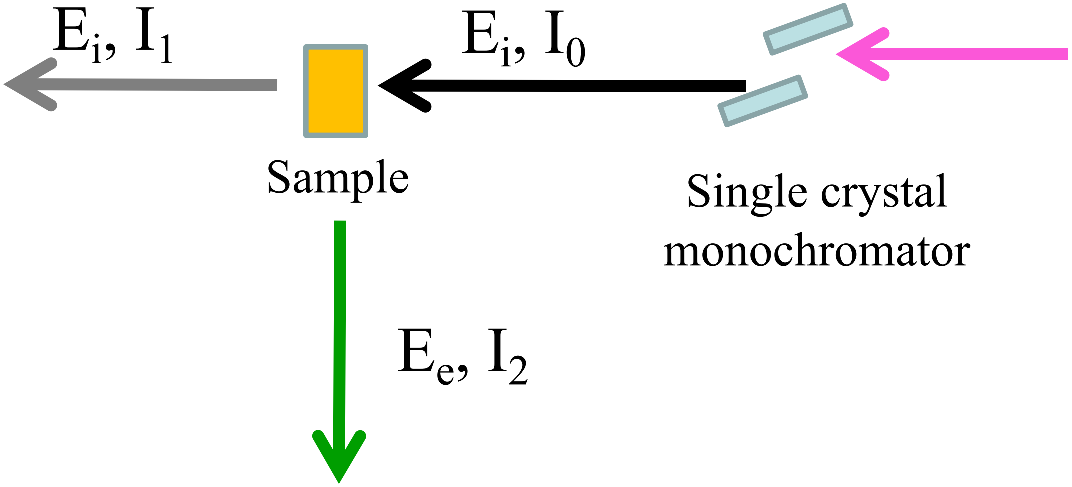

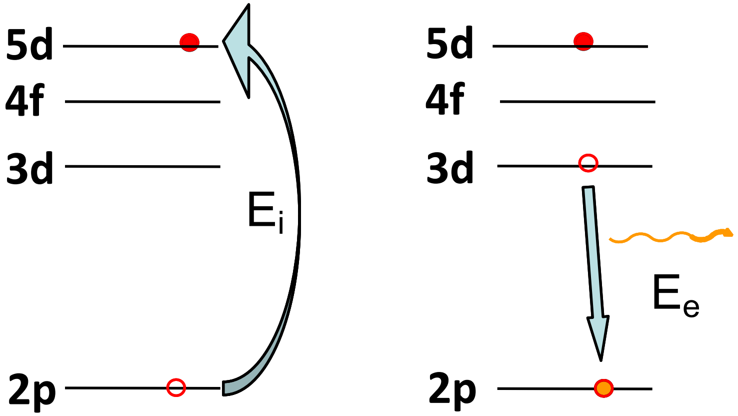

Second order process

Correctly treated with Kramers-Heisenberg equation

Hard X-ray Photon-in/Photon-out spectroscopy

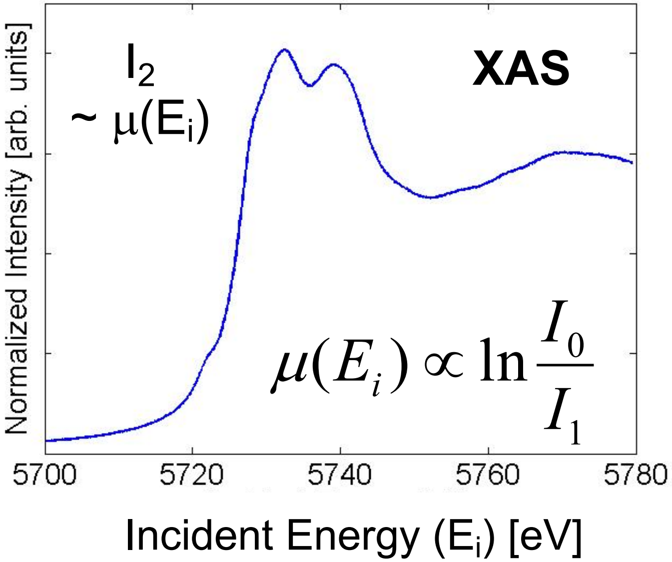

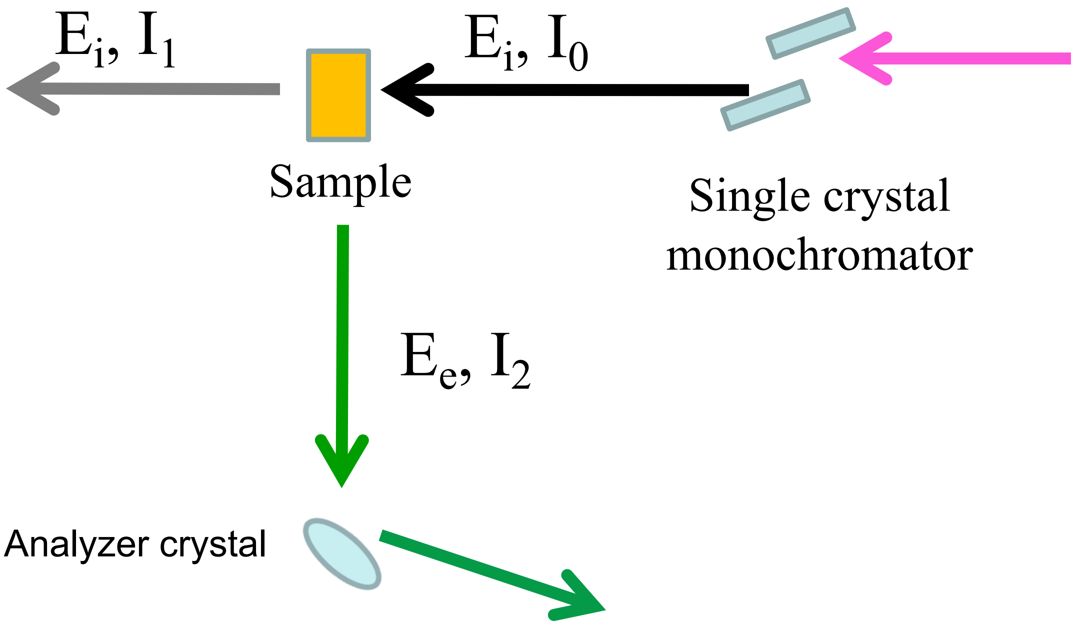

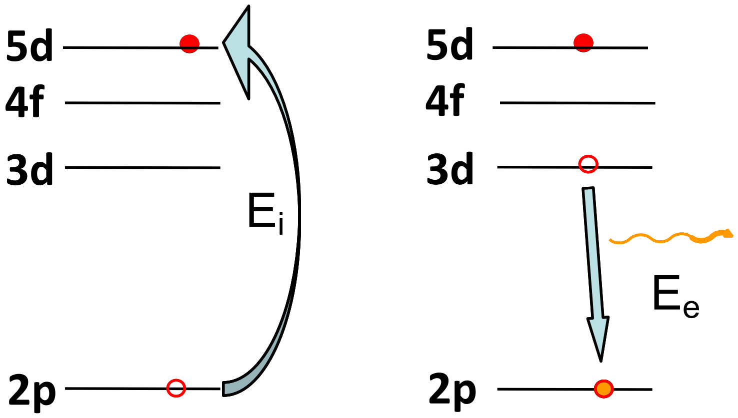

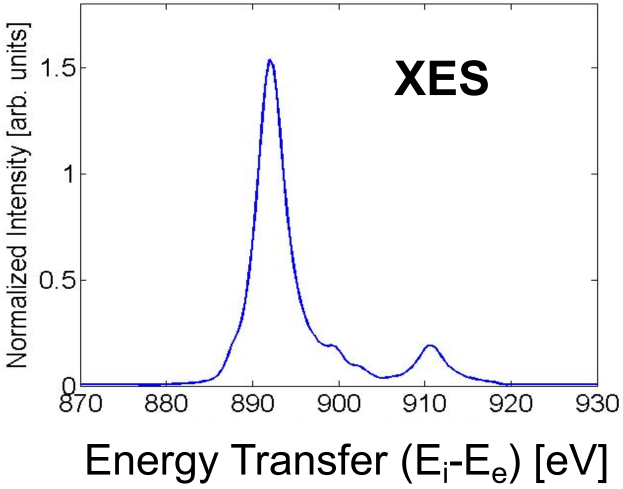

Hard X-ray Photon-in/Photon-out spectroscopy

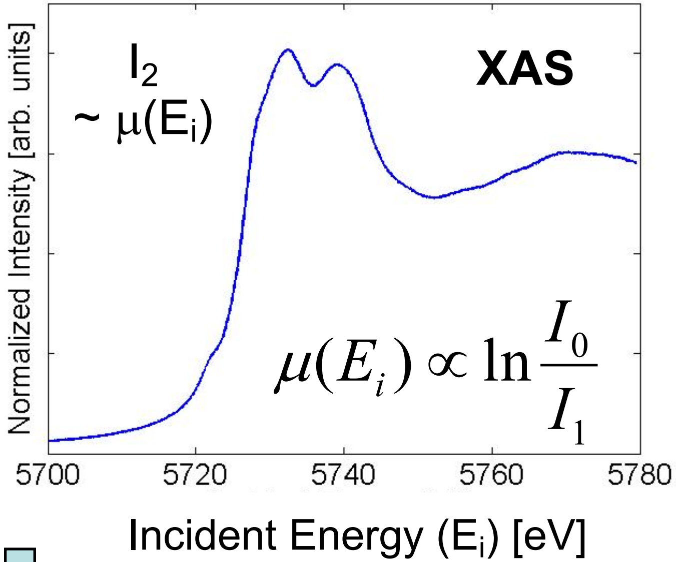

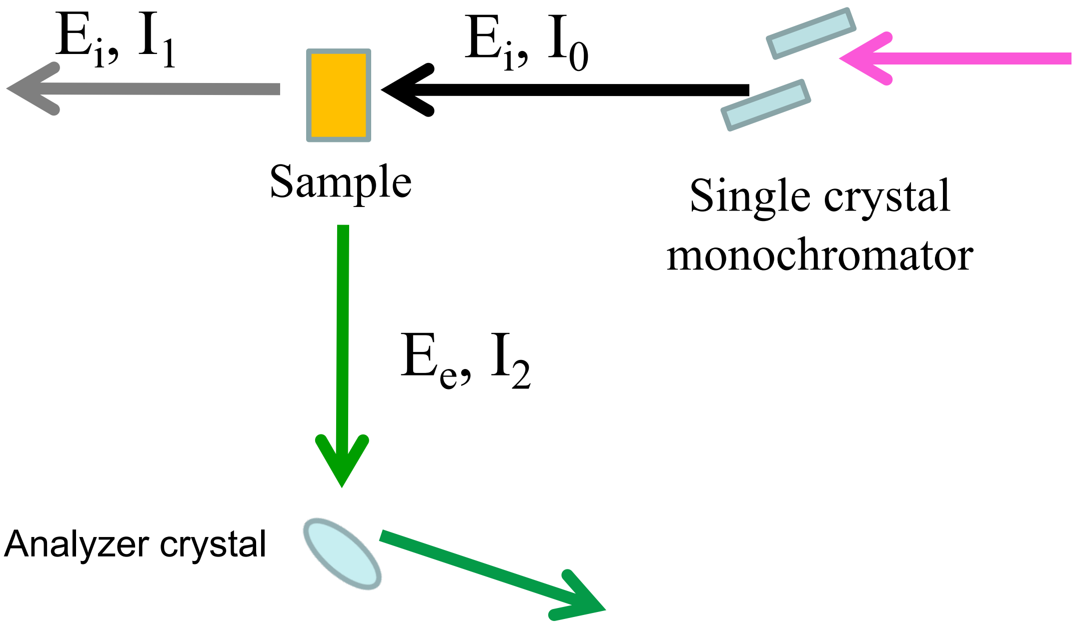

E_i, I_1

E_i, I_0

Sample

Single crystal
monochromator

E_e, I_2

Analyzer crystal

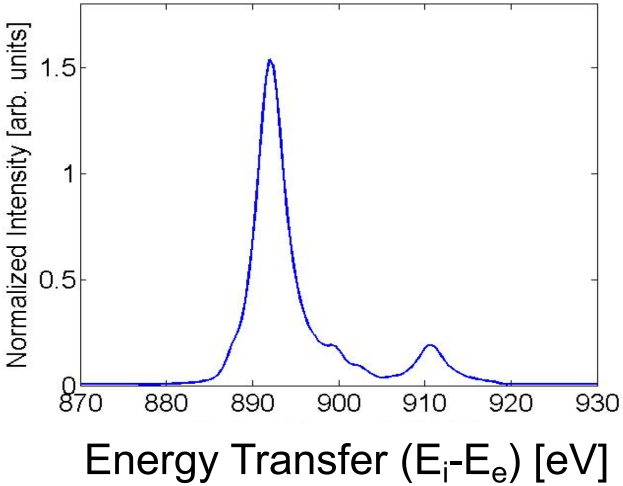

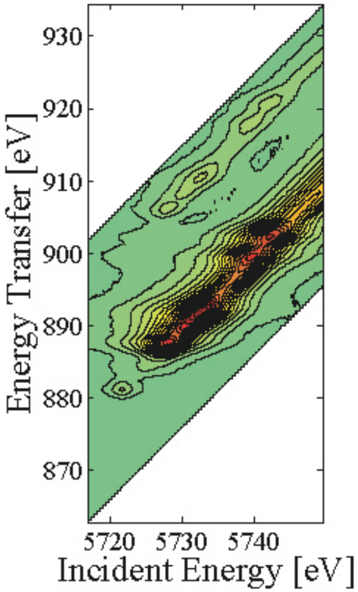

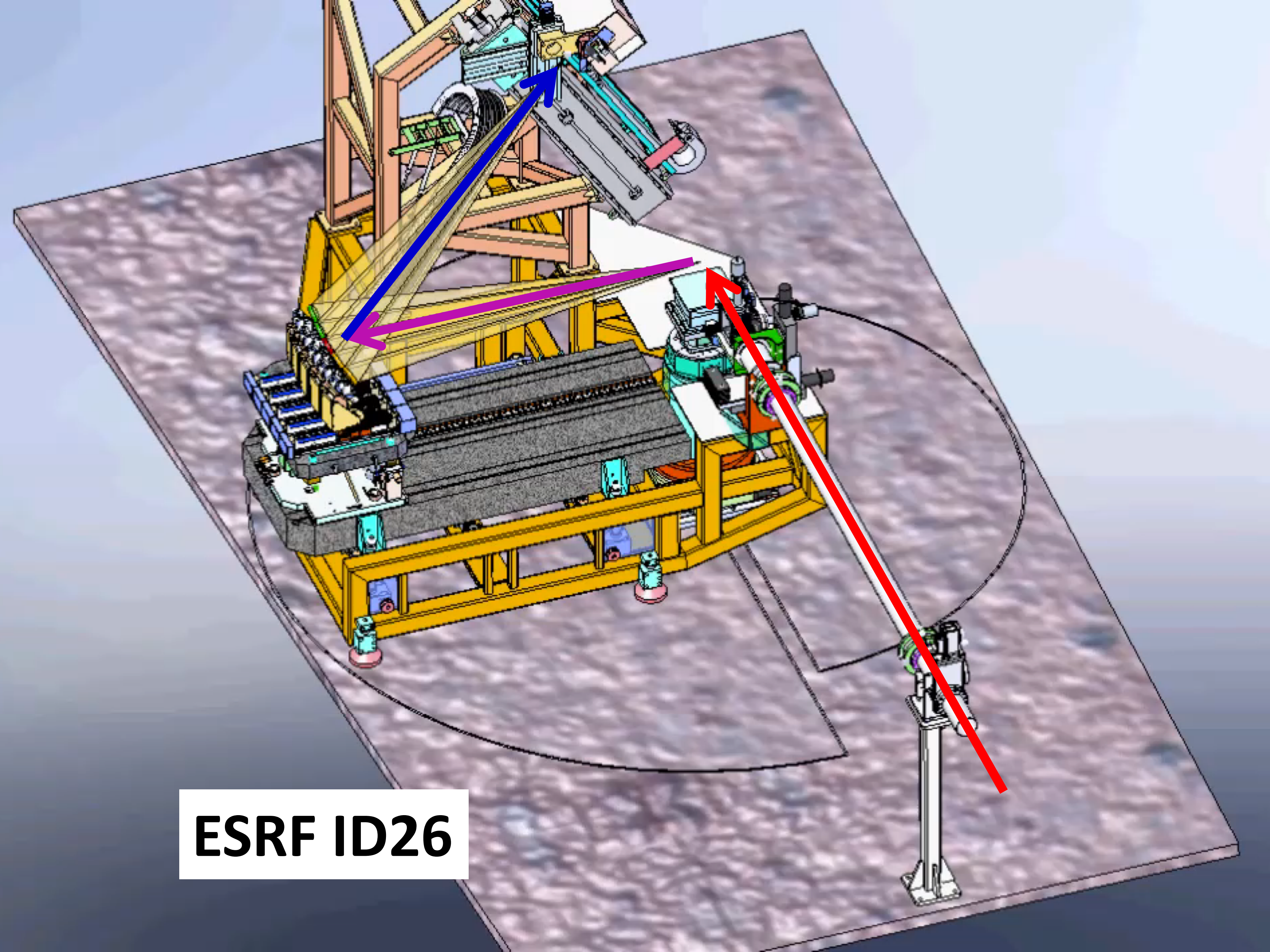

ESRF ID26

Energy diagram in photon-in/photon-out spectroscopy

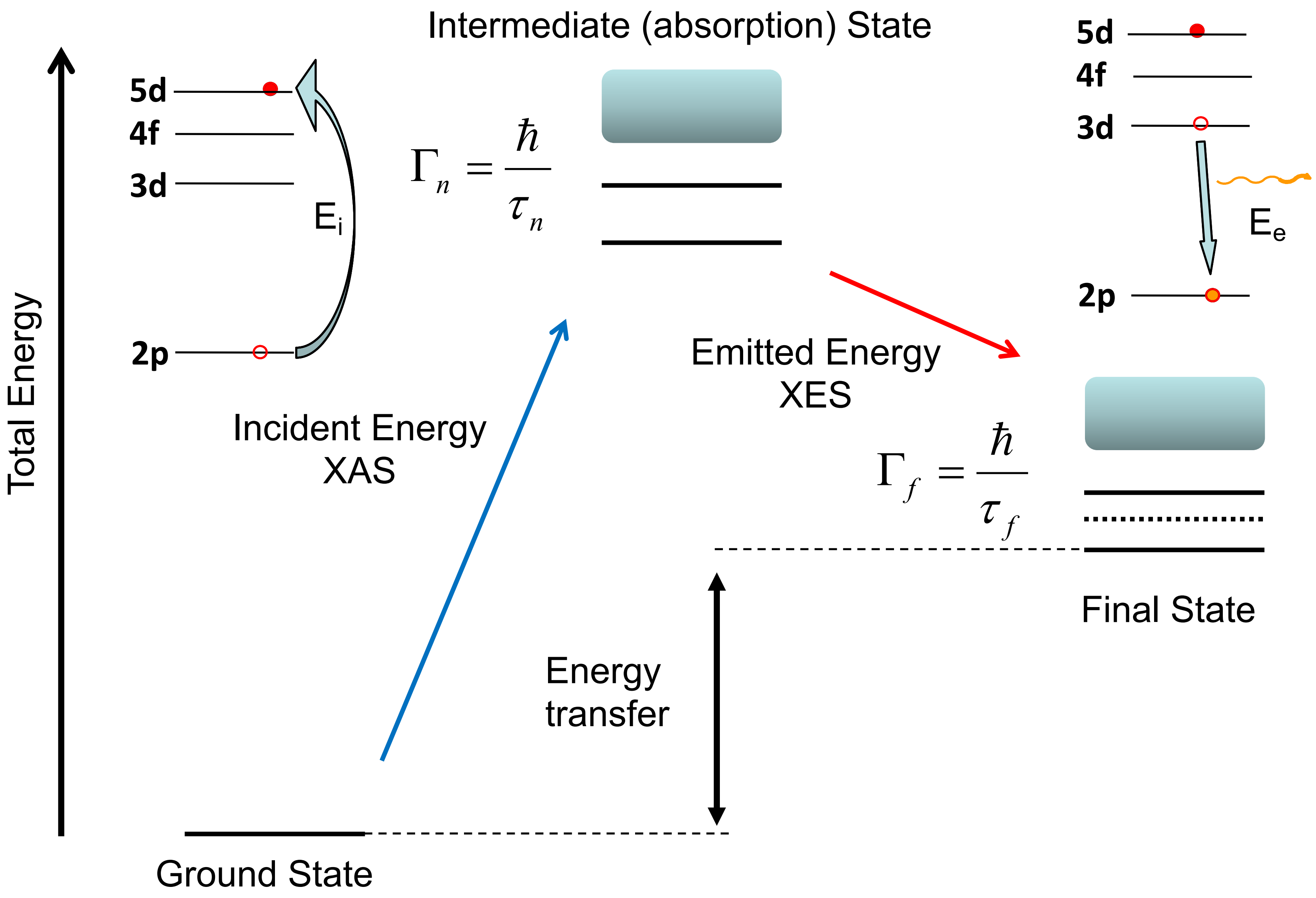

Intermediate (absorption) State

$$\Gamma_n = \frac{\hbar}{\tau_n}$$

Incident Energy
XAS

Emitted Energy
XES

$$\Gamma_f = \frac{\hbar}{\tau_f}$$

Energy
transfer

Ground State

Final State

The RIXS plane

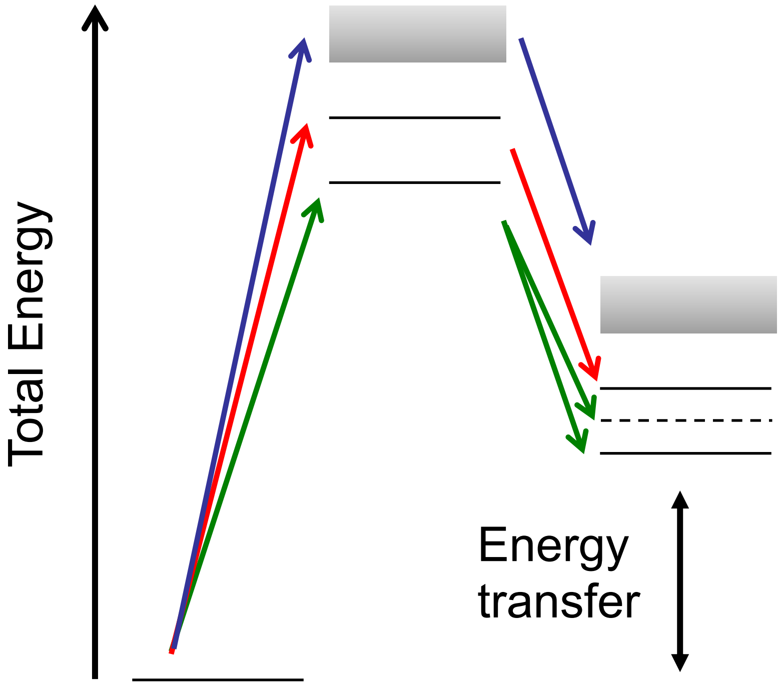

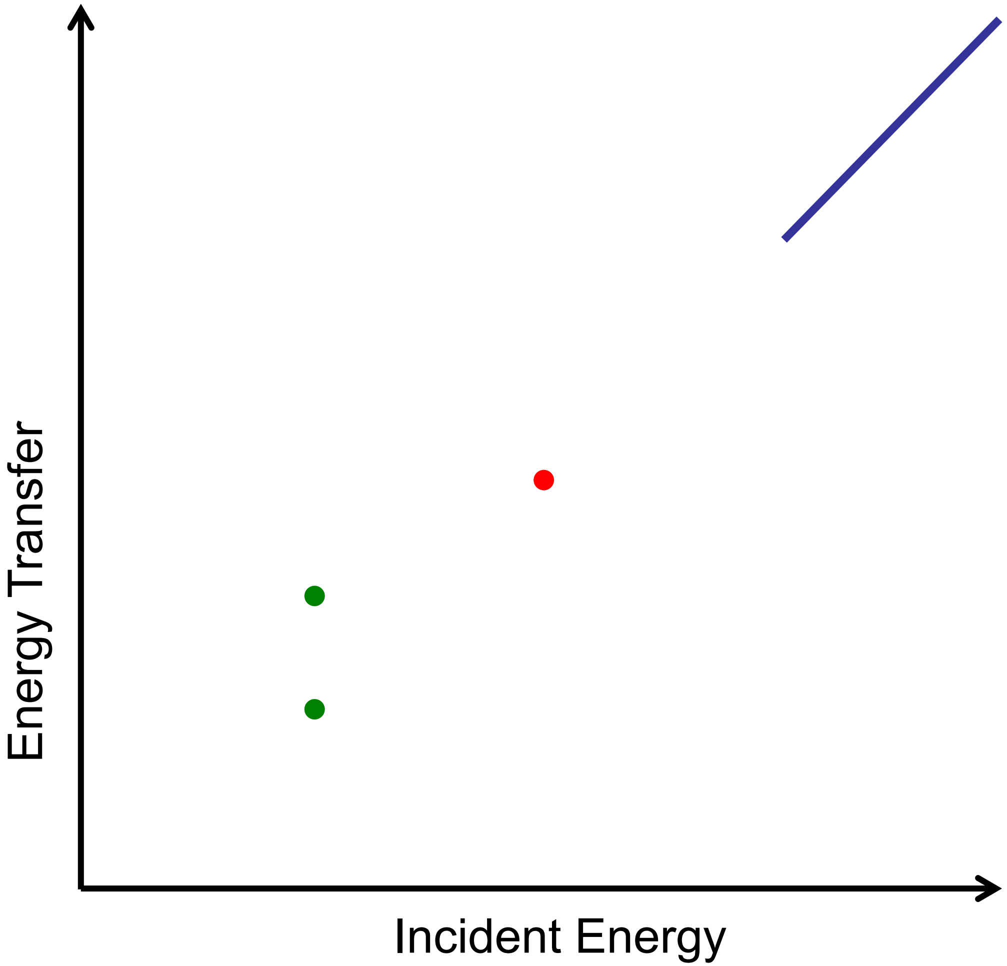

The RIXS/RXES plane

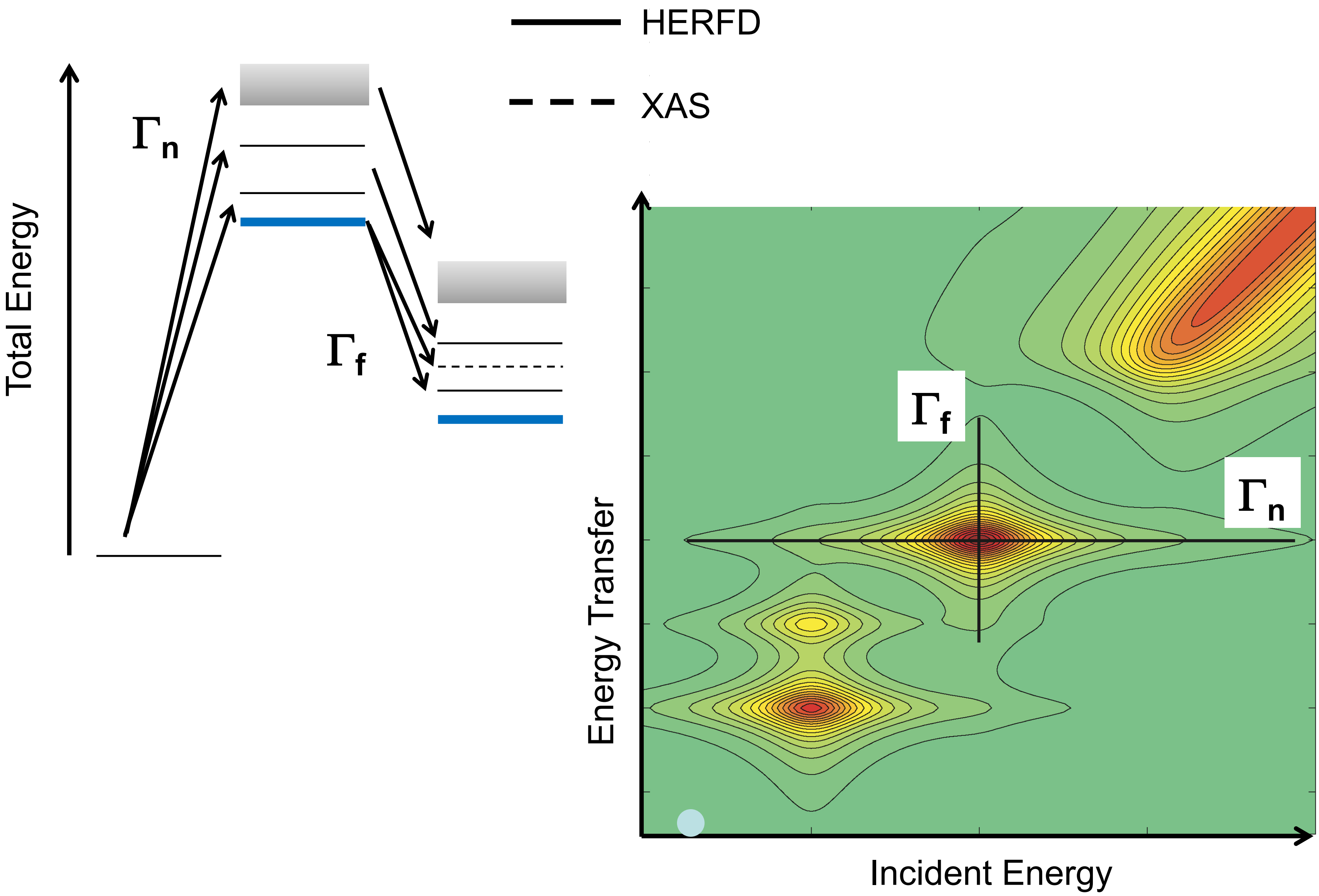

High Resolution Fluorescence Detection

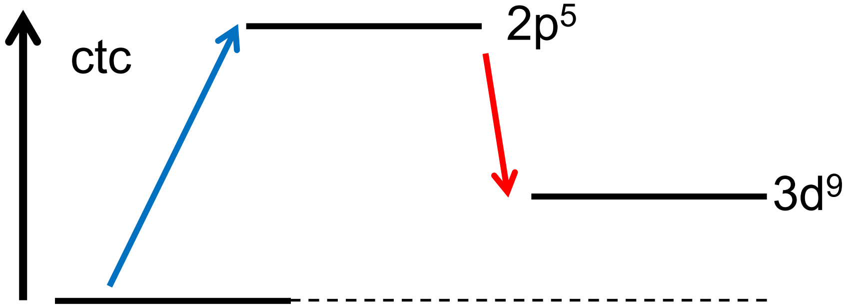

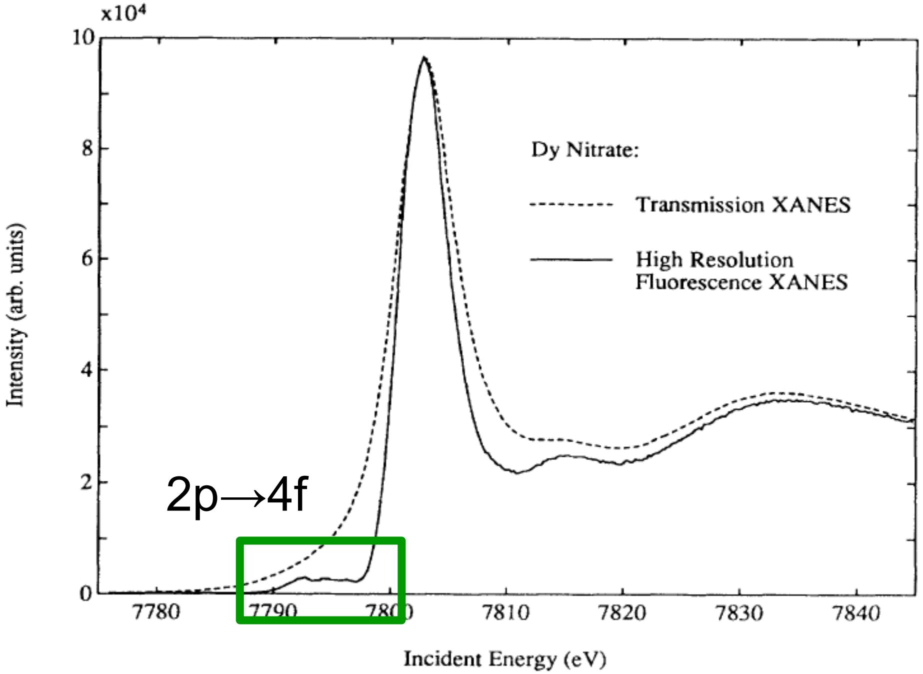

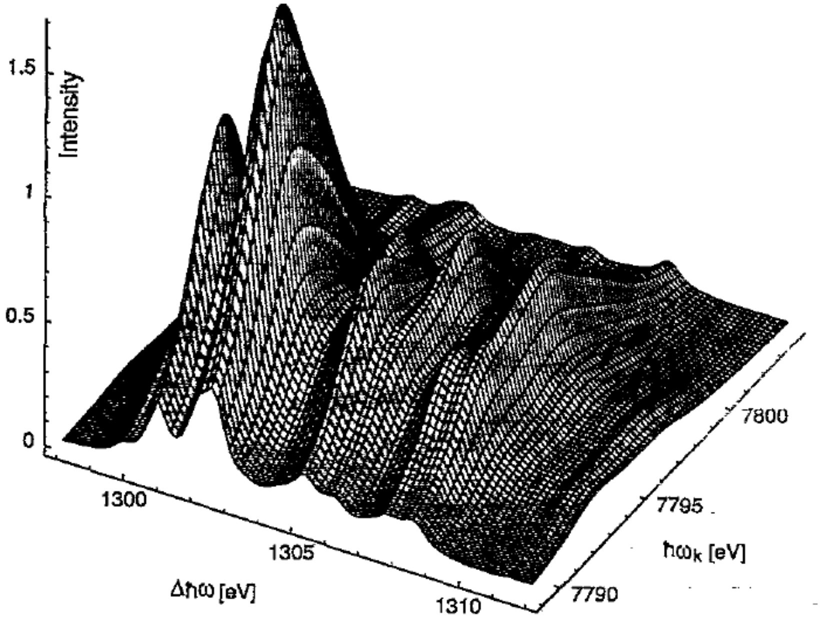

FIG. 2. Numerical calculation of the electric quadrupole → dipole part ($2p_{3/2} \rightarrow 4f$, $3d_{5/2} \rightarrow 2p_{3/2}$) of the RRS cross section at the L_3 edge of Dy^{3+}, as a function of ingoing and transferred photon energies.

Hämäläinen et al., PRL 67 2850 (1991)

Carra et al. PRL 74 3700 (1995)

CeO$_2$ XAS

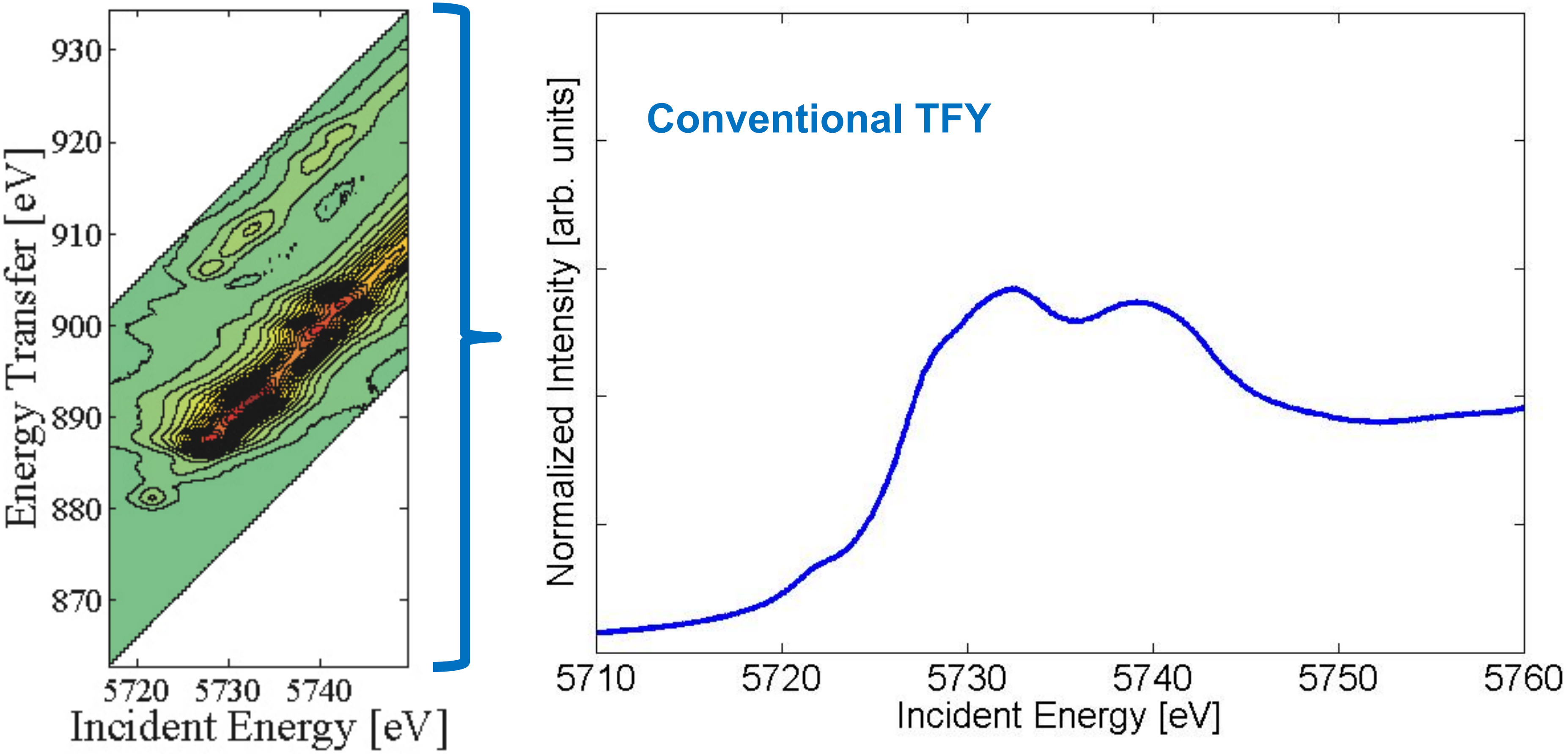
Energy Transfer [eV]
930
920
910
900
890
880
870
5720
5730
5740
Incident Energy [eV]
Conventional TFY
Normalized Intensity [arb. units]
5710
5720
5730
5740
5750
5760
Incident Energy [eV]

CeO_2 XAS

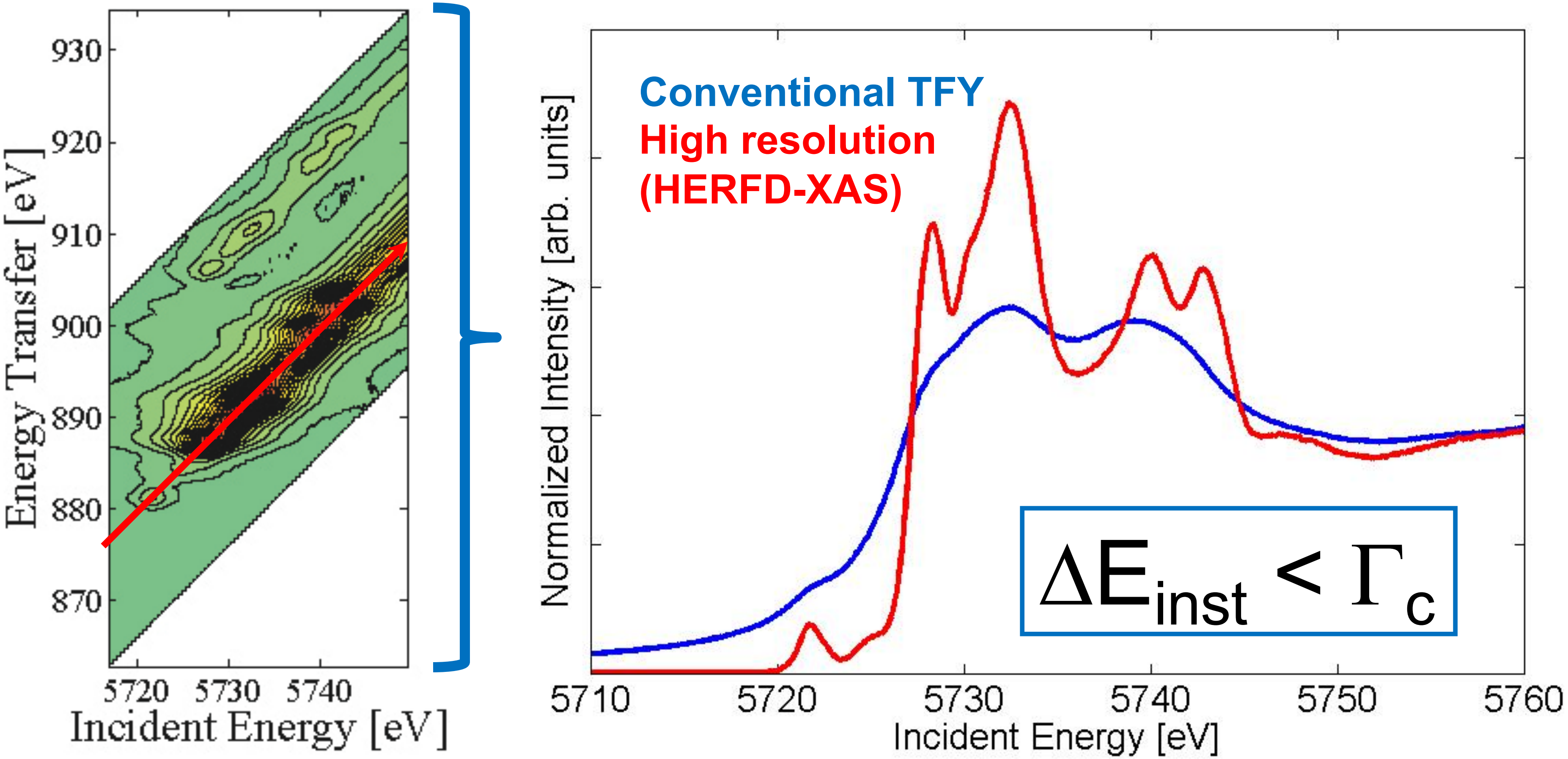

Fine structure of 5d band

$$\boxed{\Delta E_{inst} < \Gamma_c}$$

2p3d (Lα) RIXS plane in CeO_2

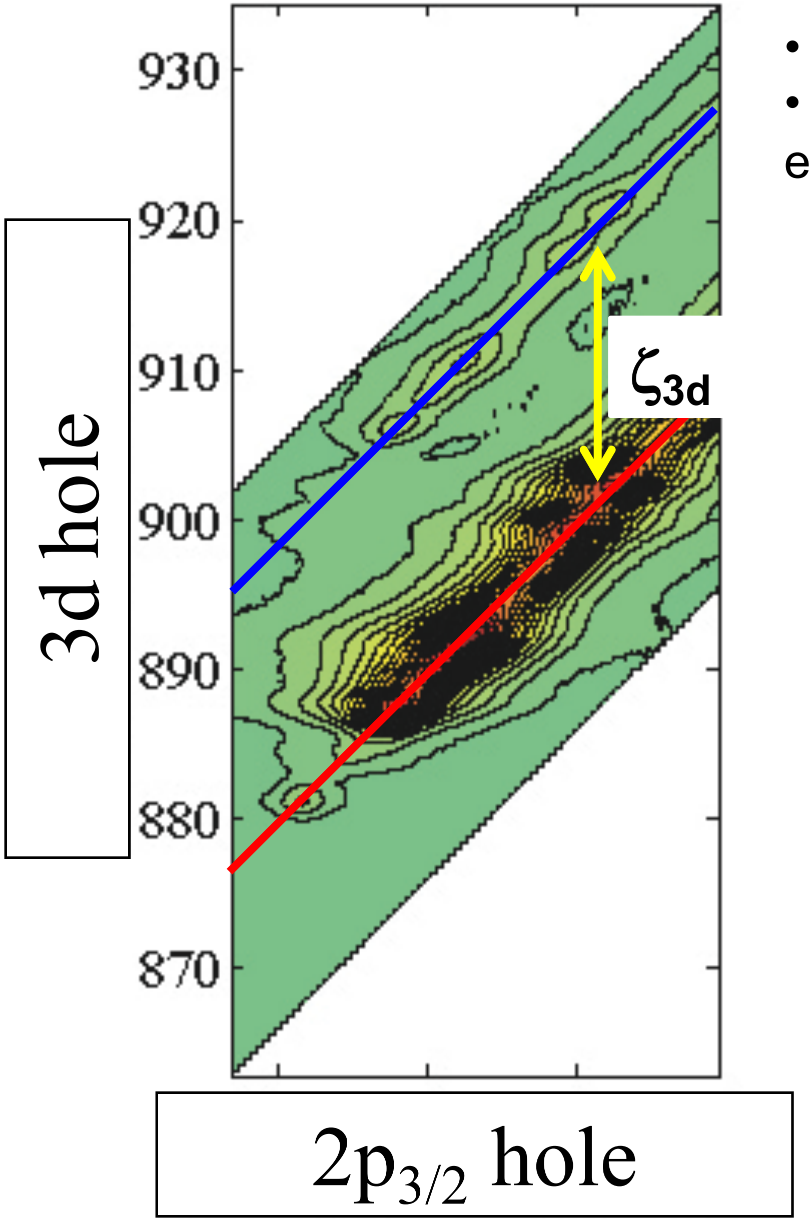

- The 3d and 2p core hole potentials are similar.
- Weak interaction of core hole with photoexcited electron

Spectral features appear along diagonal streak.

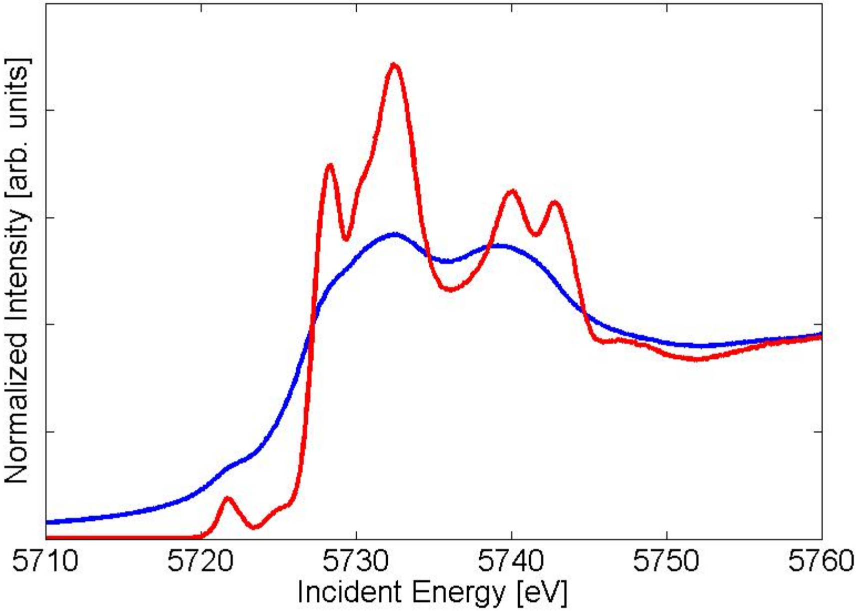

Hämäläinen et al., Phys. Rev. Lett. 67 2850 (1991)
Carra et al. PRL 74 3700 (1995)
Glatzel and Bergmann, Coord. Chem. Rev. 249 65 (2005)
Kotani et al., J. Electr. Spectr. Relat. Phenomena 184 (2011) 210–215

2p3d (Lα) RIXS plane in CeO_2

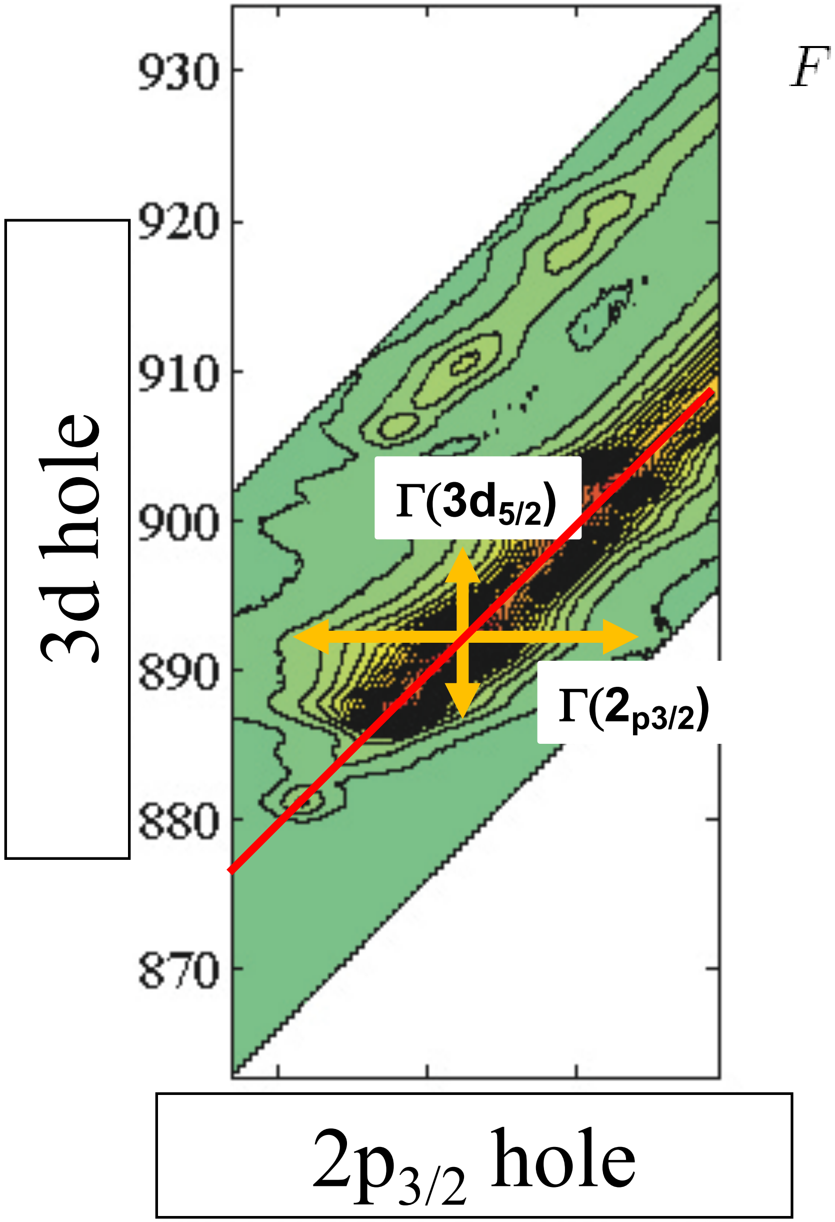

$$F(\Omega,\omega)=\sum_f \left|\sum_n \frac{\langle f|T_2|n\rangle\langle n|T_1|g\rangle}{E_g-E_n+\Omega-i\frac{\Gamma_n}{2}}\right|^2 \times \frac{\frac{\Gamma_f}{2\pi}}{(E_g-E_f+\Omega-\omega)^2+\frac{\Gamma_f^2}{4}}$$

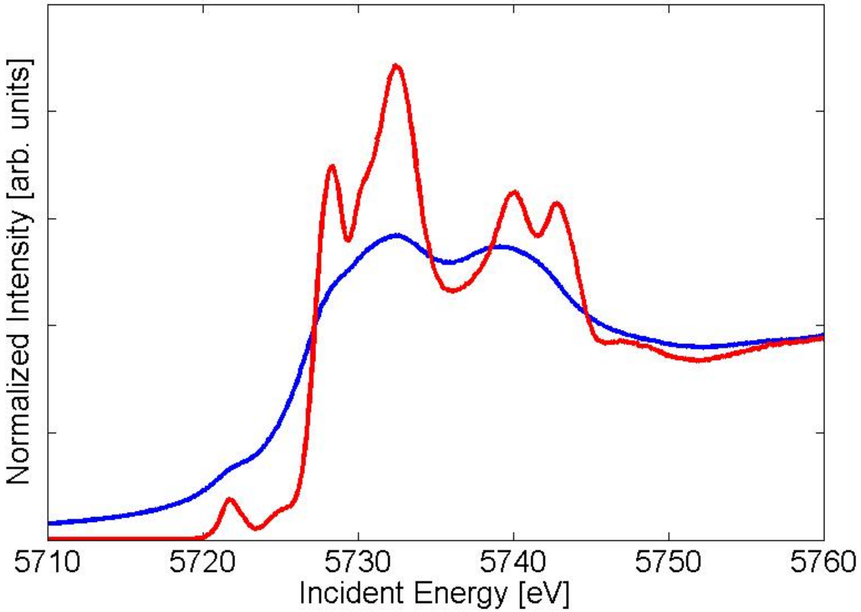

Hämäläinen et al., Phys. Rev. Lett. 67 2850 (1991)
Carra et al. PRL 74 3700 (1995)
Glatzel and Bergmann, Coord. Chem. Rev. 249 65 (2005)
Kotani et al., J. Electr. Spectr. Relat. Phenomena 184 (2011) 210–215

Direct study of the valence shell

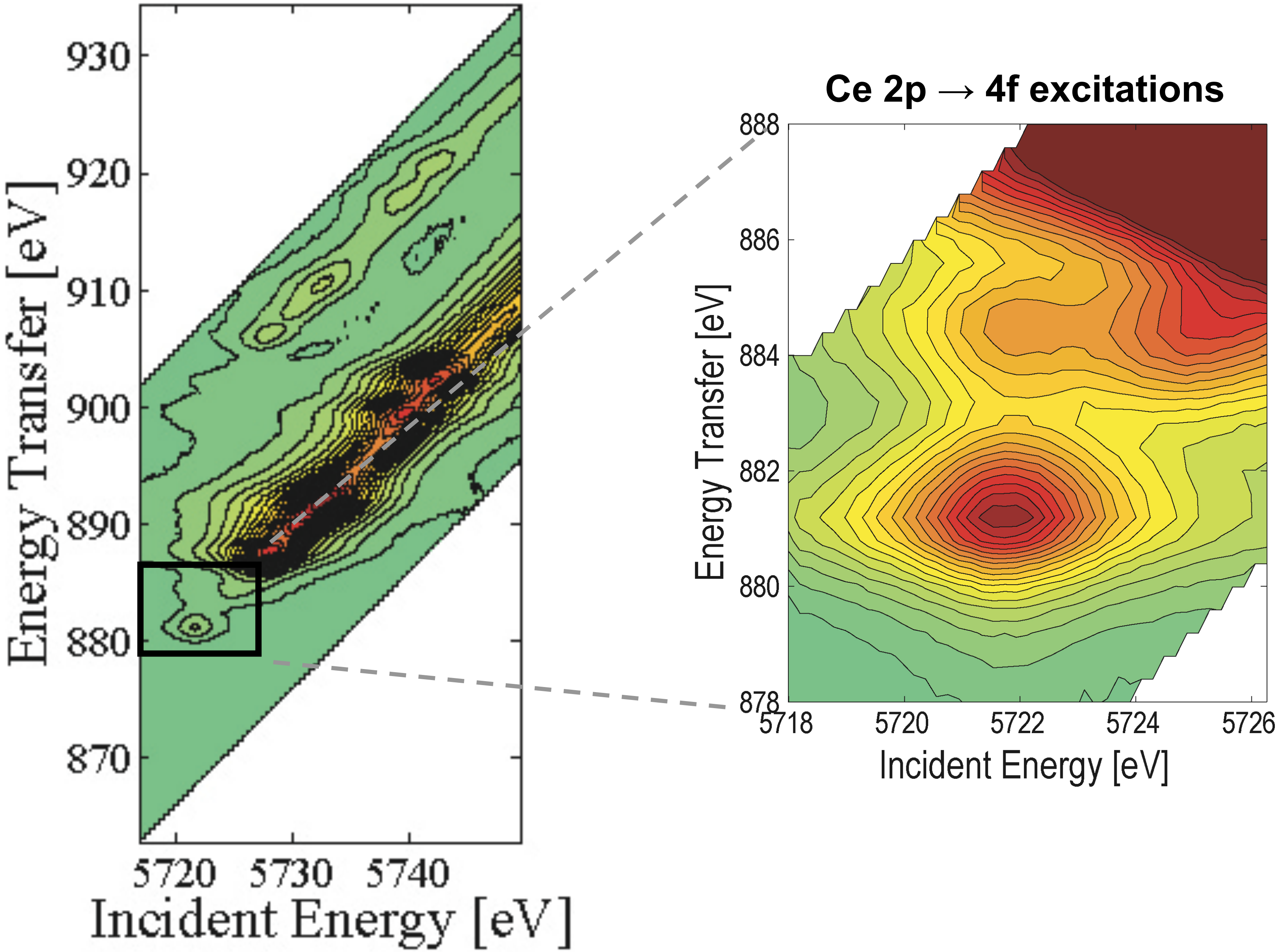

Another parameter for your energy calibration

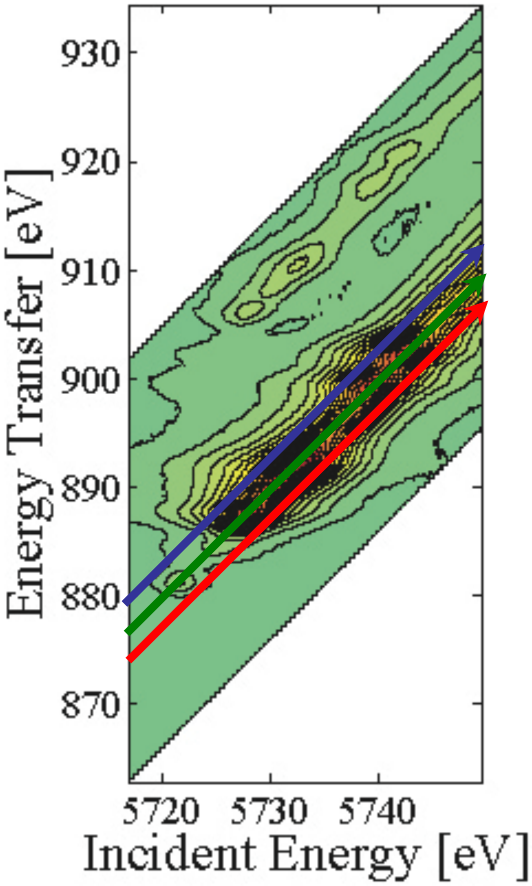

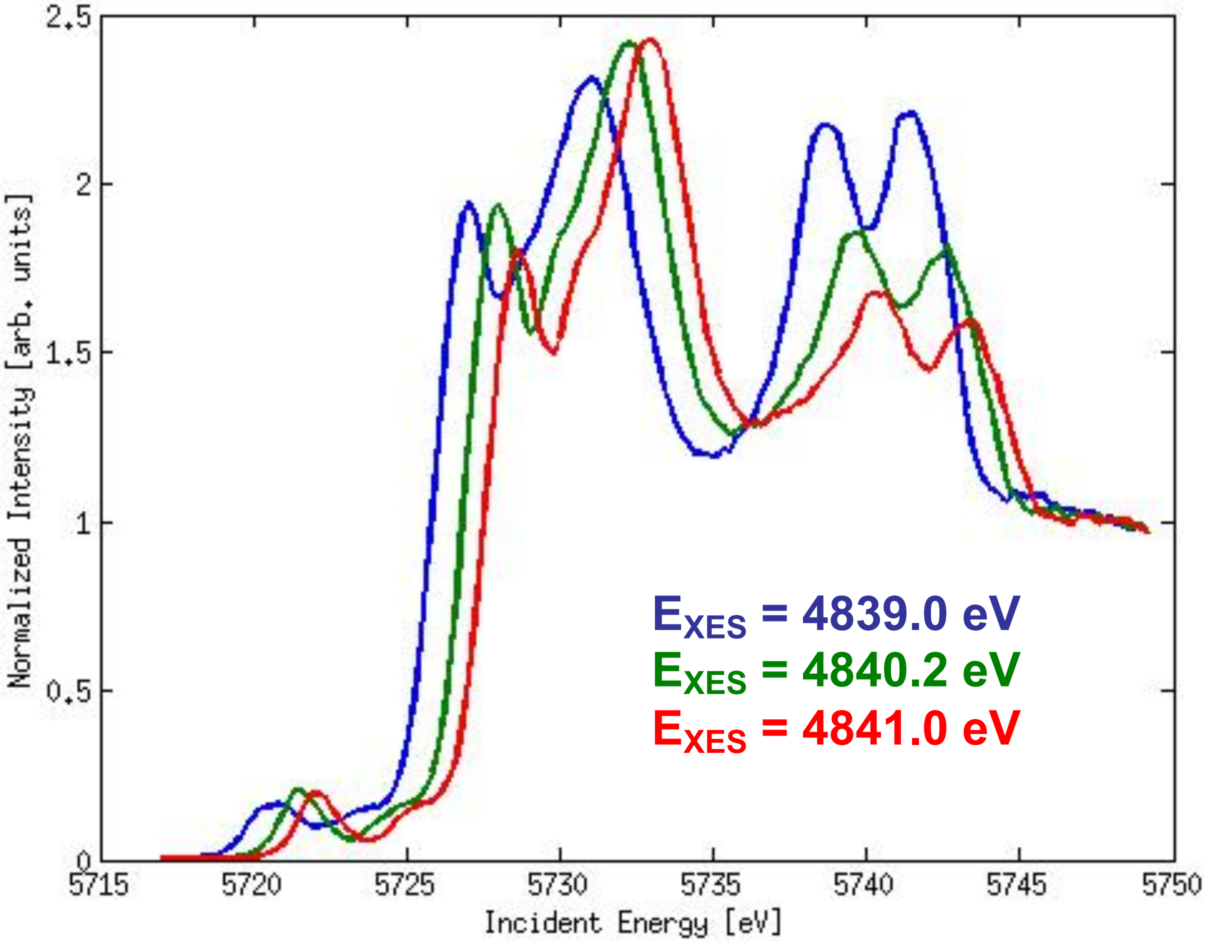

Keep E_{XES} constant !!

HERFD-XANES in Pt and W compounds

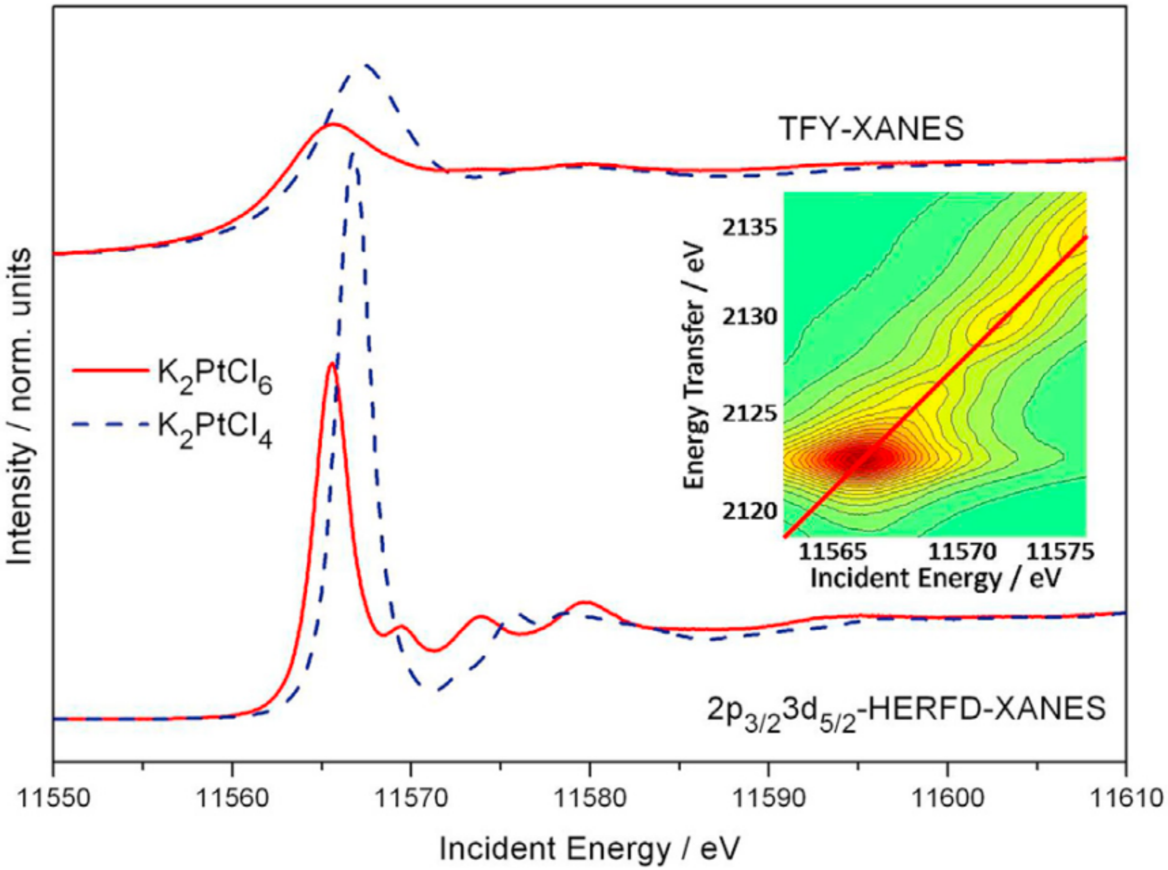

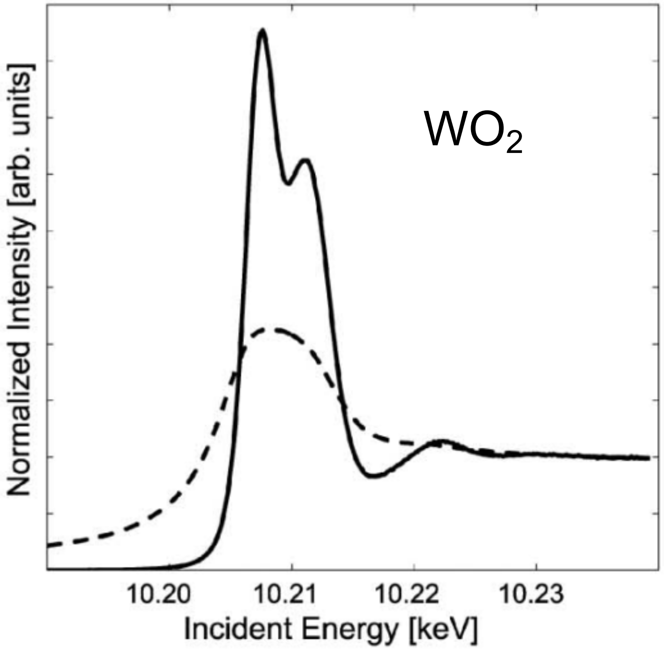

HERFD-XANES in Hg

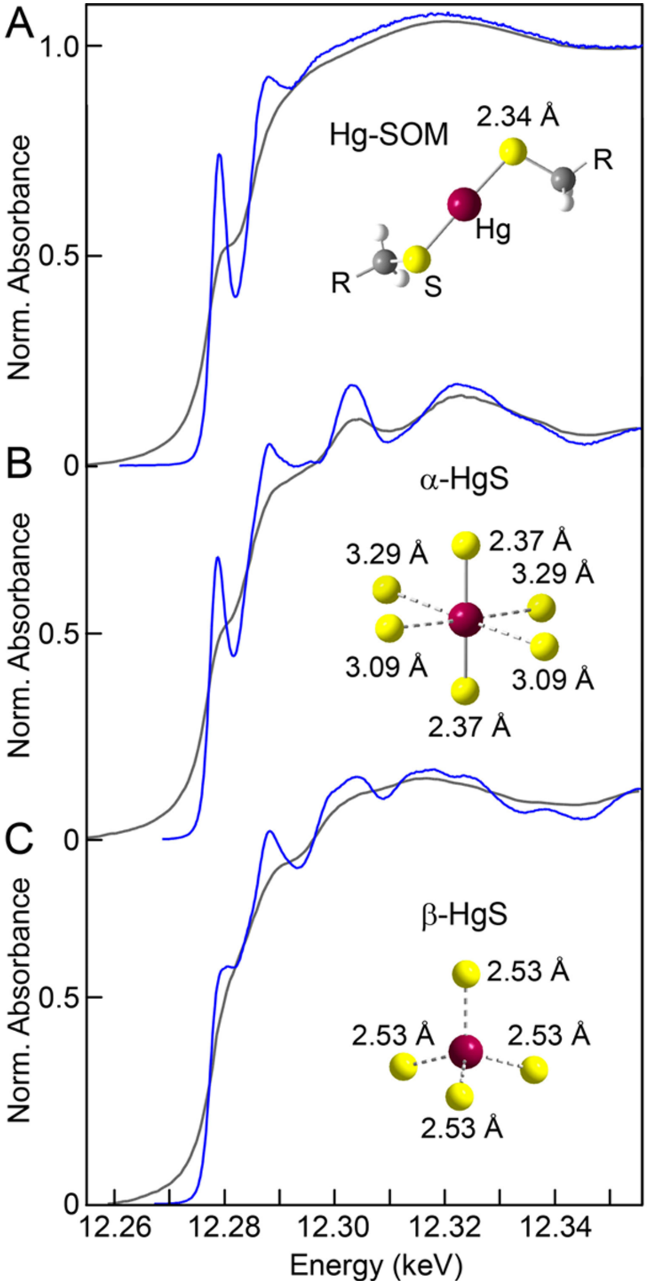

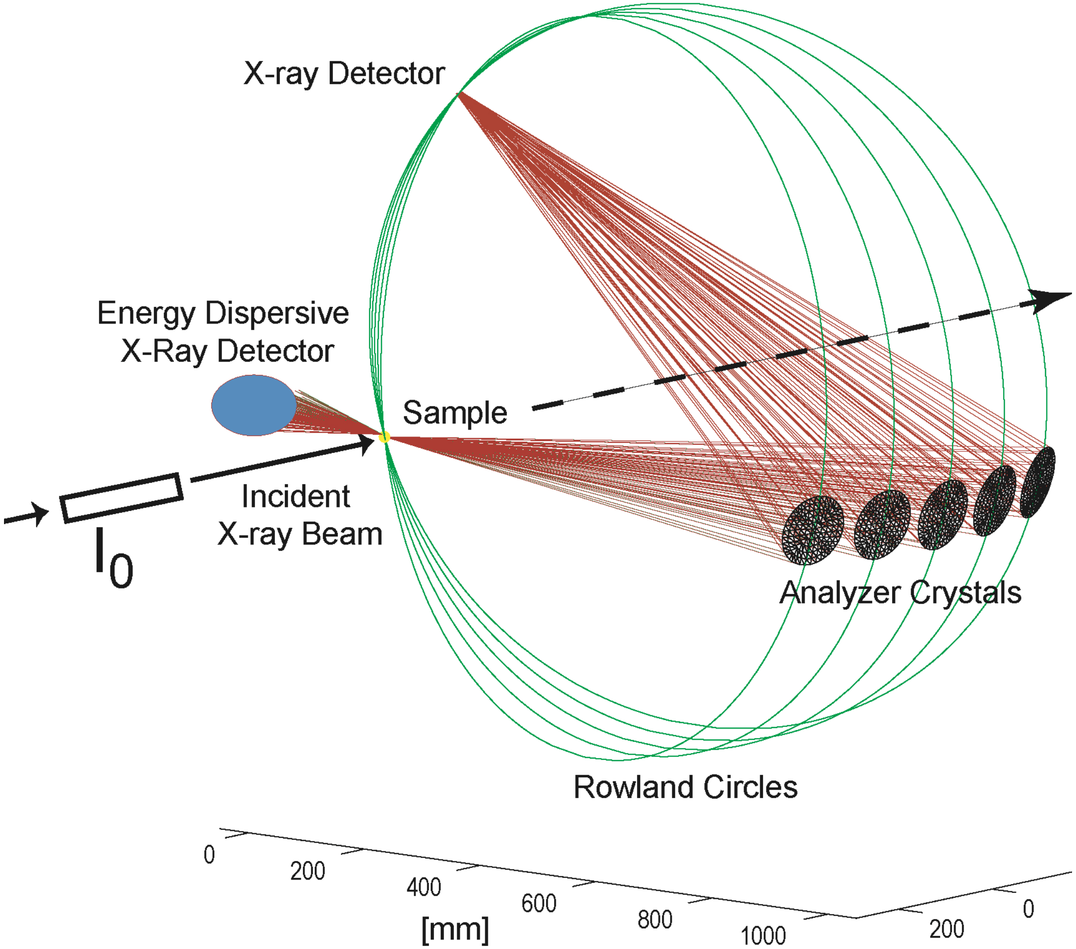

A. Manceau et al., Env. Sci. & Techn (2015)
A. Manceau et al., Inorg. Chem. (2015)

Actinides

Standard XANES at the U M4 edge

$\Delta E \sim 200eV$

Conventional

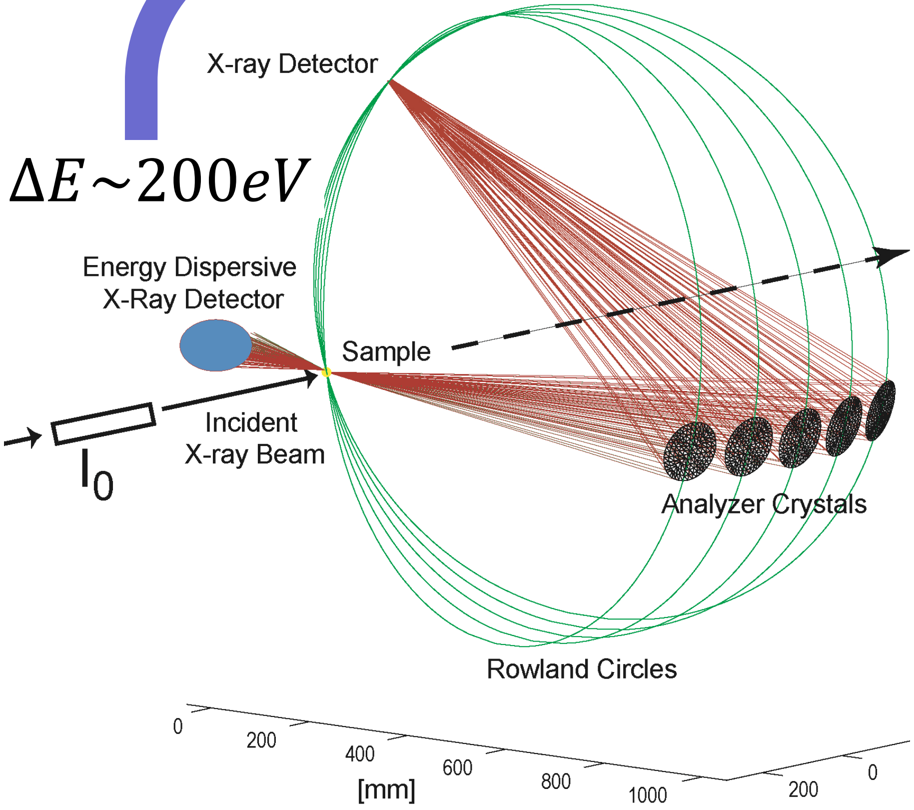

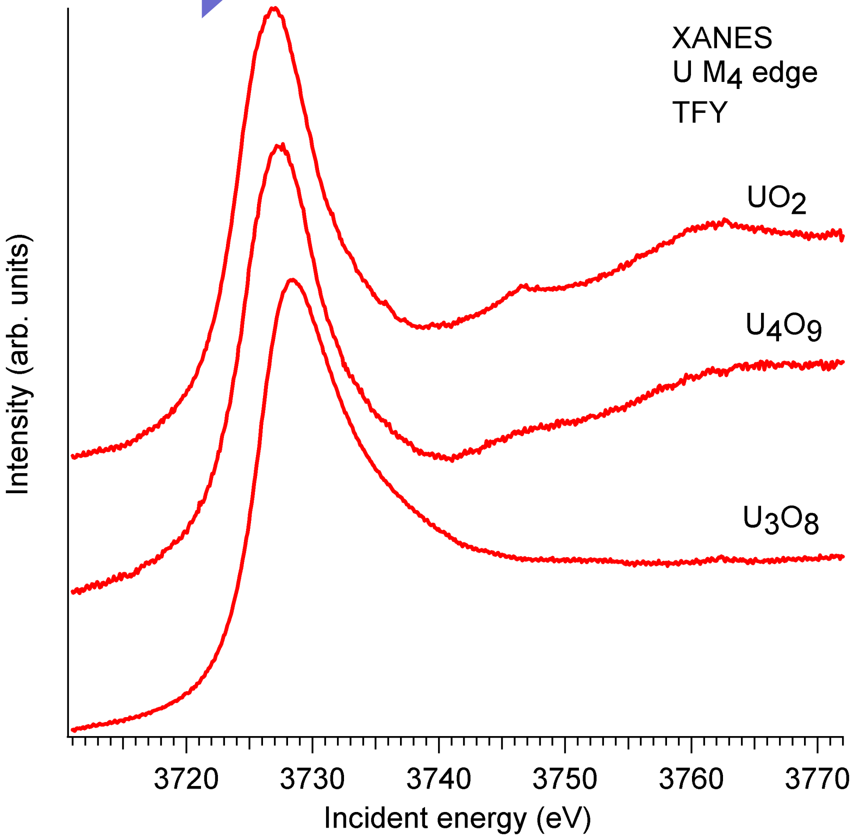

High energy resolution XANES at the U M4 edge

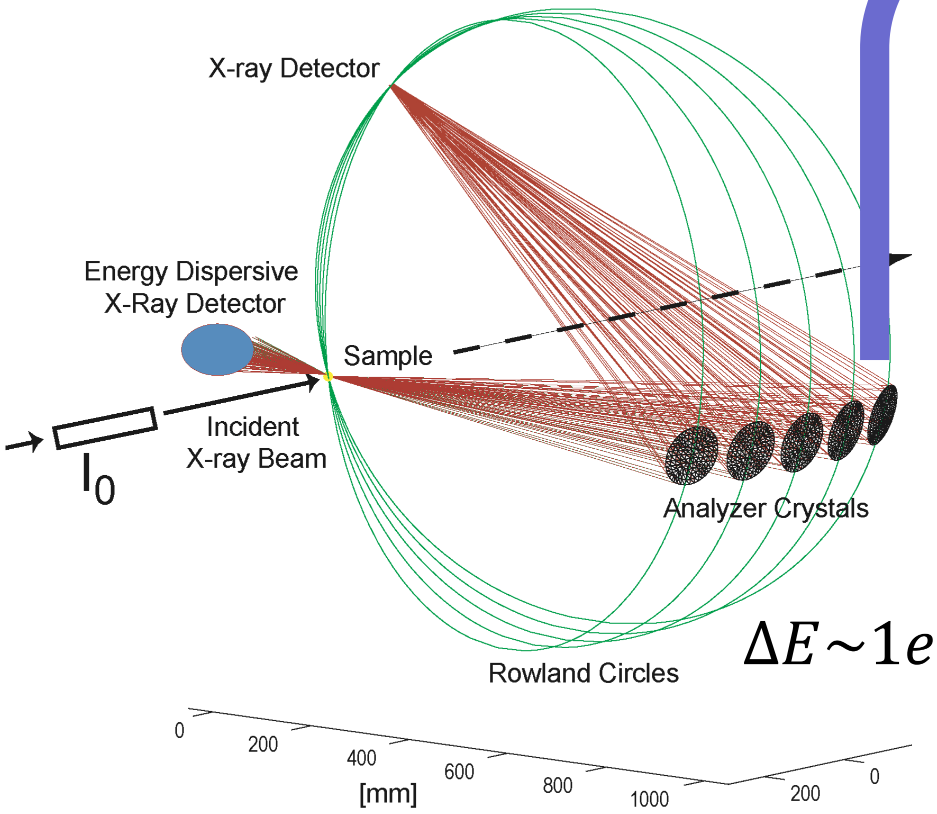

$\Delta E \sim 1 eV$

High energy resolution

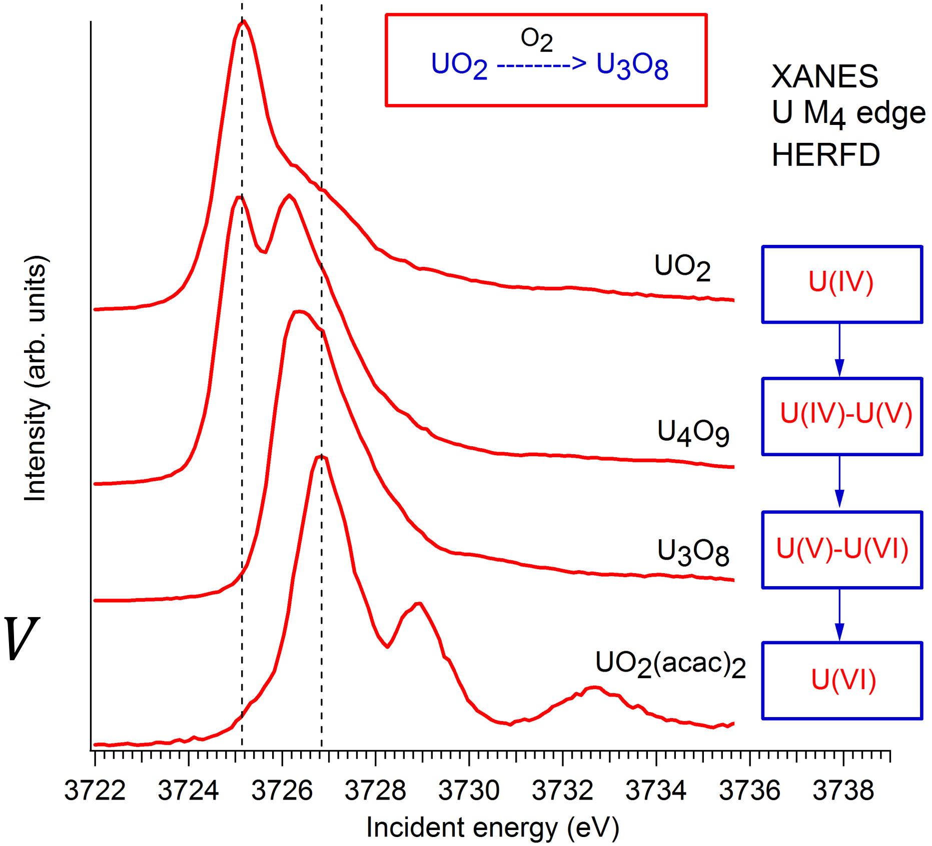

K. Kvashnina et al. PRL **111** 253002 (2013)

K. Kvashnina et al. Ang. Chemie, in press (2019)

Resonant inelastic X-ray scattering including the valence orbitals

Energy diagram in photon-in/photon-out spectroscopy

$$F^{KH}(\omega_{in},\omega_{out}) = \frac{\omega_{out}}{\omega_{in}} \sum_f \left| \sum_n \frac{\langle f|\hat{O}'^{\dagger}|n\rangle\langle n|\hat{O}|g\rangle}{E_n - E_g - \hbar\omega_{in} - i\Gamma_n} \right|^2 \delta\left(E_f - E_g - \hbar(\omega_{in} - \omega_{out})\right)$$

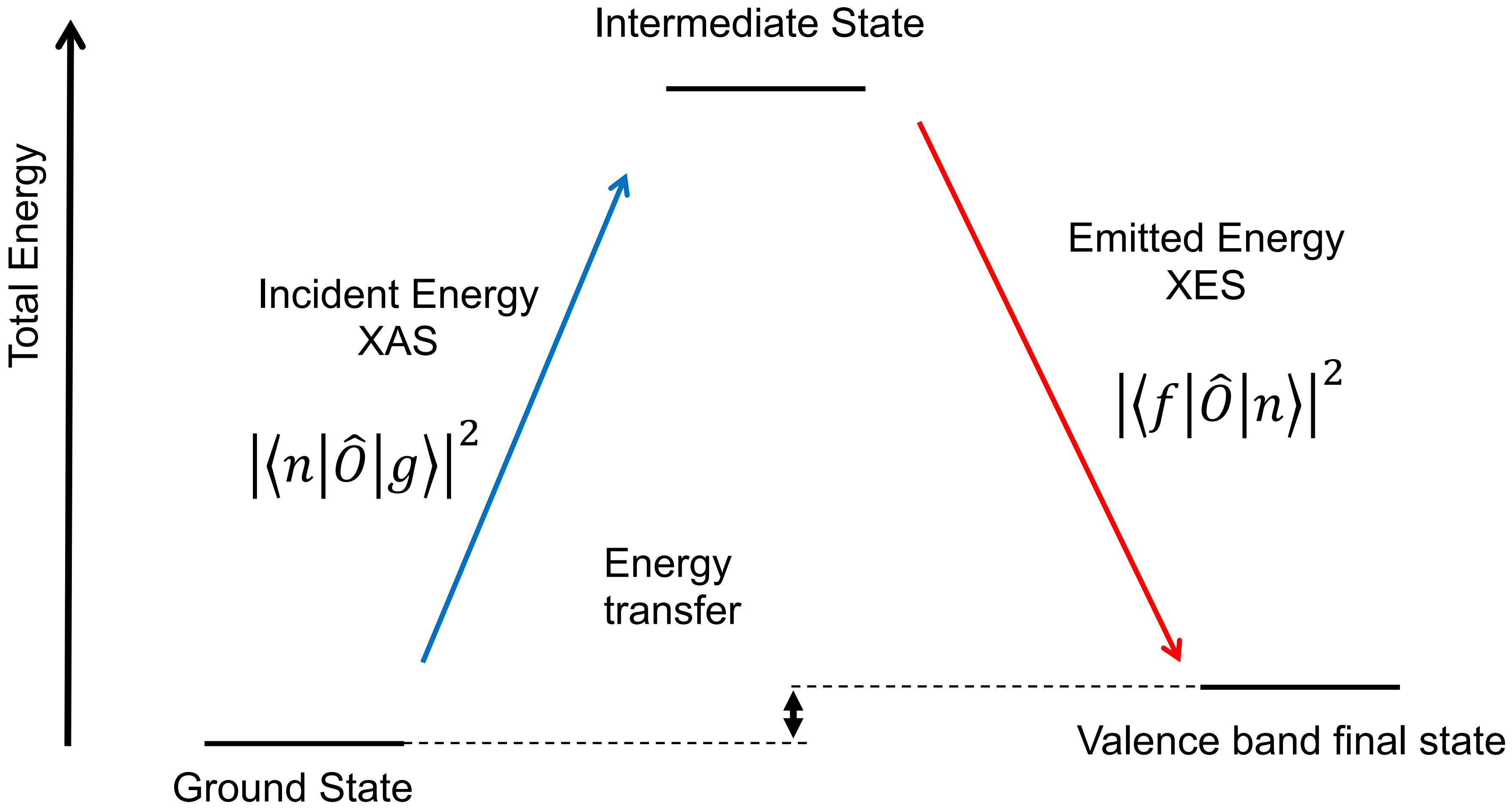

Intermediate State

Total Energy

Incident Energy
XAS

$$\left|\langle n|\hat{O}|g\rangle\right|^2$$

Emitted Energy
XES

$$\left|\langle f|\hat{O}|n\rangle\right|^2$$

Energy
transfer

Ground State

Valence band final state

Valence band UPS and surface chemistry

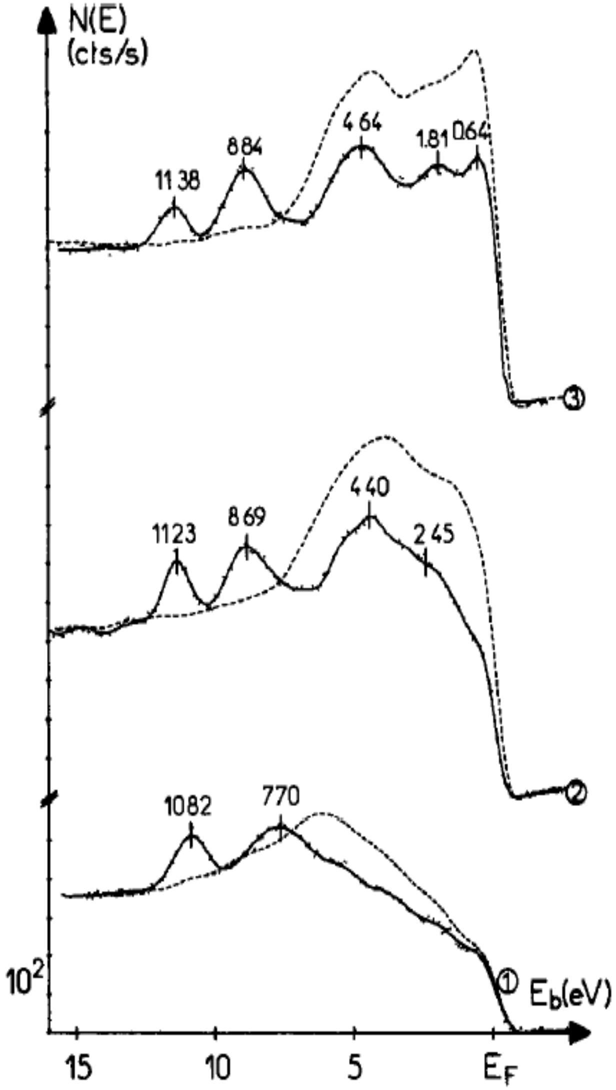

Fig. 2. UPS He II spectra of CO adsorbed on: (1) rhenium; (2) Pt–Re “alloy”; (3) platinum. The dashed curves are characteristic of the clean surfaces before exposition to CO.

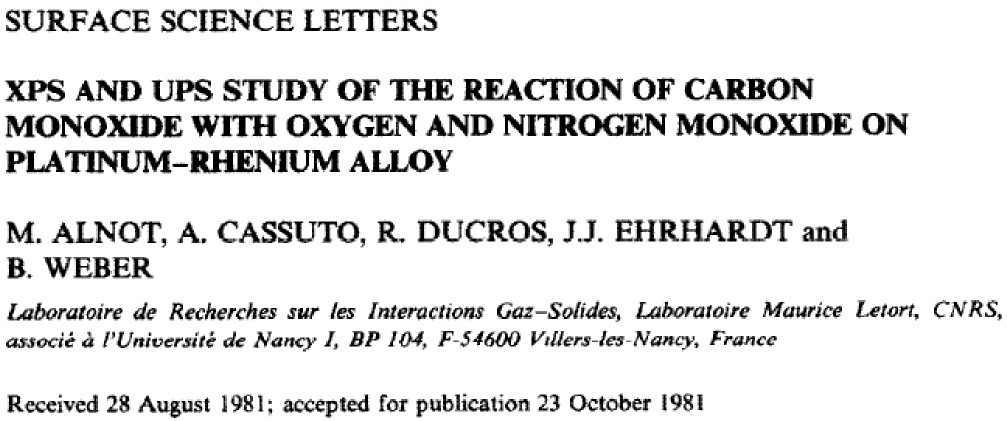
SURFACE SCIENCE LETTERS

XPS AND UPS STUDY OF THE REACTION OF CARBON MONOXIDE WITH OXYGEN AND NITROGEN MONOXIDE ON PLATINUM–RHENIUM ALLOY

M. ALNOT, A. CASSUTO, R. DUCROS, J.J. EHRHARDT and B. WEBER

Laboratoire de Recherches sur les Interactions Gaz–Solides, Laboratoire Maurice Letort, CNRS, associé à l'Université de Nancy I, BP 104, F-54600 Villers-les-Nancy, France

Received 28 August 1981; accepted for publication 23 October 1981

UHV conditions

No working conditions

Study the occupied DOS using hard X-rays.

CO oxidation over supported Pt nanoparticles

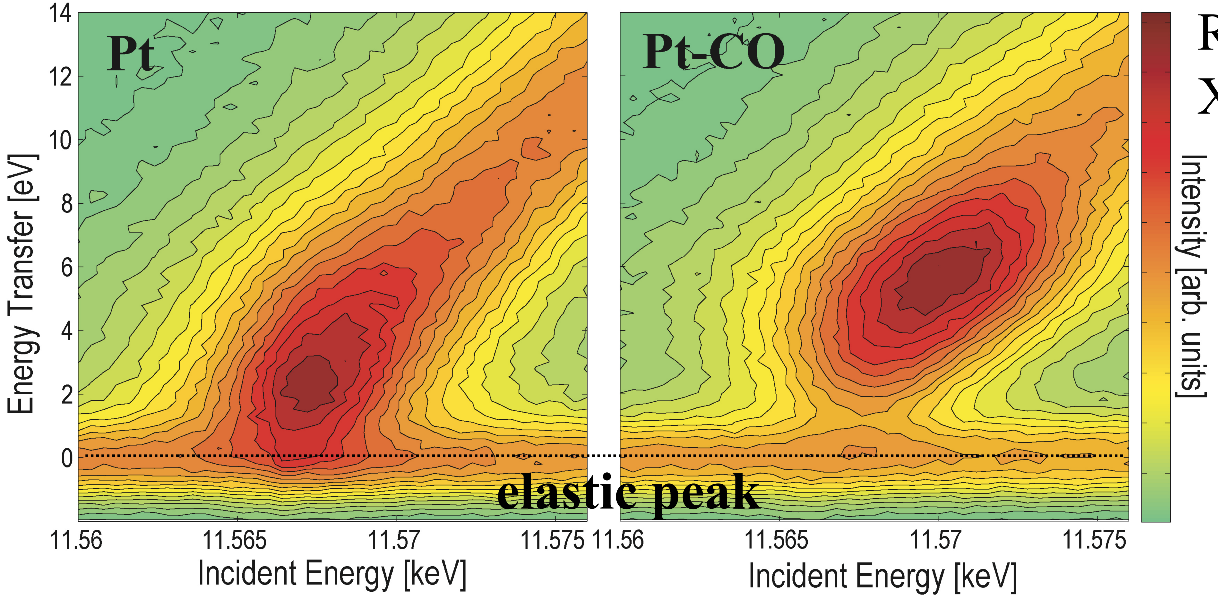

Resonant Inelastic
X-Ray Scattering (RIXS)

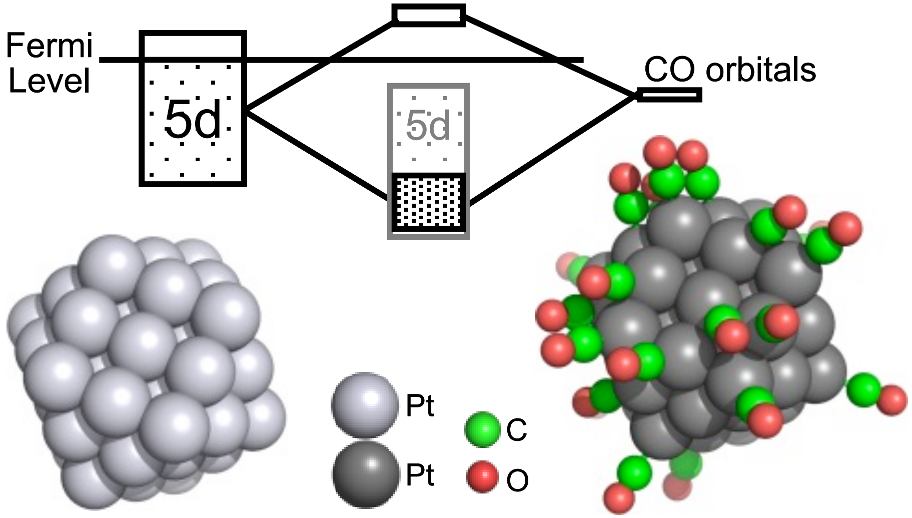

Direct observation of the Pt d-DOS under *in-situ* (*operando*) conditions

P. Glatzel, J. Singh, K. Kvashnina, J. van Bokhoven, JACS, 132, 2555-2557 (2010)

Simplifying the Kramers-Heisenberg Formula

$$F^{KH}(\omega_{in},\omega_{out}) = \frac{\omega_{out}}{\omega_{in}} \sum_f \boxed{\left| \sum_n \frac{\langle f|\hat{O}'^{\dagger}|n\rangle\langle n|\hat{O}|g\rangle}{E_n - E_g - \hbar\omega_{in} - i\Gamma_n} \right|^2} \delta\left(E_f - E_g - \hbar(\omega_{in} - \omega_{out})\right)$$

Interference changes intensities.

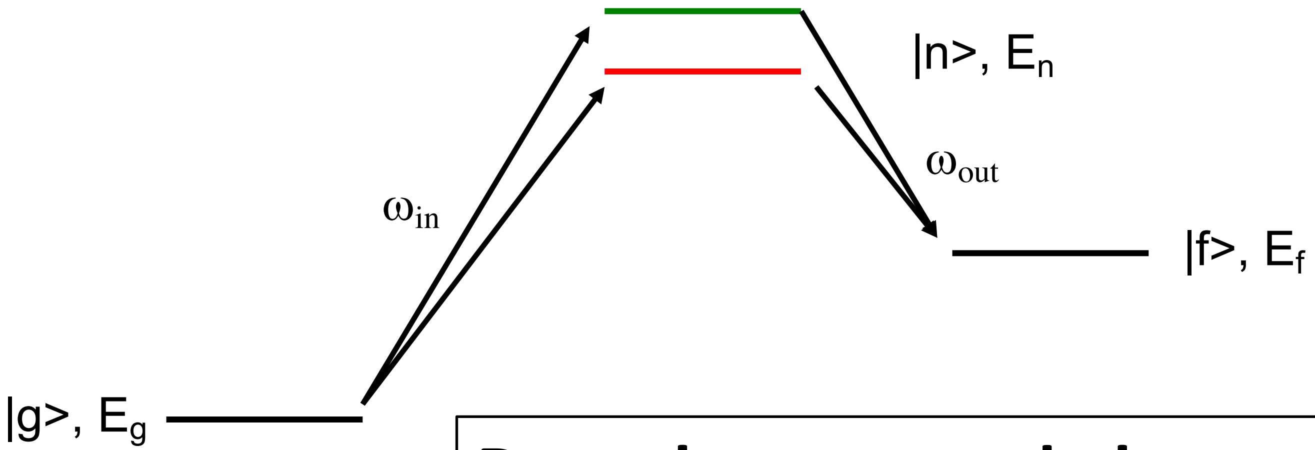

Does the scattered photon forget?

Ignore Interference and simplify:

$$F^{KH}(\omega_{in},\omega_{out}) = \frac{\omega_{out}}{\omega_{in}} \sum_f \boxed{\sum_n \frac{\text{XES} \quad \text{XAS}}{(E_n - E_g - \hbar\omega_{in})^2 + \Gamma_n^2}} \delta\left(E_f - E_g - \hbar(\omega_{in} - \omega_{out})\right)$$

Using the density of states

$$F^{KH}(\omega_{in},\omega_{out})=\frac{\omega_{out}}{\omega_{in}}\sum_f\sum_n\frac{\left|\langle f|\hat{O}'^{\dagger}|n\rangle\right|^2\left|\langle n|\hat{O}|g\rangle\right|^2}{(E_n-E_g-\hbar\omega_{in})^2+\Gamma_n^2}\delta\big(E_f-E_g-\hbar(\omega_{in}-\omega_{out})\big)$$

Approximate with density of states:

Unoccupied: $\left|\langle n|\hat{O}|g\rangle\right|^2 \to \rho'(\varepsilon_u)$

Occupied: $\left|\langle f|\hat{O}'|n\rangle\right|^2 \to \rho(\varepsilon_o)$

$$F(\Omega,\omega)=\int_\varepsilon d\varepsilon\,\frac{\rho(\varepsilon)\rho'(\varepsilon+\Omega-\omega)}{(\varepsilon-\omega)^2+\frac{\Gamma_n^2}{4}}$$

Jimenez-Mier, J. et al. *Phys. Rev. B* **1999**, *59*, 2649.

DOS calculations using FEFF84

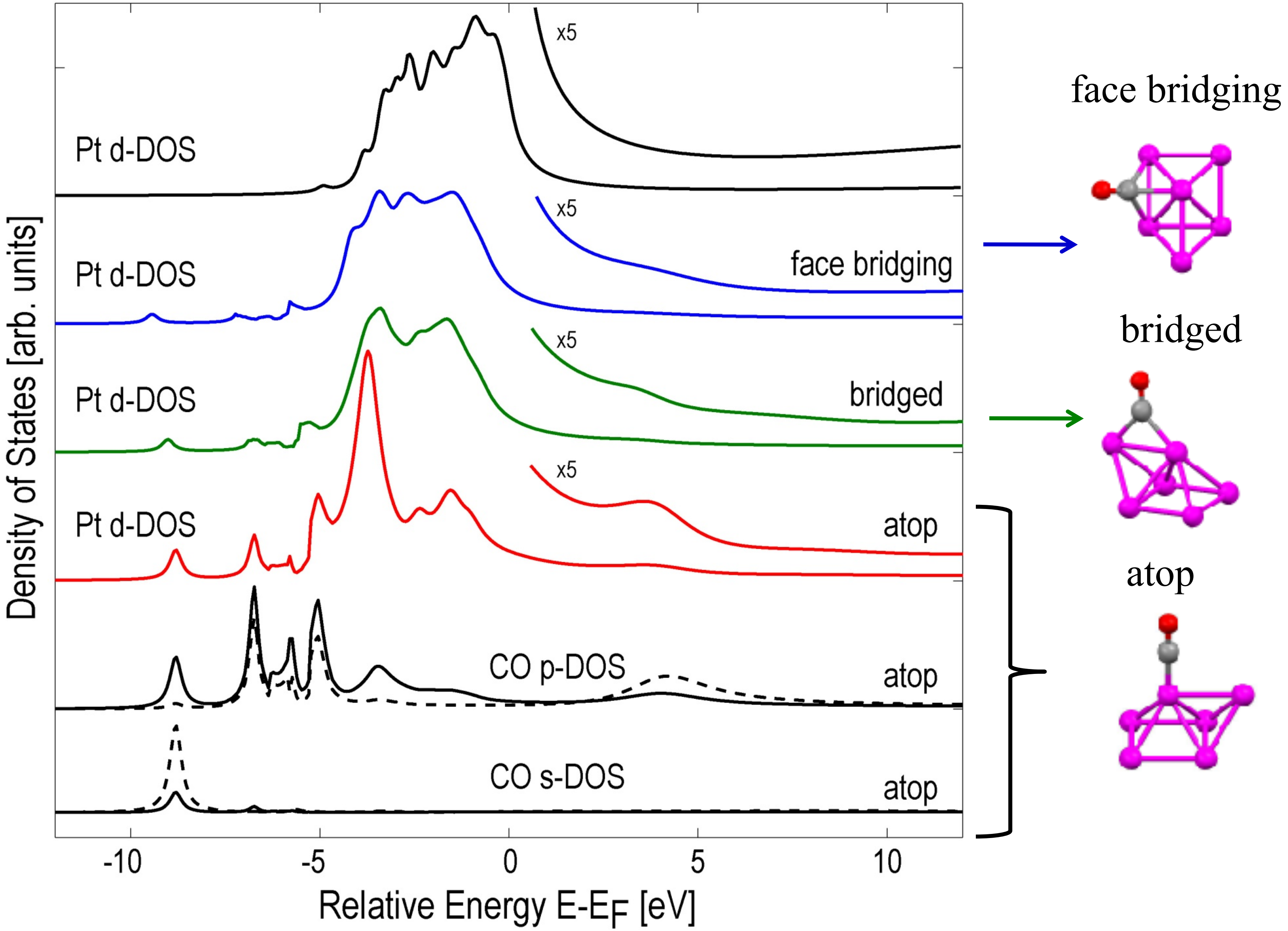

RIXS planes using FEFF d-DOS

Bare

Atop

Bridged

Face bridging

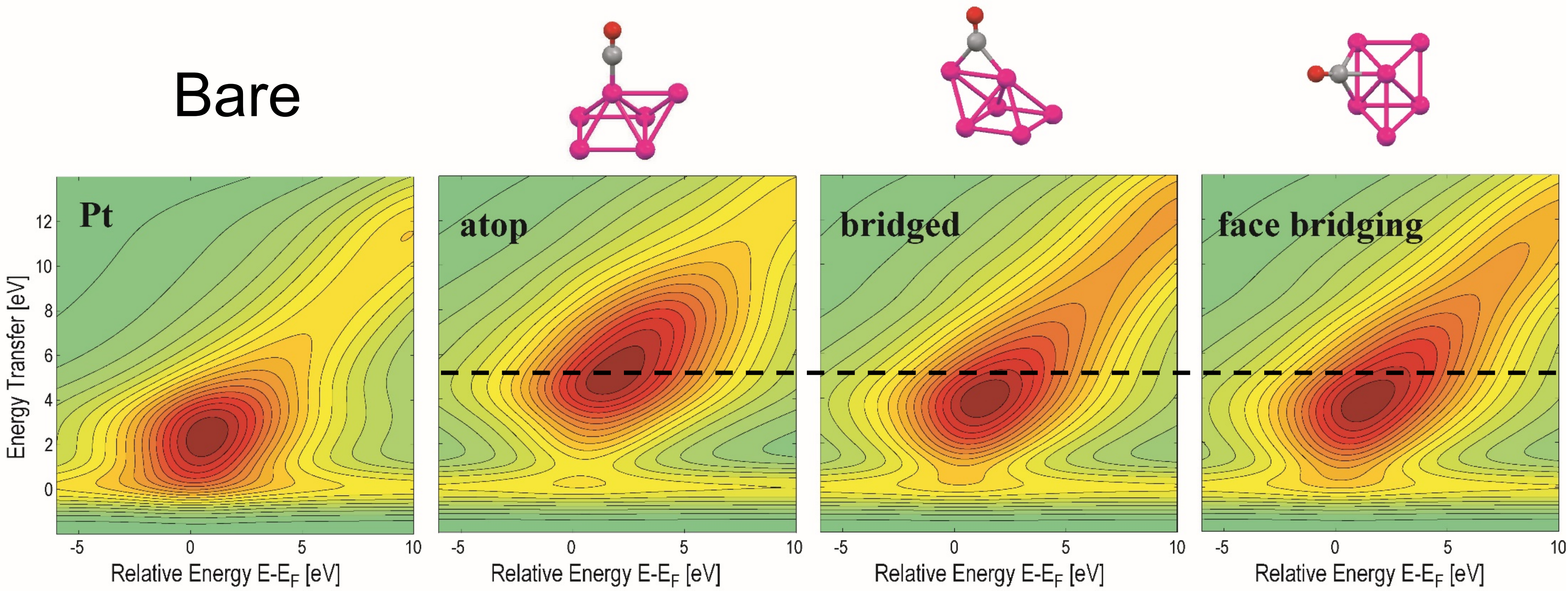

$$F(\Omega,\omega)=\int_{\varepsilon} d\varepsilon\,\frac{\rho(\varepsilon)\rho'(\varepsilon+\Omega-\omega)}{(\varepsilon-\omega)^2+\frac{\Gamma_n^2}{4}}$$

Comparison with Experiment

Pronounced change of Pt d-DOS with strong Pt-CO bond → Passivation of active Pt sites

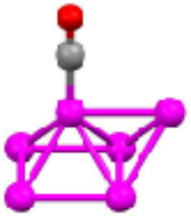

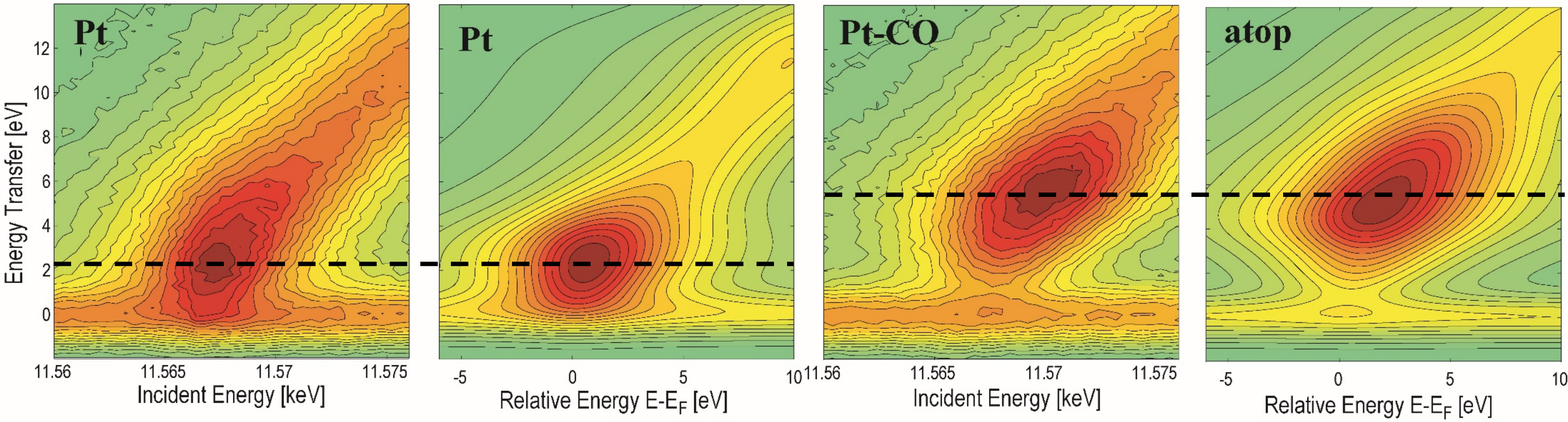

Direct probe of Pt d-DOS under *in situ* conditions

Improved instrumental resolution

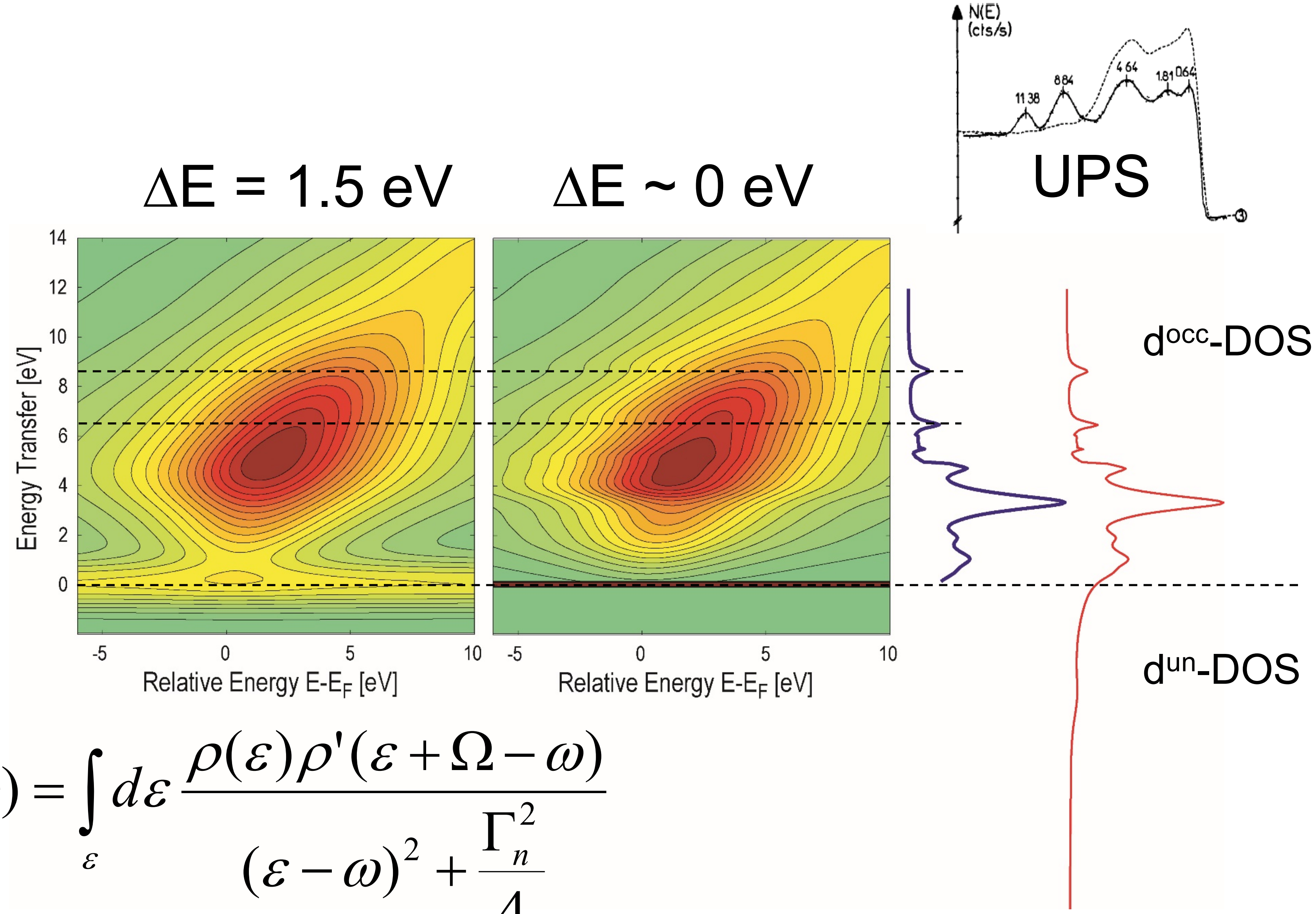

$$F(\Omega,\omega)=\int_{\varepsilon} d\varepsilon\,\frac{\rho(\varepsilon)\rho'(\varepsilon+\Omega-\omega)}{(\varepsilon-\omega)^2+\frac{\Gamma_n^2}{4}}$$

How to build a zeolitic lattice

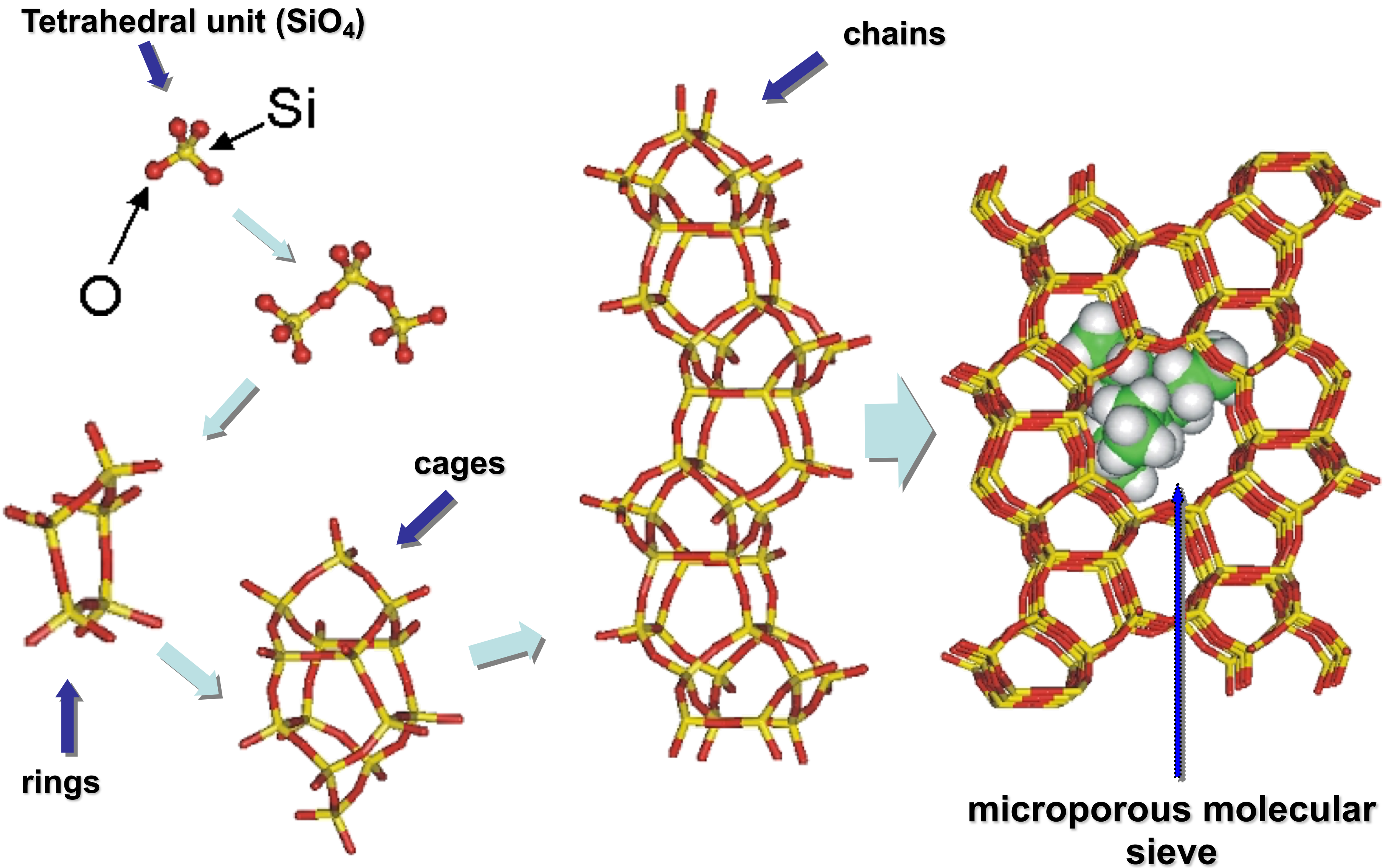

Tetrahedral unit (SiO_4)

rings

cages

chains

microporous molecular sieve

Titanium in Silicate – TS-1

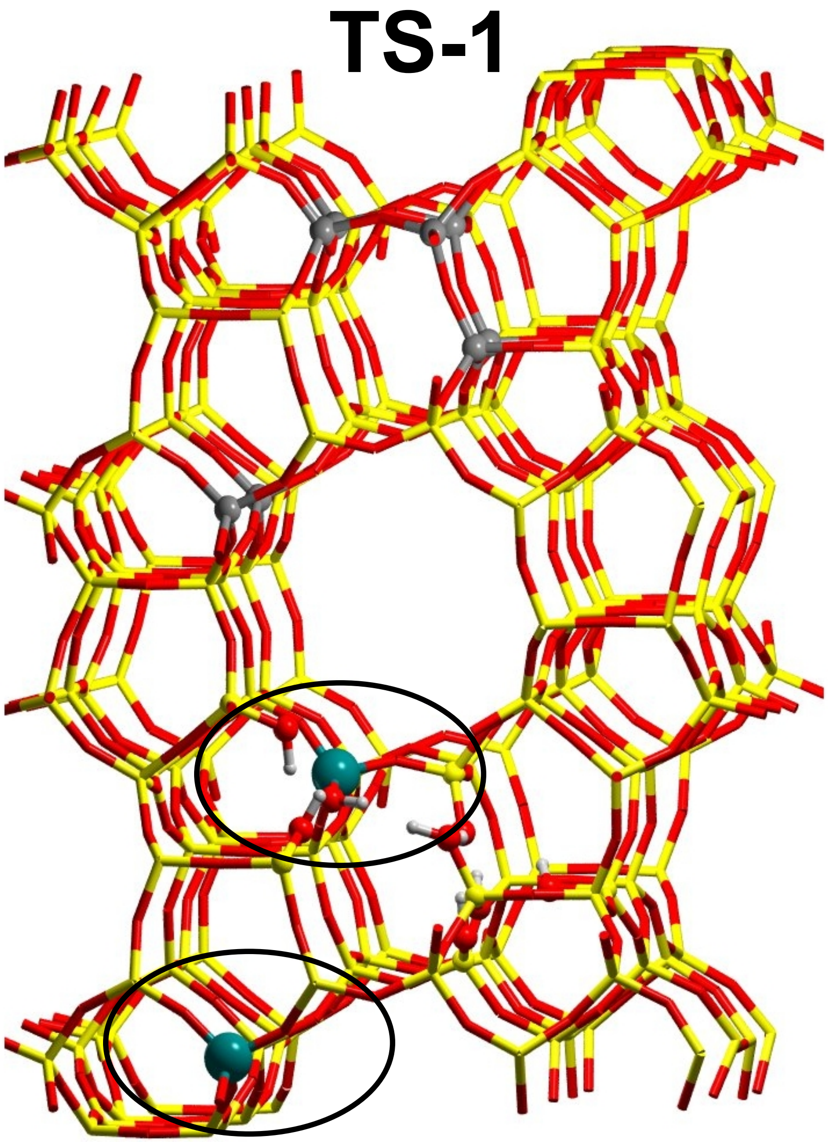

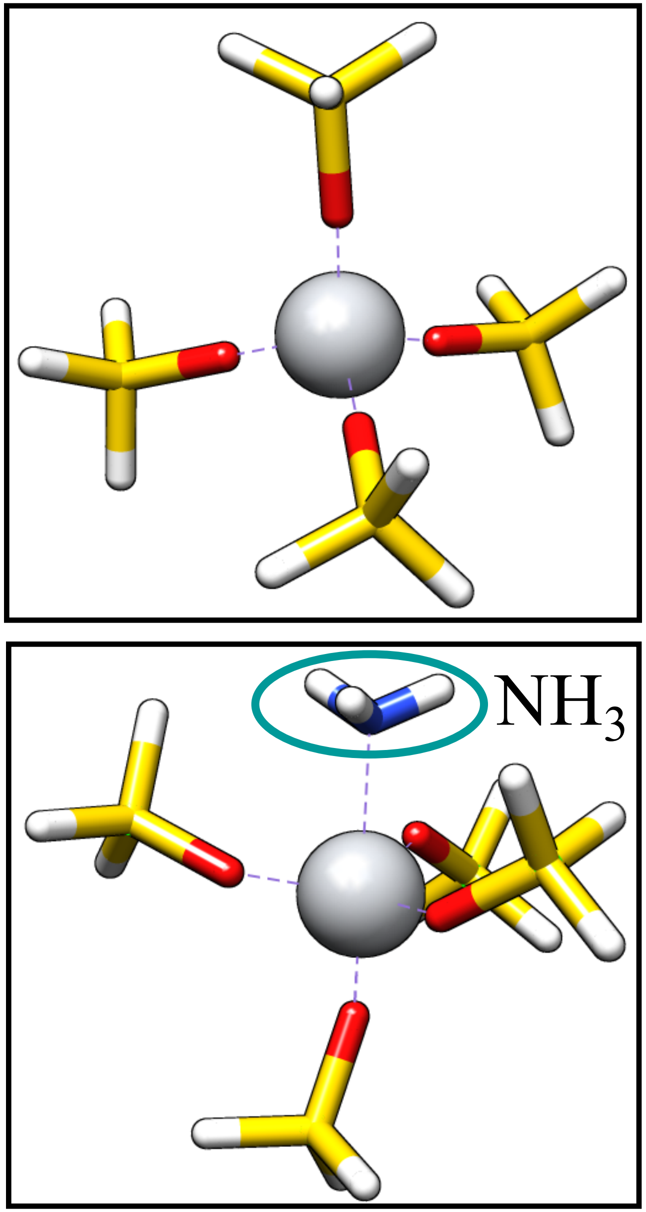

Titanium in Silicate – TS-1

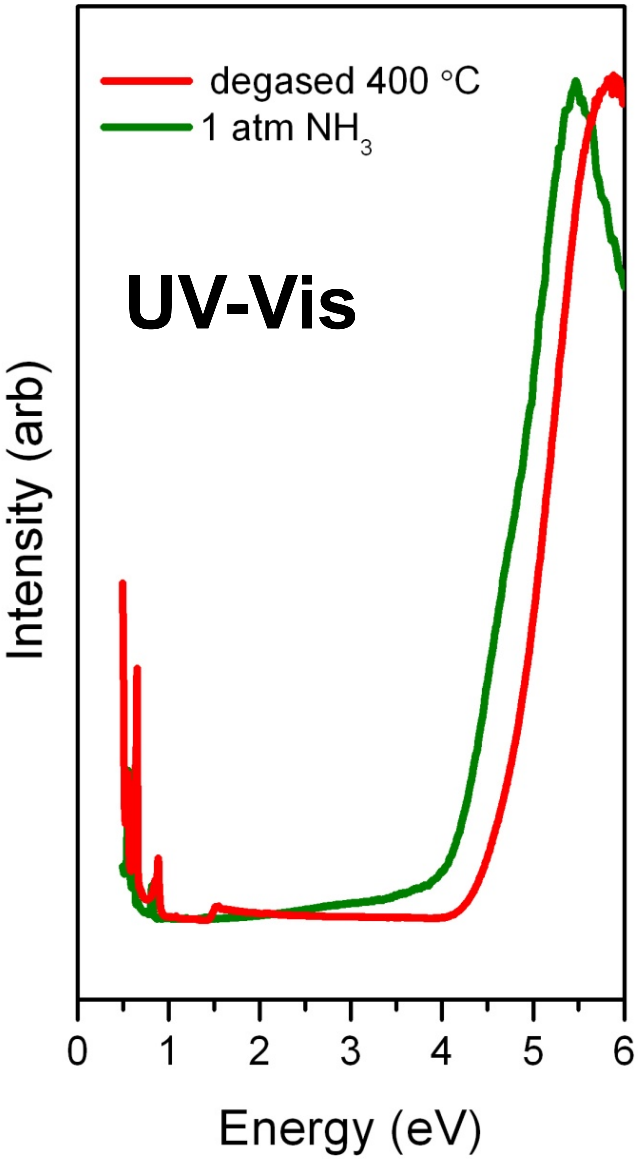

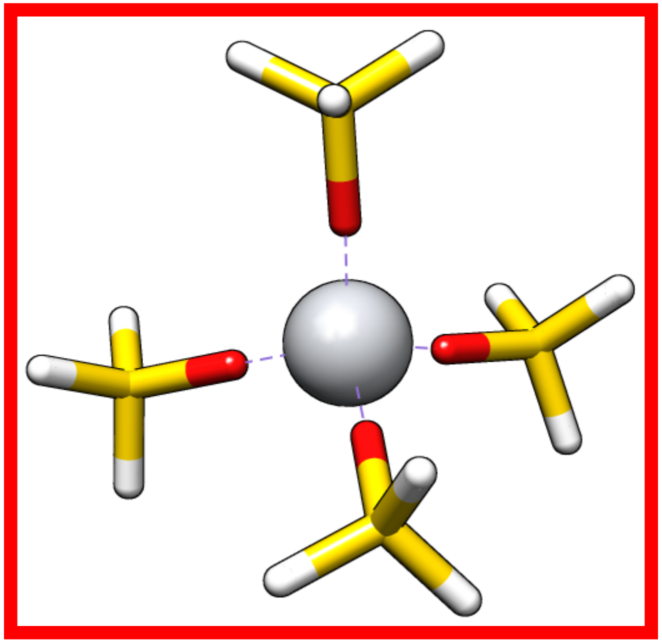

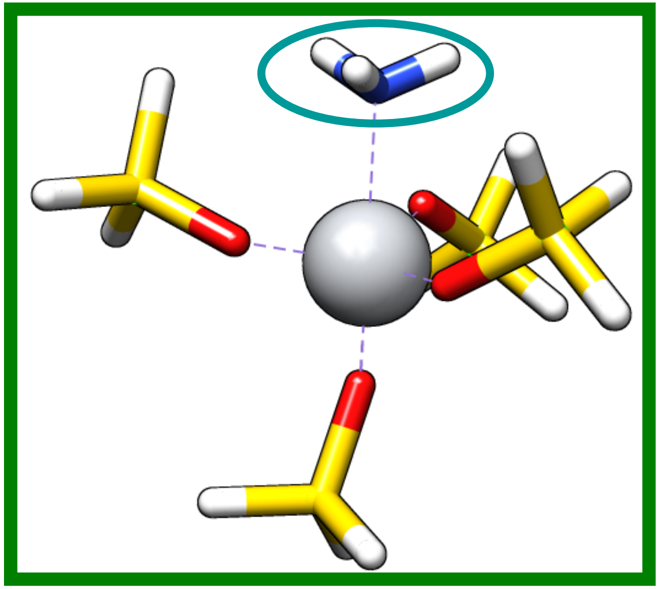

Valence Band RIXS

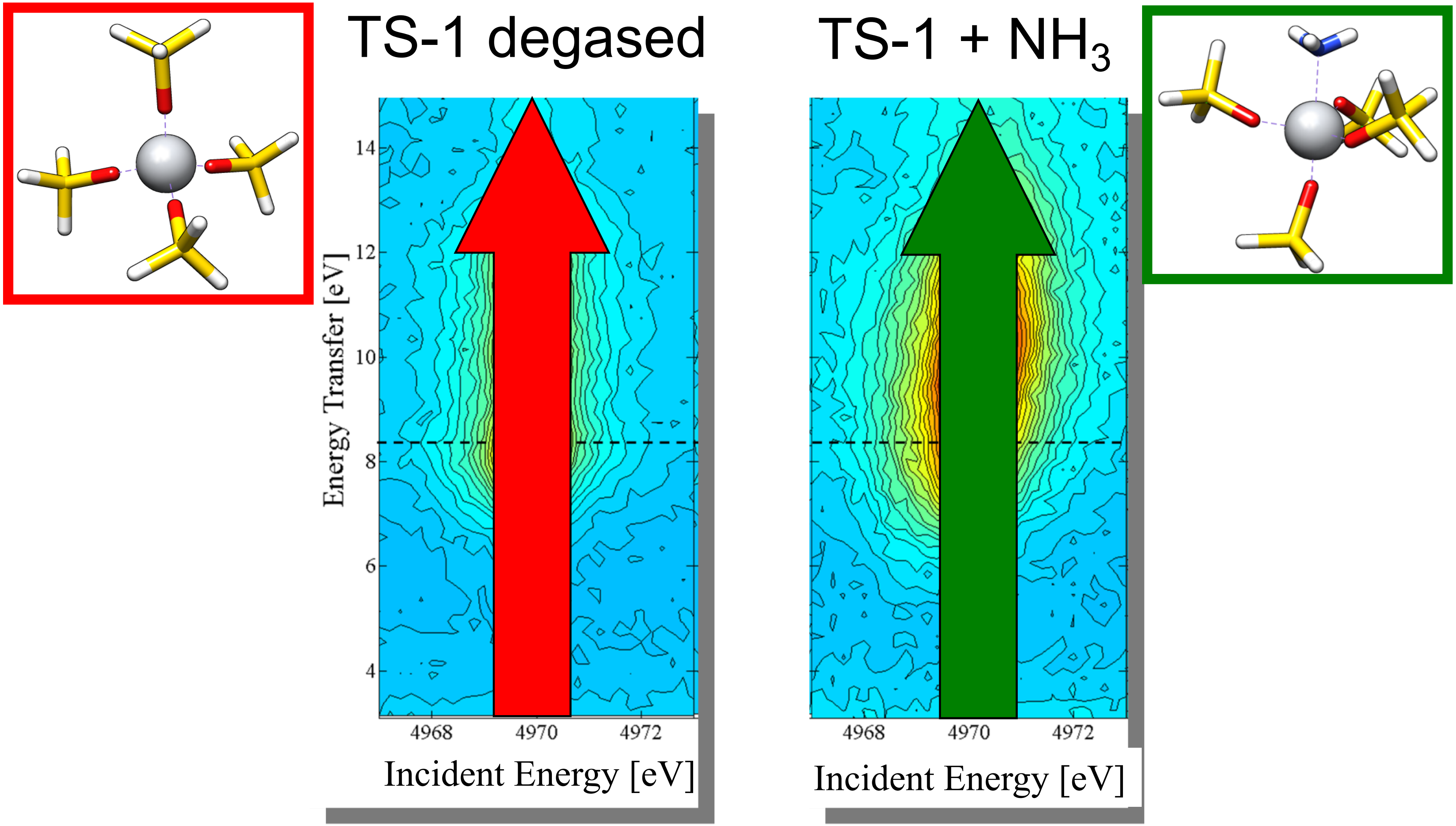

TS-1 degased

TS-1 + NH_3

E. Gallo, C. Lamberti, et al. in preparation

Comparison UV-Vis and valence band RIXS

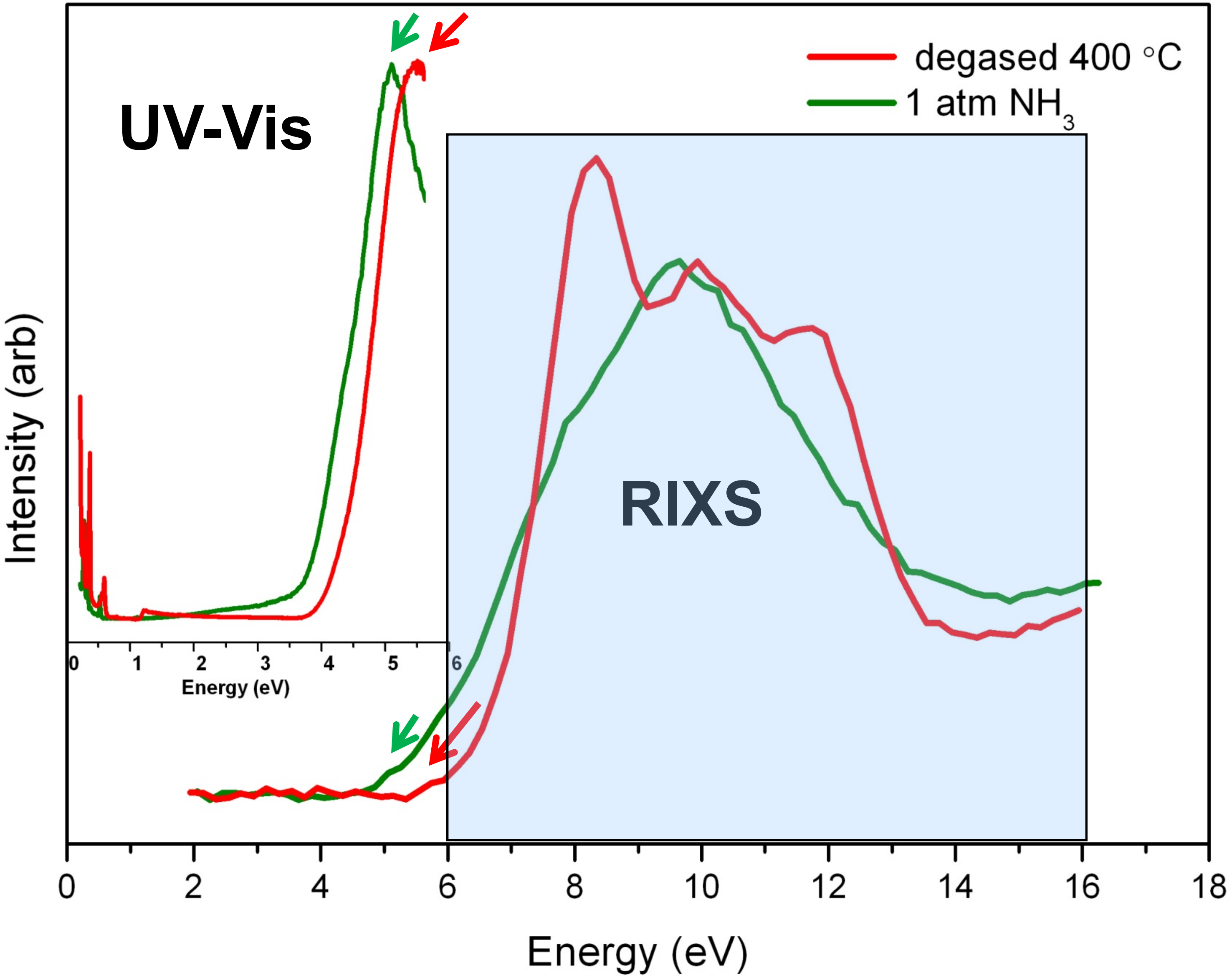

E. Gallo, C. Lamberti, et al. in preparation

DFT calculations using ORCA

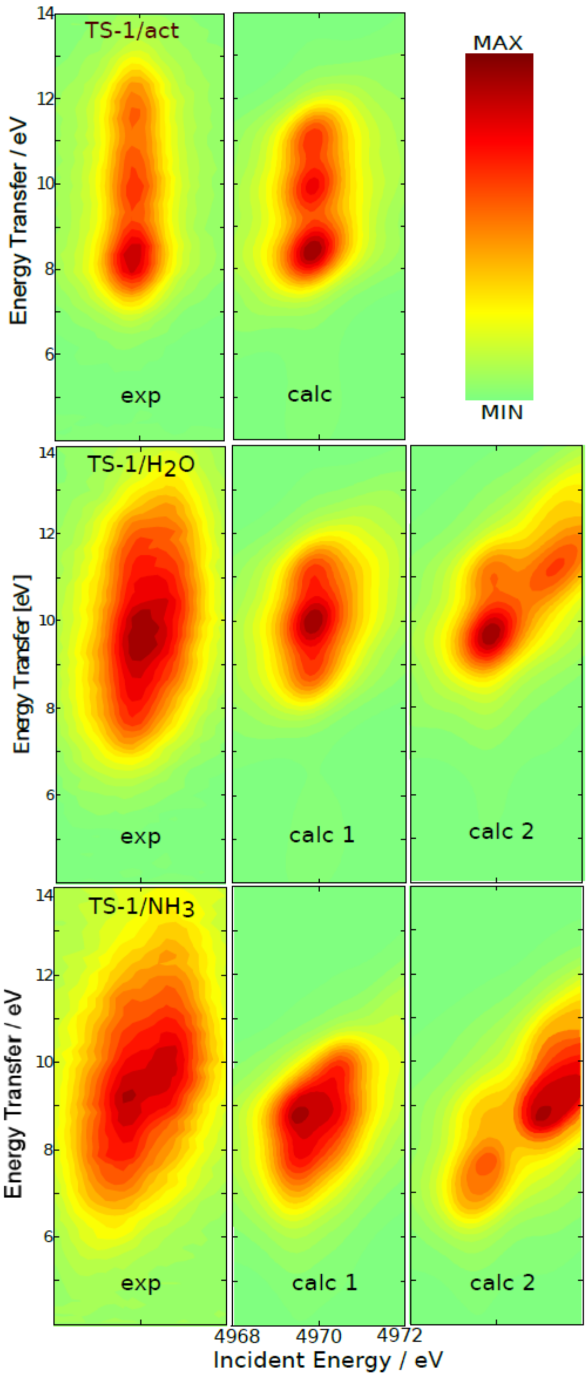

degased

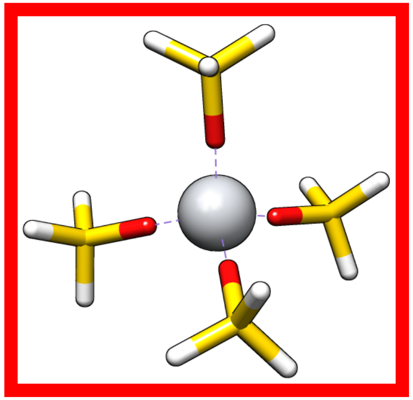

H_2O

NH_3